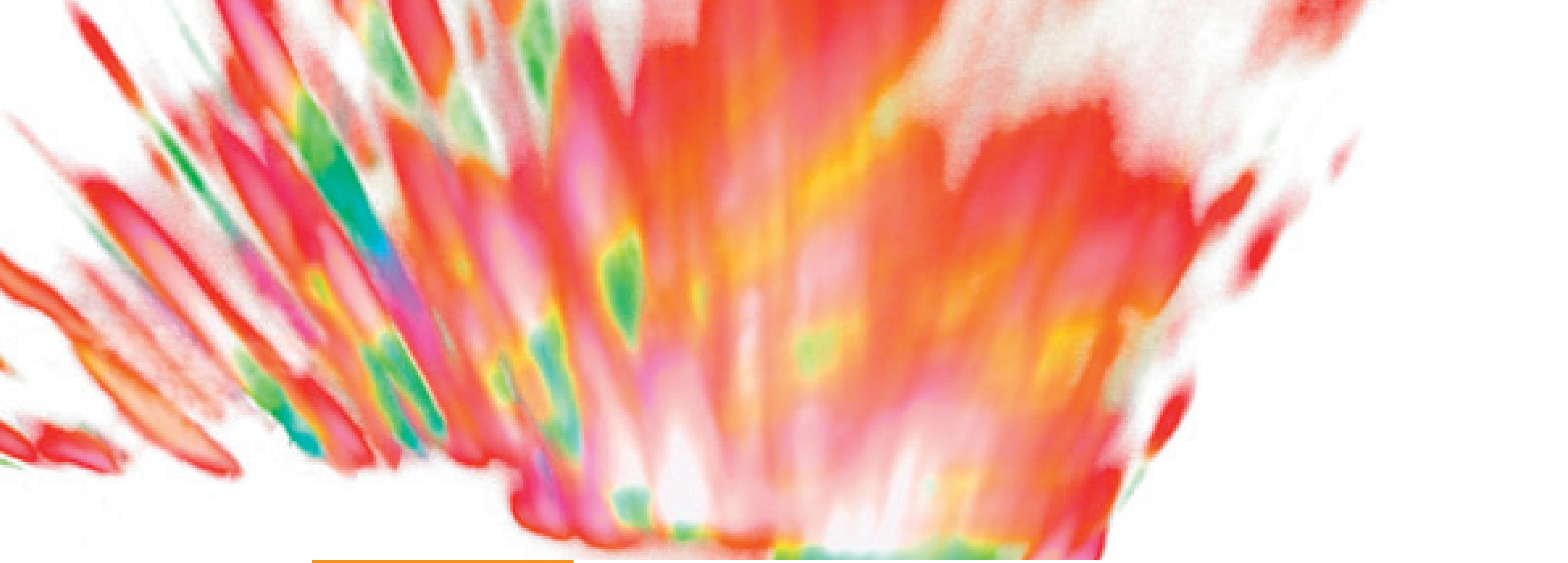

PHOTONICS

THEMENHEFT FORSCHUNG · N° 2 · 2005

Universität Stuttgart

Editorial

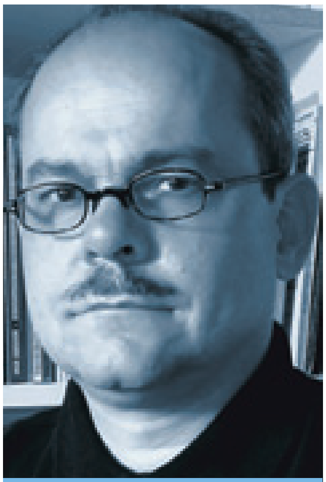

Dear reader,

the second edition of **THEMENHEFT FORSCHUNG** places its emphasis on the scientific area of Photonics, an area which is not unknown but one which is continuously expanding due to new discoveries and developments (see Welcome Address as well as the Introduction). The Universität Stuttgart is proving to be a significant home for further discoveries and applications with recognized scientific and infrastructural conditions. In the light of this, it seemed reasonable to bundle such a complex research landscape in a new **THEMENHEFT FORSCHUNG**.

All of the authors of this journal expressed the wish to write their papers in English. This is the common language in the scientific community of researchers in laser technology, quantum optics, thermodynamics or solid physics. The summary in German is designed to meet the minimal requirements of the Public Understanding of Science in Germany. I am sure, that the demand for more Public Understanding of Science in the global scientific process will create new opportunities for both sides: scientists and the public. Scientists have to translate as much as possible of their methods and results into the language of non-scientists. But non-scientists have also to be ready to learn at least some words of the language of science.

Useful roadmaps for a new field of research can generally only be drawn once the area is fully developed. Photonics is still in transit. Therefore, this **THEMENHEFT FORSCHUNG** tries to give a little in sight on ongoing research.

Dr. Ulrich Engler

Editorial details

The Themenheft Forschung is published by order of the rectorate of the Universität Stuttgart

Editorial coordination Themenheft Forschung: Ulrich Engler, Tel. +49 (0)711 121 2205; E-mail: ulrich.engler@verwaltung.uni-stuttgart.de

Scientific coordination Photonics: Thomas Graf

Authors Photonics: Mohamed Benyoucef, Peter Berger, Manfred Berroth, Friedrich Dausinger, Martin Dressel, Adolf Giesen, Harald Giessen, Bruno Gompf, Thomas Graf, Tobias Heist, Sven Hensler, Felix Hoos, Michael Jutzi, Erich Kasper, Jürgen Köhler, Berthold Leibinger, Peter Michler, Wolfgang Osten, Tilman Pfau, Christof Pruss, Uwe Rau, Markus B. Schubert, Jürgen Stuhler, Jörn Teipel, Sven Marcus Ulrich, Jürgen H. Werner

Layout Themenheft Forschung: Zimmermann Visuelle Kommunikation, Gutenbergstraße 94 A, 70197 Stuttgart
Cover photo by Frank Luerweg

Print and Advertising: Alpha Informations GmbH, Finkenstraße 10, 68623 Lampertheim, GERMANY, Tel. +49 (0)6206 939-0, Fax +49 (0) 6206 939 232; Internet: http://www.alphawerbung.de; Sales management: Peter Asel

Stuttgart, November 2005

ISSN 1861-0269

zurück zum Inhalt

Welcome address by the rector

The new **THEMENHEFT FORSCHUNG** is dedicated to one of the outstanding research fields of the Universität Stuttgart – Photonics. It is well known: light matters in Stuttgart. The interaction of basic quantum optics research, applied photonics, material sciences and mechanical engineering is a unique advantage of the photonics research at and around the Universität Stuttgart. There are hardly any other centres with a comparably versatile, interdisciplinary and complete pervasion of photonics research activities – not only in Germany but also worldwide.

The clustering and the accentuation of all the photonics activities around the Universität Stuttgart is a strategic goal of both the university and the ministries of Baden-Württemberg and shall feature distinct emphasis on the transfer of photonic technologies into engineering and manufacturing.

The Universität Stuttgart will expand teaching on optical sciences with an own Master degree on optical engineering. The promotion of young scientists will additionally be supported by the implementation of a graduate school focused on the phenomena of light-matter interactions.

An important premise for a sustainable growth of photonics is a competitive research excellence from basic science to application-oriented engineering that strategically generates the innovations needed for the future of our economy.

This holistic approach could not be fully represented in our **THEMENHEFT FORSCHUNG**; nevertheless the subject area reaches from the basic research in atom optics, single photon sources and new holograms to the new developments on lasers, silicon based photo detectors or solar cells.

I thank the scientific coordinator, Prof. Graf, and all the authors of our university very much for their contributions and their additional effort for the necessary public understanding of science. My special thanks goes to Berthold Leibinger and his well informed and inspiring words about the future of the scientific region in Stuttgart with regard to optical technologies.

Prof. Dr.-Ing. Dieter Fritsch

zurück zum Inhalt

Photon technology

The comprehensive interpretation of "photonics" includes an incomparably large spectrum of technologies and applications. Originating from the photon and created equivalent to electronics, it had first been used with optoelectronic applications. Today photonics stands for the modern so-called "optical technologies". The properties of the photon to transmit energy and information without moving a mass allow fascinating technical solutions. Laser light opened the doors to novel scientific disciplines. Quantum optics, non-linear optics and atomic optics are fascinating new worlds with rules and properties very different from those intuitively known to mankind.

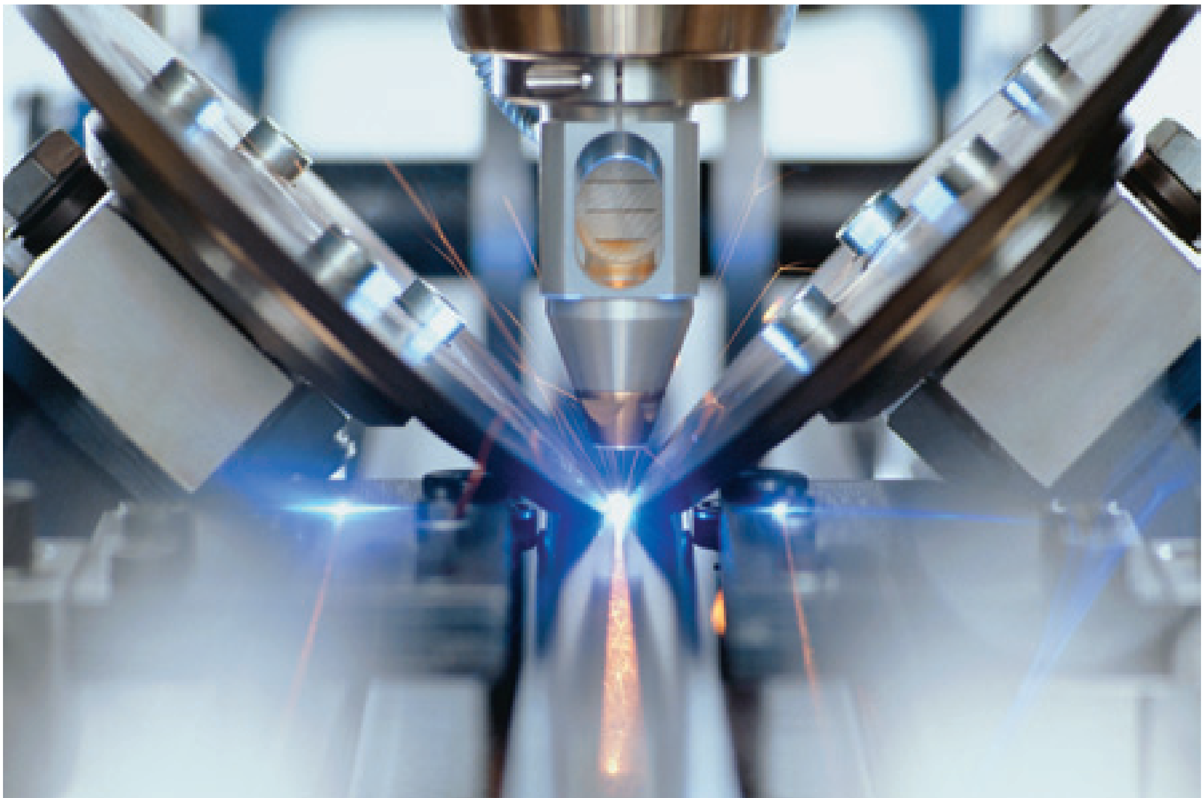

Sunlight is a basic precondition for life on Earth. Since humans have walked the earth they have followed the rhythm of the sun, moon and star light. By taming fire man created his first artificial source of light. For the evolution of mankind, this was a very important step. But only after hundreds of thousands of years did the technological breakthrough of optics occur. Early scientists learned to understand the concept of classic light and invented spectacles, the telescope and the microscope, among others. Mankind started to utilize light by inventing optical instruments that allowed the discovery of the universe, bacteria and photography. Electricity enabled another breakthrough. With easy and efficient electrical lighting mankind became emancipated from the sun.

The "light revolution" came with the invention of the maser and the laser. The laser has become a basic artificial light source for science and industry. It is light of a new quality that can be adapted to specific needs. Light finally not only enables vision but it has become a versatile tool. This breakthrough is envisioned by many statements that call the 21st century the "century of the photon."

The center of a new technology

The photon, the light quantum postulated by Einstein, is the combining element of all photonic disciplines. The difference to classic light and optics is the utilization of the specific properties of the photon that are not available with "ordinary" thermal light.

The key property of laser light is the coherence that results in high spectral and spatial resolution as well as interference phenomena. Interference is the basis for holography and various imaging techniques. It is now possible to create laser light pulses a million or even billion times shorter than a billionth of a second. The single frequency property of laser light is used in detection and measurement applications. In manufacturing technologies the high spatial resolution enables contact-free, high performance cutting and welding of various materials including stainless steel by focusing high power laser light onto a small spot. The high frequency and spectral purity of laser light allows the coding and transfer of huge amounts of data. Single photon emitters allow the utilization of the quantum properties of the photon, for example for quantum cryptography.

Despite the very different applications, all photonic disciplines have in common the interaction between light and material. Photonics therefore goes far beyond the boundaries of light. The spectrum of "light optics" ranges from infrared to ultraviolet. In contrast, the more energetic X-rays and the "tera incognita" of the terahertz waves between microwaves and infrared light also belong to the photonic spectrum. And even the atomic laser can be linked to photonics. "Atomic optics" has become possible only with laser light. While in optics material is used to manipulate light, here light manipulates material.

Photonics research is indispensible for future economic growth

The economic impact of photonics cannot be underestimated. Already today, photonic technologies play an important role in many key industry sectors like production, information and communication, imaging and detection. Photonic systems from laser machines to components for infrastructure and consumer products worth hundreds of billion of Euros are shipped around the world. While the markets of established photonic applications are still rapidly growing, many more applications are yet to come. These new applications currently in development in science and industry are indispensable for our future economic growth.

Research and industry are tightly interconnected. Basic research builds the underlying structure for innovations that industry can distribute in the market. While the long term success of industry is based on excellent research, only economic success enables the society to finance research. This basic relation is very relevant for photonics. Today, we can hardly estimate the impact of all the photonic research – parts of which are illustrated in this book. But we know that it is of key importance for our future economic success. The German government has realized the importance and initiated a national research program for "optical technologies".

A short trip through photonic research at the Universität Stuttgart highlights the various links and interactions in which new applications are born. Once, the laser was called a solution for an unknown problem. But then it helped to invent previously unthinkable new methods and gain spectacular new insights. The example of the laser shows that even though science needs some orientation towards marketable results, free basic research is very important for the discovery of new technologies. This is the domain of state-

THE AUTHOR

PROF. DR.-ING. E.H.
BERTHOLD LEIBINGER

Chairman of the Supervisory Board of the TRUMPF Group

Contact
TRUMPF GmbH + Co. KG
Johann-Maus-Str. 2
71254 Ditzingen
Internet: www.trumpf.com

funded research. There is no doubt that the close collaboration of science and industry is important, but this should not result in shrinking funding for basic research!

Excellent photonic cluster in the Stuttgart vicinity

The region surrounding the Universität Stuttgart provides every opportunity for successful photonic research, development, production and marketing. Research is represented as well as the complete value chain from the specialized supplier to the user. Local utilization of regional competence and knowledge pairs with global marketing of the products. This so-called photonic cluster has also been identified through an early study for the German state of Baden-Württemberg on strategic future investments. The study led to strategic funding of basic research by the Landesstiftung Baden-Württemberg and the founding of Photonics BW as the local photonic network.

The photonics research at the Universität Stuttgart and neighboring research institutes is an example of an excellent science cluster. Compared to other national optics locations, it is marked by the largest interdisciplinary network and a strong penetration of photonics in manufacturing technologies and engineering that allows very efficient transfer of basic research into innovations. The interplay of quantum optical basics, applied photonics, material research, production technologies and engineering are an important advantage of the Stuttgart photonics cluster.

The photonic challenges are manifold and interdisciplinary as is apparent on the following pages. The extension of the fundamental barriers of photonic components falls into the domain of physical basics. Then there is the need for the extension of technical barriers and finally the extension of the process capabilities of photonics systems and processes. •

Berthold Leibinger

zurück zum Inhalt

Research on lasers and laser applications

Since its invention and the first experimental demonstrations the laser has long overcome its initial image of being a solution for a yet unknown problem. In fact this technology has now reached an essential economical importance both as an independent industry as well as a key technology and mainspring for innovations in other industrial sectors. But also in science the laser has never lost its attractiveness and continues to open up new fundamental research opportunities ranging from microbiology and medicine over material processing and nano-science to fundamental research on light-matter interactions and quantum phenomena.

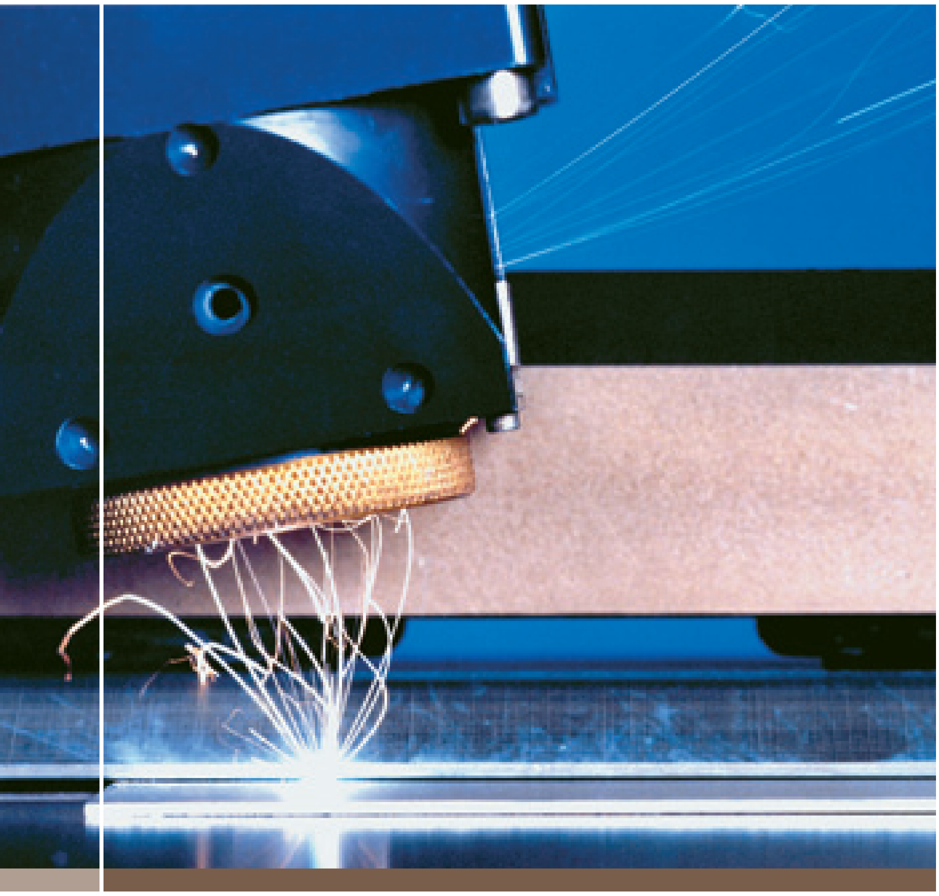

The research on lasers and their applications at the Universität Stuttgart is concentrated at the Institut für Strahlwerkzeuge (IFSW). It follows a holistic approach and spans the whole range from laser physics and laser development to laser applications and fundamental research on laser material processing. The aim is to generate essential innovation and competitive advantage in a wide field of manufacturing applications. For manufacturing purposes, the laser is indeed a universal tool as it covers all production processes defined by the German industry standard DIN 8580. That is to say: primary forming, deforming, separating, joining, coating, and altering material properties. All these laser applications in manufacturing have gained significant impulses with the improvements of the laser sources in the recent few years. And the actually most prominent and reputed laser worldwide, the thin-disc laser, is an invention of the IFSW. But also in the past, the IFSW has contributed key innovations for instance to the CO_2-lasers that are leading the global market today.

Still, this successful technology transfer would not have happened without a sound scientific but practical demonstration of where and how the laser technologies are superior to conventional manufacturing methods. This is why the holistic research approach with the merge of the newest laser sources with cutting-edge research on laser material processing was and is so important. Many of the most successful laser techniques in a wide range of manufacturing applications are a result of this approach. Among these are the solution of welding instability problems with double-focus techniques, an essential leap in precision with the invention of helical drilling with the development of a corresponding trepanning optics, the investigation and development of novel nozzles for laser material processing as well as fundamental research on the dynamics of light-matter interactions that led to a sound understanding of laser processing techniques.

All these research results have meanwhile found their way into widespread industrial implementations, and prove that the photonics research in Stuttgart indeed is at the leading edge of science and that the technology transfer to the innovative industry of the region is very efficient. This successful research environment shall be demonstrated with a few exemplary developments highlighted in the following.

1. The Thin-Disk Laser

The thin-disk laser concept allows to build diode pumped solid state lasers with simultaneously highest output powers, highest efficiency and best beam quality. Nearly all operational modes of solid state lasers and laser amplifiers such as continuous wave, pulsed operation with pulse durations between femtoseconds and nanoseconds can be realised with this design and in most cases with clearly superior properties as compared to other laser concepts.

One of the outstanding features of the thin-disk laser is its excellent beam quality which results from the face cooling of the laser disk. **(01)** shows the principle of the thin-disk laser design. The laser crystal is shaped as a disk with a diameter of several mm (depending on the output power/energy) and a thickness of 100 µm to 200 µm depending on the laser-active material, the concentration of the laser-active ions (the so-called doping level) in the thin-disk crystal and the excitation design (the so-called "pumping" of the laser material). The disk is coated to work as a highly reflective mirror on its back side for both the laser and the pump wavelengths and anti-reflection coated on the front side for both wavelengths. This disk is mounted with its backside on a water-cooled heat sink using indium-tin or gold-tin solder. This technique allows a very stiff fixation of the disk on the heat sink without deformation of the disk which acts as a backside-mirror of the laser resonator. To reduce the stress during the soldering process as much as possible the heat sink is made from a heat expansion matched material (Cu-W). The heat sink is water-cooled by impingement cooling using a multi-nozzle design inside the heat sink.

Due to this mounting and cooling technique the temperature gradients inside the laser crystal are mainly coaxial to the disk axis and the laser beam axis. Within the homogeneously pumped central area of the disk the temperature distribution is very uniform in radial direction. Therefore, these temperature gradients only slightly influence the laser beam propagating there and back through the disk. As compared to rod laser systems the thermally induced deformations and non-uniform refractive index changes (both causing lens effects and aspherical disturbances) are reduced by more than one order of magnitude in the thin-disk laser design. The stress induced birefringence is even more reduced and can be neglected for real laser systems. Additionally, due to the large surface-to-volume ratio the heat dissipation from the disk into the heat sink is very efficient thus allowing the operation at extremely high volume power densities in the disk (up to 1 MW/cm^3 absorbed pump power density).

ZUSAMMENFASSUNG

Dank seiner einmaligen Anwendungsvielfalt erfreut sich der Laser eines seit seiner Erfindung ungebrochenen und beispiellosen Siegeszuges in allen gesellschaftlichen, industriellen und wissenschaftlichen Bereichen. Das Institut für Strahlwerkzeuge (IFSW) verfolgt dabei einen ganzheitlichen Forschungsansatz der die Entwicklung neuer Laserstrahlquellen mit der Erforschung laserbasierter Materialbearbeitungsprozesse und der dafür benötigten Komponenten verbindet. Die Arbeit des IFSW wird hier anhand ausgewählter Beispiele aus den drei genannten Themenkreisen illustriert. Aus dem Bereich der Laserentwicklung wird das am IFSW erfundene und heute bereits sehr erfolgreich industriell umgesetzte Scheibenlaserkonzept vorgestellt. Die Forschung auf dem Gebiet der Materialbearbeitung mit Laserstrahlen hat wesentlich zum industriellen Erfolg des Scheibenlasers beigetragen und wird anhand der Erkenntnisse z.B. beim Bohren oder beim Schweißen illustriert. Dass es für den erfolgreichen Einsatz des Strahlwerkzeugs Laser mehr braucht als Laserstrahlen, Linsen und Spiegel zeigt der Bericht über aerodynamische Komponenten, welche einerseits zum Schutz der optischen Elemente eingesetzt werden und andererseits die für den Bearbeitungsprozess erforderlichen Druck- und Strömungsverhältnisse erzeugen.

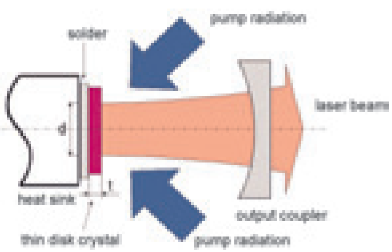

01

The principle of the thin-disk laser design.

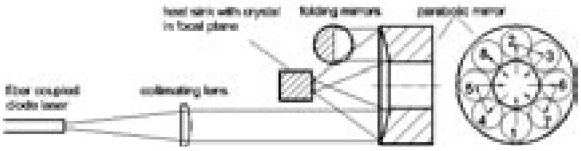

02

Pumping design for the thin-disk laser with 16 pump beam passes.

The disk can be pumped in a quasi-end-pumped scheme. In this case the pump beam hits the crystal under an oblique angle as shown in **(01)**. Depending on the thickness and the doping level of the crystal only a small fraction of the pump radiation is absorbed in the laser disk. Most of the incident pump power leaves the crystal after being reflected at the back side. By successive re-directing and imaging of this part of the pump power again onto the laser disk the overall absorption of the pumping beam can be increased. A very elegant way to increase the number of pump beam passes through the disk is shown in **(02)**. The radiation of the laser diodes for pumping the disk is first homogenized either by fibre coupling of the pump radiation or by focusing the pump radiation into a quartz-rod. The end of either the fibre or the quartz rod is the source of the pump radiation which is imaged onto the disk using the collimating lens and the parabolic mirror. In this way a very homogeneous pump profile with the appropriate power density in the disk can be achieved which is necessary for good beam quality. The unabsorbed part of the pump radiation is collimated again at the opposite side of the parabolic mirror. This beam is re-directed using two mirrors to another part of the parabolic mirror where the pump beam is focused again onto the disk, this time from another direction. This re-imaging procedure can be repeated until all the (virtual) positions of the parabolic mirror have been used. At the end the pump beam is re-directed back to the source thereby doubling the number of pump beam passes through the disk. In this way up to 32 passes of the pump radiation through the disk have been realized and more than 90 percent of the pump power is absorbed in the disk.

Using multiple pump beam passes through the disk results in a thinner disk and/or a lower doping concentration thus reducing the thermal effects like thermally induced lenses and stress in the disk. Another advantage is that the effective pump power density is increased (nearly 10 times for 16 pump beam passes) so that on the one hand the demands to the power density (beam quality) of the pump diodes are reduced and on the other hand also quasi-three-level laser materials (e.g. Ytterbium doped) can be used with this design.

When operating the disk in this set-up the output power or energy can easily be scaled just by increasing the pump spot diameter keeping the pump power density constant. Also, there is no need to increase the brightness of the pump laser diodes.

Very high laser output power can be achieved from one single disk by increasing the pump spot diameter while keeping the pump power density constant. The slope efficiency and the optical efficiency are nearly independent of the pump spot diameter. To date more than 4 kW power has been demonstrated from one single disk (Trumpf Laser). The high efficiency of the thin-disk laser results also in a very high electrical efficiency of the total laser system which is higher than 25 percent for industrial lasers with 4 kW output power and a beam propagation factor M^2 of less than 20.

An alternative way to scale the output power is the use of several disks in one resonator. More than 6.5 kW laser power has been demonstrated so far using 2 and 4 disks in one resonator (Trumpf Laser). Due to the moderate thermal effects in the disks the beam quality is nearly independent of the power and is at least 3 times better (for commercially available thin disk lasers) than that of rod lasers with the same output power.

Depending on the demands from materials processing the high-power thin-disk lasers in the kW power range are operated with a beam propagation factor (beam quality) M^2 of about 20 that means that the focusability of the laser beam is 20 times inferior to the theoretical limit ($M^2 = 1$). But beyond this beam quality, the thin disk laser design offers the possibility to operate high power lasers also with the diffraction-limited beam quality ($M^2 = 1$) due to the moderate thermal effects and the small optical distortions in the disk. Using an appropriate resonator design it is possible to achieve high laser output power with high optical efficiency.

Simulations show that scaling of the output power of one single disk is only limited by amplified spontaneous emission (ASE) if the pump spot diameter becomes larger and larger. Fortunately, the optical gain of lowly doped Yb:YAG is rather small so that ASE will occur only at very high pump power levels. For a 9 at. percent doped disk with a thickness of 200 µm the power limit occurs at a pumping power beyond 50 kW so that much more than 20 kW laser power can be extracted in cw-operation from one single disk.

This power level (20 kW) can be increased much more by further increasing the pump spot diameter. The limitation set by ASE can then be overcome by using a disk with an un-doped cap on top of the disk thus reducing the average radial gain by the square of the ratio between un-doped and doped material.

The simulations also show that the laser power level for diffraction-limited mode operation can be increased to the same power level as for multi-mode operation. The reason for this behaviour is that the aspherical contribution to the residual thermal lens of the disk inside a top-hat pump profile is extremely small (less than 10 nm optical path difference) and independent of the pump spot diameter itself. The resulting phase step at the edge of the pumped region can be compensated for by using simple adaptive optics.

Besides the outstanding properties of the thin-disk laser design for cw-operation it is also well suited for pulsed laser systems especially if high average output power is required. Till today, pulsed thin-disk laser systems have been developed and demonstrated for the ns, ps, and fs pulse duration ranges (10^{-9}, 10^{-12}, and 10^{-15} seconds, respectively). All systems show an excellent beam quality and high efficiency.

Scaling the pulsed energy of one single disk is limited more severely by ASE than in the case of cw-operation since the gain under low repetition rate conditions is much higher as compared to the cw-operation of a disk. Nevertheless, using an un-doped cap on top of the disk will result in achievable pulse energy levels far beyond 10 J from only one single disk. This energy can be further increased by using multiple disks in one resonator.

Up to now several companies already offer thin disk lasers on the market for different applications. These lasers are covering the power range from several watts up to several kW for materials processing. **(03)** shows a thin disk module for the power range up to 500 W.

Using thin disk lasers for materials processing will considerably increase the process efficiency for many applications. Due to the good beam quality of thin disk lasers deep penetration welding becomes possible also for thin materials as well as remote welding at high power. In summary, the increase of laser and process efficiency will result in substantial cost reduction of laser manufacturing.

In future, new materials will be investigated with the goal to increase the power, the energy and the beam quality even further. Laser output powers of much more than 10 kW and energies of more than several J will be possible. New materials will open new markets for new wavelengths and with the semiconductor thin disk lasers customized lasers for specific markets will become feasible.

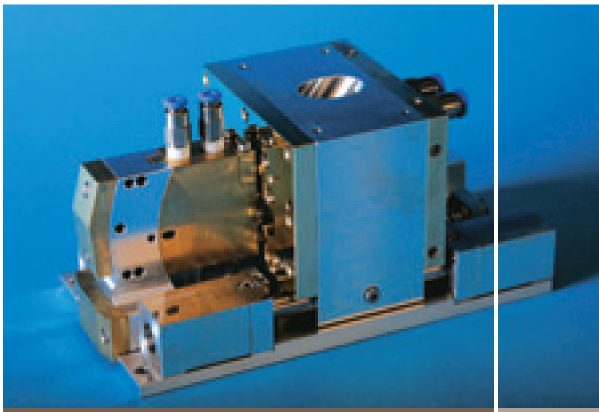

03

Thin-disk laser module for up to 500 W laser power.

2. Understanding Laser Material Processing

As stated in the introduction, strong synergetic effects result from simultaneous but linked developments and research in the fields of laser systems and their applications. The basic understanding of photonic production processes in one hand allows defining the direction of laser development. Early tests of newly developed systems on the other hand offer the chance to investigate, prove and demonstrate their potential and thus open new markets.

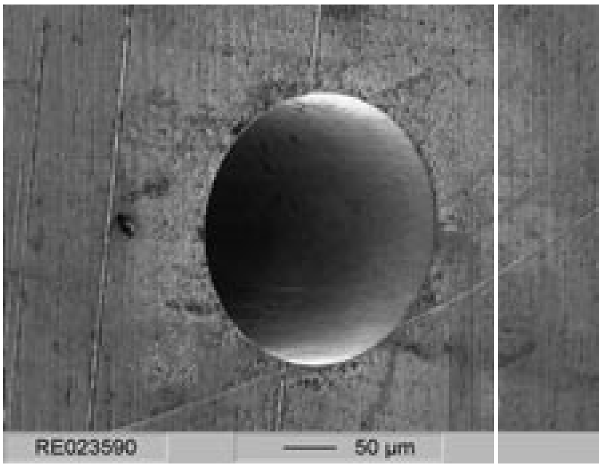

04

Hole produced in 1 mm thick steel with an experimental picosecond laser developed at the IFSW.

A recent example lies in the field of micro machining **(04)**. Whereas the majority of research groups propagated the recipe to increase accuracy by reducing the pulse duration down to the femtosecond region (1 fs = 10^{-15} s), fundamental theoretical investigations and experimental findings at the IFSW showed, that pulses shorter than 1 ps (= 10^{-12} s) do not offer further advantages for the processing of metals and that the highest precision can be reached with 10 ps long pulses. This conclusion superseded the development of complicated and expensive laser systems.

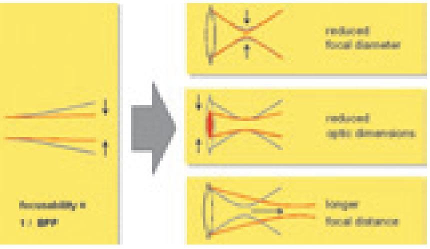

05

Benefits of improved focusability: reduced focal diameter (top), reduced optics dimensions (middle) or extended working distance (bottom).

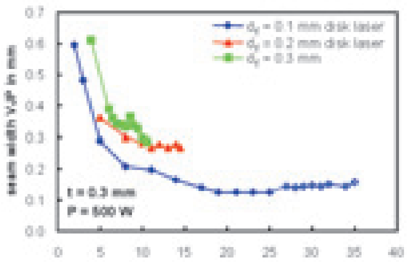

06

Welding performance of a thin-disk laser (focus diameters 0.2 and 0.1 mm) compared to a conventional system (focus diameter 0.3 mm), both operated at 500 W, when applied to steel sheets of 0.3 mm thickness.

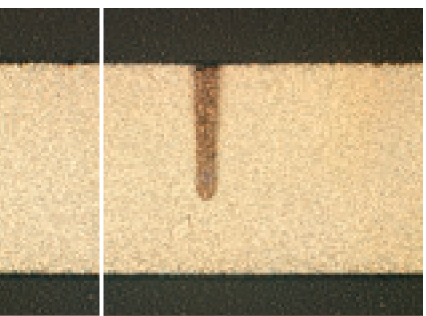

07

Cross sections through a 2.5 mm deep weld seam in steel achieved with a 3 kW thin-disk laser at a velocity of 9 m/min.

One of the first findings of the research at the IFSW was that an ideal laser for welding should offer high efficiency, a short wavelength (1 µm) and good focusability.

Both conventional laser systems used for welding, CO_2 lasers and lamp pumped Nd:YAG systems, could not meet all requirements. CO_2-lasers offered the advantages of high efficiency, low cost and strong focusability. Nd:YAG lasers, on the other hand, convinced production engineers by their short wavelength allowing beam conduct through flexible glass fibres.

The search for a laser concept able to fulfil all of the above requirements led to the invention of the disk laser. Industrial lasers based on this concept now combine the advantages of the conventional work horses.

With the thin-disk laser or generally with a laser of equal focusability such as the fiber laser, one can achieve either a significant reduction of the focus diameter by using the same focal length or an even stronger reduction of the dimensions of the focusing optics when maintaining the focal diameter **(05)**. In the latter way, accessibility is improved, integration in the handling device is facilitated and the dynamics of the system is improved due to the smaller moving mass. A third option to benefit from stronger focusability is to extend the distance between optics an workpiece which enables highly productive techniques such as remote welding which uses rapid beam deflection to eliminate non-productive times. In this case, the working volume accessible with scanner optics scales with the third power of the focusability. The remote welding is presently introduced in car body manufacturing and allows to substitute resistance spot welding to a large extent.

In addition to the advantages for system layout described above, higher focusability allows to overcome current limitations of the welding process. **(06)** demonstrates this in the case of welding thin sheets with low power. The maximum welding speed for full penetration is 35 m/min with a focus diameter of 0.1 mm of a disk laser which is three times faster as compared to the attainable speed with a larger focus diameter of 0.3 mm obtained from a conventional laser.

In welding of thicker materials the disk laser enables extremely slim weld cross sections **(07)** which so far could only be achieved with electron beams. In this way heat distortions can be minimized in welding of precise workpieces such as transmission components.

3. Gas-dynamical Components for Laser Material Processing

In order to ensure efficient processes with high-quality outcome, not only the laser process itself but also the environment of the process needs to be controlled and optimised. The result of laser material processing is very much influenced by the composition of shielding gases, pressure and gas flow circumstances.

These specific gas-dynamical conditions required to attain the desired results are usually limited to a small volume around the interaction region of the laser beam with the workpiece. In most cases this is accomplished very efficiently and effectively with appropriately designed gas nozzles.

The gases control requirements, however, are as diverse as the many different laser applications themselves. Additionally, gas-dynamical components often are also used to prevent the contamination of the expensive and sensitive optical elements. Especially the focusing optics and optical sensors close to the interaction zone are very vulnerable to damage caused by smoke and droplets generated by the highly dynamic laser-matter interaction. The degradation and the subsequent destruction of these optical components can again be prevented by appropriate gas cross-jets which are generated by specifically dedicated nozzles to deflect both smoke and droplets. The challenge in the combined use of shielding gas and cross-jets lies in the potential aero dynamical interaction of the different gas flows. In particular one must prevent that the cross-jet which protects the optical components draws the shielding gases off the workpiece.

To date a large variety of gas-dynamical components have been and still are being investigated and optimised for a wide variety of different laser material processing applications at the IFSW. As an illustration of the corresponding work, three interesting concepts shall be highlighted in the following: gas nozzles for high-power cutting with CO_2 lasers, a cross-jet nozzle for the protection of optical components and a gas-dynamical device to reduce the ambient pressure in the interaction zone to improve the rate of ablation with ultra-short laser pulses.

In the field of laser cutting the development of nozzles concentrates on the applications with inert gases as they require particularly high pressures and high flow velocities to efficiently remove the melt out of the gap. Compared to this task, the requirements for oxygen-assisted cutting are much less demanding. Due to the immediate required momentum interaction of the gas with the melt, the nozzle is usually very close to the workpiece surface which means that the laser beam has to be directed collinearly with the nozzle axis and focused through the nozzle opening onto the workpiece.

It is known since many years that the commonly used conical or conical-cylindrical nozzles cannot transfer high pressures over larger distances in the generated free jets. This is due to a gas-dynamic shock wave caused by the sudden deceleration of the gas in the jet impinging the workpiece. These shock waves get more pronounced the higher the velocity of the gas is that hits the workpiece surface. The gas velocity at the exit of conical nozzles is equal to the speed of sound and it significantly increases within a few millimetres of distance from the nozzle. Therefore the impact pressure on the workpiece is significantly reduced by the shock losses with increasing distance from the nozzle.

At distances larger than the diameter of the nozzle further shocks arise that get more and more pronounced with increasing gas pressure in the nozzle. Those shocks can be completely avoided by using specially shaped nozzles, the so-called Laval-nozzles. Simultaneously, the shocks mentioned first are limited in strength. The advantage of the Laval-nozzle therefore is the constant impact pressure on the workpiece over much larger distances in the free jet. However, due to the high gas consumption of Laval-nozzles, the use of conical nozzles is still favoured where short distances to the workpiece are possible and the investigations to optimise the according gas dynamics is still an important part of the implementation of laser cutting applications.

Novel gas nozzle designs are also required for the cases where no transmitting optical windows or lenses can be used in the focusing optics due to the high laser powers that have become available more recently. In this case the inner gas pressure cannot be built up between the focusing lens or a window and the nozzle opening. To solve this problem ring-shaped nozzles and the combination of several nozzles were successfully investigated in the past few years. With the combination of two Laval-nozzles, for instance, the two jets can be merged to form one single jet that propagates collinearly with the laser beam. The inherent asymmetry of this implementation can be avoided by the use of a ring-shaped Laval-nozzle as shown in **(08)**.

All optimisations and new developments of nozzles for laser cutting require a sound understanding and detailed investigations of the gas-dynamics and the melt flow in the cutting gap. Experimentally this is investigated with appropriately scaled models **(09)** and interferometric methods or, especially more recently, with direct observation with high-speed camera equipment.

The same applies to the investigation and the development of cross-jets for the protection of the optical components particularly in laser welding applications **(10)**. It was shown that an efficient deflection of droplets requires the cross-jet to be placed as closely as possible to the workpiece surface. The gas velocity should be as high as possible to ensure the strongest possible deflection angles. This required the development of a special gas-dynamic nozzle that on the one hand provides the desired droplet deflection but on the other hand avoids the shielding gases form being drawn off the workpiese surface.

Another interesting gas-dynamical component was derived from very early investigations of aerodynamic windows that were

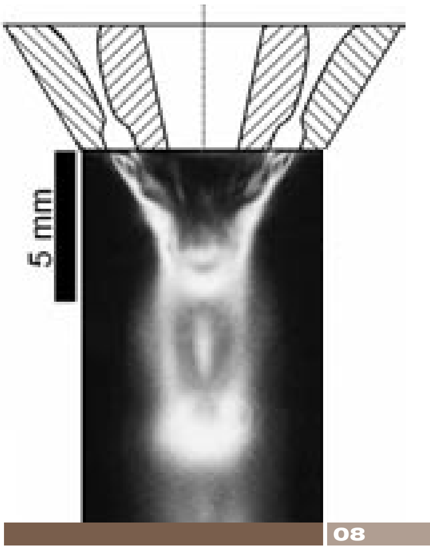

08

Schlieren picture of the gas jet produced by a ring-shaped Laval-nozzle with a gas pressure of 1 MPa and a gas flow of 350 bar×lt/min.

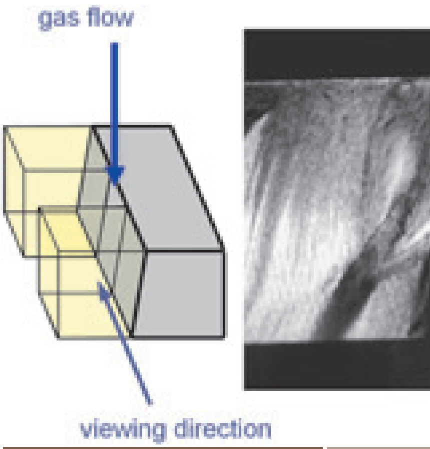

09

Experimental simulation of the melt flow in a cutting gap reproduced with optically transparent walls. A mixture of soot in petroleum is used to simulate the liquid melt flow.

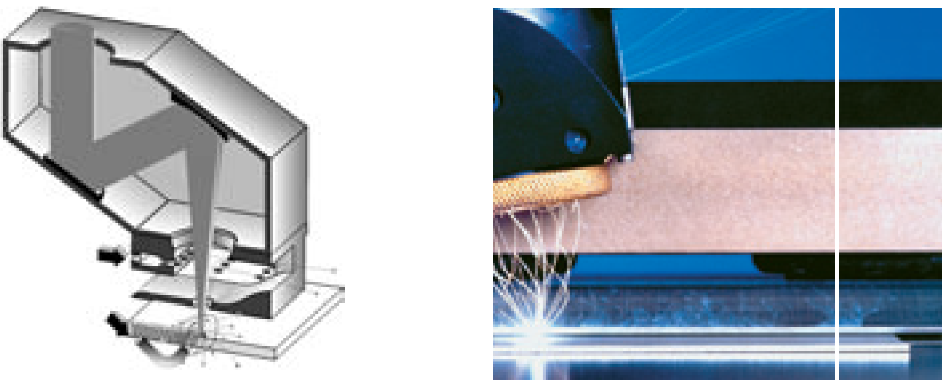

10

Left: set-up with the cross-jet (top arrow) nozzle which avoids the disturbance of the shielding atmosphere (bottom arrow). Right: deflection of the spilling by the cross-jet.

used to seal high-power CO_2 lasers. The knowledge on this technology now is exploited to reduce the ambient pressure to enhance the rate of ablation with ultra-short laser pulses. It has been shown that a reduction of the ambient pressure from approximately 1 bar to 0.1 bar can increase the ablation rate by at least one order of magnitude. The advantage of using an aerodynamic window as shown in **(11)** lies in the small evacuated volume just at the place where it is needed rather than evacuating larger chambers that house the whole workpiece.

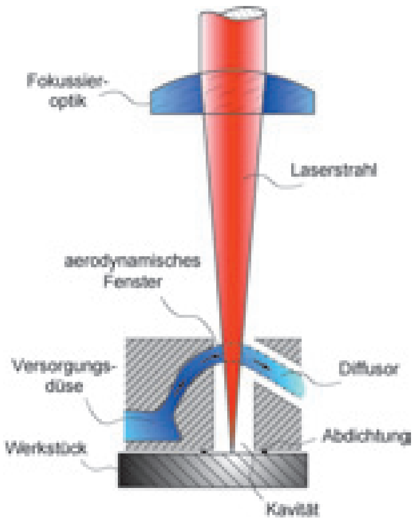

11

Aerodynamic window to increase the rate of ablation with ultra-short laser pulses.

4. Conclusions and Outlook

Summarising the past 20 years of laser research at the IFSW it can be concluded that one of the outstanding strengths is indeed the holistic research approach. Only by mastering every single aspect from the generation of laser beams to the fundamentals of the highly complex laser-matter interaction processes including the influence of the gas-dynamic environment at the interaction zone it is possible to successfully transfer novel and innovative technologies from academia to industry and generate the economic and societal benefits that we have seen so far.

This is an experience that will also be valid for the future. The holistic approach will be perpetuated although the research topic naturally will change. Once the thin-disk laser will have exceeded the 10 kW level the scientific interest will gradually shift from power scaling to shaping of custom mode properties. As the usual linearly or circularly polarised diffraction limited Gaussian modes not always – if not rarely – are the most suitable beams for given applications, the generation of modes with unconventional polarisation and/or intensity distributions will offer further potential of innovations. These all the more if the mode properties can be changed online during laser operation. On the other hand, the emergence of multi-kW lasers with nearly diffraction limited custom modes will create the necessity to develop novel optical fibres that allow to transmit the laser power without deteriorating the customised beam properties.

As in the past, it will be the research on laser applications that will point the direction of the laser research by assessing which of the above visions can be exploited in practice. Additionally, due to the fast and widespread implementation of the laser especially in manufacturing, there is a natural need for an improved quality assurance of laser machining processes. As this can only be achieved with a sound fundamental understanding of the highly dynamic laser machining processes the research on the laser-matter interaction, the complete numerical simulation of all relevant processes and the development of novel and better diagnostic tools is currently being reinforced with significant efforts. •

Peter Berger
Friedrich Dausinger
Adolf Giesen
Thomas Graf

SUMMARY

Thanks to its unparalleled versatile applicability the laser enjoys an ever increasing popularity in all societal, industrial and scientific fields. The Institut für Strahlwerkzeuge (IFSW) contributes to this success by following a holistic research approach that links the development of novel laser sources with the investigations on laser material processing and on the thereto required components. The efforts of the IFSW are illustrated with selected examples from these three research areas. The thin-disk laser concept that was invented at the IFSW has already successfully been transferred to industry. The industrial success of the thin-disk laser was significantly stimulated by the research on the applications as illustrated with knowledge gained from investigations on drilling or welding. That the successful application of lasers involves more than light, lenses and mirrors is seen from the examples given on aerodynamic components that are being developed both to protect the expensive optics and to provide the ideal environment for optimised machining processes.

THE AUTHORS

From left to right: Dipl.-Ing. Peter Berger, *Prof. Dr. rer. nat. habil.* Friedrich Dausinger, *Prof. Dr. phil. nat. habil.* Thomas Graf, *Dr. rer. nat.* Adolf Giesen.

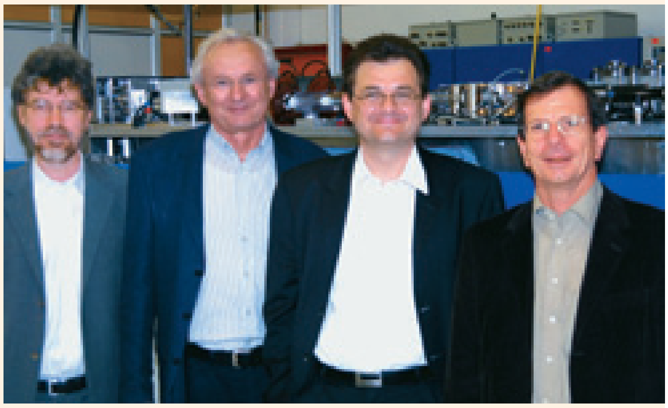

Contact
Institut für Strahlwerkzeuge (IFSW), Universität Stuttgart,
Pfaffenwaldring 43, 70569 Stuttgart, Germany
Tel. +49 711 685 6840, Fax +49 711 685 6842
Internet: http://www.ifsw.uni-stuttgart.de, http://www.fgsw.de

Peter Berger

was born in Wiesloch, near Heidelberg, in 1954. After study of aero and spaceflight technologies he received his diploma at the Universität Stuttgart in 1980. From 1981 to 1986 he was with the Institut für Aero- und Gasdynamik, where he worked in the field of the design of supercritical cascades for compressors and turbines. Since 1987 he is with the Institut für Strahlwerkzeuge (IFSW). Here he is responsible for topics concerning fluid and thermodynamics and he is leading the group working on basic research in laser materials processing.

Friedrich Dausinger

received his Ph.D. degree after the study of Physics at Max Planck Institut für Metallforschung in 1977. Then at Robert Bosch GmbH, among other responsibilities leading the laser application laboratory. Since 1986 at Institut für Strahlwerkzeuge (IFSW) of the Universität Stuttgart. In 2000 appointed to Professor after qualification for lecturing in Mechanical Engineering with a publication on energy coupling and process efficiency in laser materials processing. Presently deputy director of the institute and head of laser application group. Additionally director of non-profit company Forschungsgesellschaft für Strahlwerkzeuge (FGSW) mbH. Friedrich Dausinger is Fellow of Laser Institute of America, Corresponding Member of Russian Academy of Engineering Sciences and regular member of the German Wissenschaftliche Gesellschaft Lasertechnik e.V., WLT (Scientific Society for Laser Technology).

Adolf Giesen

studied physics at Bonn University, and received his Ph.D. degree in 1982. From 1982 to 1986 he was with DLR (former DFVLR, the German Aerospace Establishment), where he was responsible for resonators, optics and discharge technology in the CO_2-laser developing group. Since 1986 at the Institut für Strahlwerkzeuge (IFSW) of the Universität Stuttgart. Head of the department for laser development and laser optics, working on diode pumped solid state lasers (thin disk laser) and on characterization of laser beams and of optical components used with lasers.

Thomas Graf

was born in Lugano, Switzerland, in 1966. He received the physics M.Sc. degree in 1993 and the Ph.D. degree in 1996 from the University of Bern, Switzerland. As a post-doctoral research associate he was engaged in research on high-power solid-state lasers with high beam quality, beam-shaping for diode-laser bars, and thermodynamics of optical systems at the University of Bern until 1997. He then joined the University of Strathclyde in Glasgow, Scotland (UK) where he was engaged in research on non-linear optics and passively mode-locked multi-Watt all-solid-state lasers. In April 1999 he was appointed head of the High-Power Lasers and Material Science Group at the Laser Department of the Institute of Applied Physics, University of Bern (Switzerland) where he was awarded the venia docendi in 2001 and where he was nominated assistant professor in April 2002. In June 2004 he was appointed as university professor and director of the Institut für Strahlwerkzeuge (IFSW) at the Universität Stuttgart. He is currently interested in high-power all-solid-state laser systems, laser beam shaping and laser applications in manufacturing.

Silicon-based photodetectors for high-speed integrated optical receivers

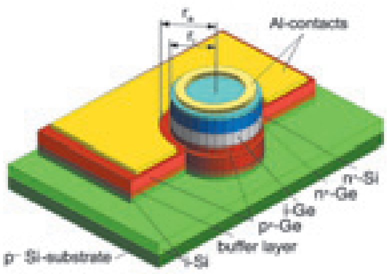

One of the main tasks of communication engineering is to provide the transmission of a certain amount of data over a long distance in a short period of time. We all use electrical and wireless data transmission systems day by day but one of the oldest methods to transmit information is using light signals. Simple fires, light houses, a mirror to reflect the sunlight or a torch. The amount of data to be transmitted and also the data rate is rather limited, of course. The real revolution in optical data transmission was caused by the commercial use of optical fibers in the 1980ies.

With the optical fibers it was possible to transmit digital data between continents on commercial transmission lines with data rates from several Mbits/s up to several Gbit/s nowadays. Actually, in laboratory experiments the transmission of more than 10 Tbit/s over a single fiber was demonstrated. A single ISDN phone call requires only 64 kbit/s. The maximum data rate of these systems is mainly limited by the electronic circuits in the transmitter and receiver, not by the fiber itself. Therefore the main interest of the researchers is to develop faster electronic components. On the other hand, the open market forces the researchers to develop cheap components, which is contradictory in a way.

1. Silicon and Germanium as detector material

One solution to get fast and cheap devices is to use the well established silicon based technology for integrated circuits and just add the photodetector in the same process. This allows fabricating fully integrated pure Silicon photodetectors in a commercial CMOS process that work at data rates up to some Gbit/s. An example of a 2 GBit/s CMOS-receiver with integrated photodiode and preamplifier designed at the Institut für Elektrische und Optische Nachrichtentechnik (INT) is shown in **(01)**. This receiver can be used in plastic optical fiber (POF) links that work in the visible range or can be integrated e.g. together with a processor core for fast optical memory access.

The optical fiber communication systems operate in the infrared region, mostly at 1.5 µm and in some cases at 1.3 µm. There are so called transmission windows of the fibers with low absorption allowing long distance transmissions. But Silicon photodetectors are able to detect light only in the visible range (wavelength from 0.4 µm to 0.8 µm) up to a wavelength of approximately 0.85 µm. Thus Silicon photodetectors are not suitable for infrared light even though highly desired due to the monolithic integration with complex circuits.

In recent years, the element Germanium was added to pure Silicon to improve significantly the performance of transistors, which are key elements in electronic circuits. The so called SiGe-technology is very fast and more cost-efficient than other technologies used for high-speed circuits, e.g. GaAs or InP. Another advantage of Germanium is the ability to detect light with wavelengths up to 1.6 µm.

Using the compound semiconductor Silicon-Germanium (SiGe) the absorption coefficient in the infrared region rises with higher Germanium contents. Pure Germanium absorbs photons of 850 nm 65 times better than pure Silicon. An overview of the absorption of some common semiconductor materials is shown in **(02)**.

Pure Germanium is well suited for photodetectors in fiber optical communication systems, but there are some restraints in combination with the Silicon technology.

First of all the growth of a Germanium layer on a Silicon substrate is very sophisticated due to the lattice mismatch of about 4 percent. Only thin Germanium layers up to some nanometers grow perfectly but are strained. If the thickness increases, the layers are relaxed but the density of defects and dislocations increases. A modified process, developed at the Institut für Halbleitertechnik (IHT) at the Universität Stuttgart [2], uses low temperature growth to force the defects to arise at the materials interface and not in the Germanium bulk. This was a very important step in order to get good device properties.

The second restraint is the dark current. The basic physical structure of a photodetector device is a pn-diode with an intrinsic absorber material between the p- and n-region. This pin-photodiode is operated in reverse bias, i.e. in an ideal device the current is negligible when there is no light. Actually, in real devices there is a current even when there are no photons – the so called dark current.

One part of the dark current is the diffusion current caused by carriers entering the intrinsic region driven by diffusion. This part is proportional to the square of the intrinsic carrier density of the material which is $2.5 \cdot 10^{13}$ cm^{-3} in Germanium and $1.6 \cdot 10^{10}$ cm^{-3} in Silicon. Thus Germanium photodiodes will have a dark current which is about six orders of magnitude higher than in Silicon.

The other part of the dark current is the recombination current which depends on the crystal quality of the material. As mentioned, there is a lattice mismatch between the Silicon and the Germanium crystal introducing defects that feed this recombination current. The recombination current is furthermore proportional to the intrinsic carrier density and to the thickness of the intrinsic absorber region.

In **(03)** the current versus voltage characteristic of a SiGe photodiode designed at the INT and fabricated at the IHT is shown. With increasing reverse voltage the dark current (solid line) raises some orders of magnitude. With illumination at 1298 nm with a power of about 1 mW, the photodiode delivers a photocurrent (dashed line) of about 0.1 mA. The dark current may be completely avoided if the photodiode works at low bias voltages or even without it (zero bias operation). The photodiodes realized by the mentioned cooperation of IHT/INT proved their ability to be operated under zero bias conditions. This was obtained by a proper choice of thickness

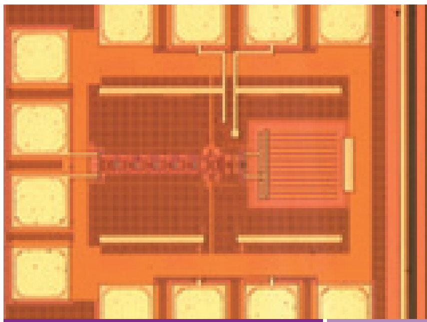

01

Optical CMOS-receiver with fully integrated photodiode for 2 Gbit/s [1].

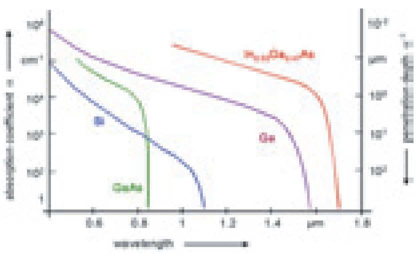

02

Absorption coefficients and penetration depth of common semiconductor materials [3].

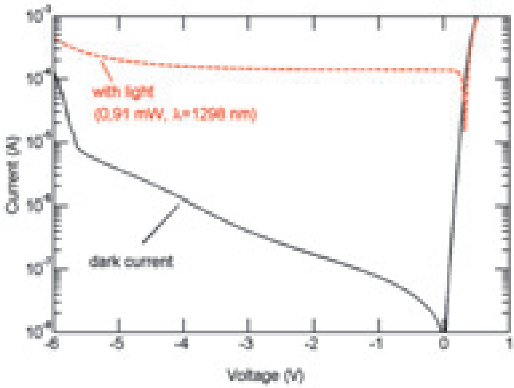

03

Current versus voltage characteristic of a SiGe photodiode designed at the INT and fabricated at the IHT with (dashed line) and without (solid line) illumination at 1298 nm.

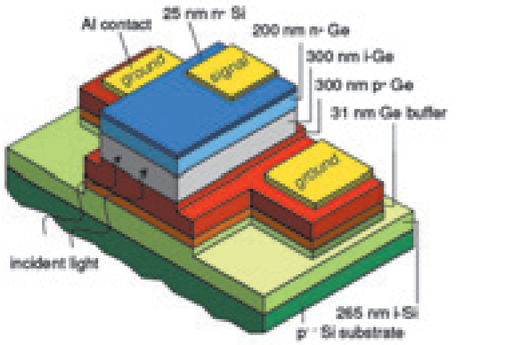

04

SiGe waveguide detector [4].

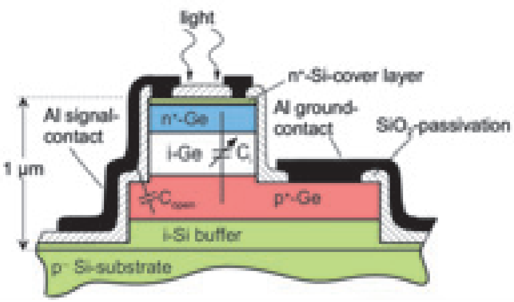

05

Cross section of a Ge on Si pin-detector.

and doping of the device to extend the space charge layer across the absorbing region only by the built-in potential.

The quantum efficiency, i.e. the ratio of generated electrons in respect to the total number of incoming photons, is 23 percent at 850 nm, 16 percent at 1300 nm and 3 percent at 1550 nm. This is, of course, far away from the desired 100 percent. One reason for this is the absence of an antireflection coating, thus approximately one third of the incident light is lost by Fresnel reflection at the detector's surface. Another limitation is the thin absorber region, which is only 300 nm in this device. The longer the wavelength the more light passes trough the intrinsic region, because the absorption coefficient gets smaller and smaller towards the infrared.

2. Lateral or vertical structures?

Commonly the photodetector is grown layer by layer on a substrate and the light hits the detector perpendicularly to the surface. This is a vertical structure and the coupling of the light is easy – just by placing a lens or a fiber above the detector. Furthermore, each detector can be tested during the manufacturing process without cutting the wafer. This is an important point for cost reduction during fabrication.

But to overcome the poor sensitivity due to weak absorption in the thin layers of vertical diodes, so called waveguide photodetectors were build. Here the absorber is shaped as a thin, narrow but very long rectangular waveguide. The light travels parallel to the surface through the detector structure and the absorption length can be up to some millimeters, depending on the length of the waveguide.

A waveguide is formed by a region with a high refractive index, which is surrounded by a material with lower refractive index. In a SiGe compound the refractive index increases with increasing Germanium content. This effect can be used to build up waveguide detectors based on the SiGe material. An example of a SiGe waveguide detector is shown in **(04)**.

The light is coupled to a waveguide made of a 300 nm pure Germanium layer. To inject the light into the waveguide a lateral facet has to be created. In order to make the waveguide accessible for fiber coupling, first the waveguide of the diode is cut perpendicularly to the wafer surface with a dice saw. After this first step, the waveguide has a length of several hundred micrometers. Scanning Electron Microscopy (SEM) inspection reveals a considerable roughness of the end facet resulting in high coupling losses. In a second step two tilted cuts perpendicular to the end facet are performed. This cutting procedure yields a triangular, prism shaped cantilever, which is broken off. Now the waveguide has a length of approximately 30 µm and exhibits a smooth end facet.

As the fabrication and the coupling of the light to the detector are difficult, we returned to the vertical structure. A schematic cross section of this is shown in **(05)**.

The basis is a Silicon substrate with a doping concentration as low as possible to avoid high-frequency losses. The detector consists of a 300 nm p^+-doped contact layer, a 300 nm absorber layer and a 200 nm n^+-doped contact layer. A thin n^+-doped Silicon layer improves the top ohmic contact. In terms of speed and time required for growth of the layers, a thin absorber of only a few 100 nm is favorable. Then a Germanium content of close to 100 percent is necessary to get enough sensitivity.

The structure of the complete detector needs only two etching steps. First a mesa is etched out of the n^+- and the intrinsic Germanium. The etching depth has to be controlled precisely not to hurt the p^+-Ge contact layer. If so, this would thin out the p^+-Ge contact layer and increase its resistance leading to a degradation of the detector's RC-time constant.

A second etching process structures the p^+-contact. It is removed partially to reduce the capacitance C_{open} to the overlap capacitance of the Aluminum signal trace and the p$^+$-Ge contact as shown in **(05)**. By this step of the process, the total device capacitance is reduced close to the intrinsic diode capacitance C_i. The pin-structure is isolated by a 500 nm Silica (SiO_2) layer with windows opened for the metallic Aluminum contact.

A top view REM picture is shown in **(06)**. The two steps of the mesa etch are apparent as outer circles. The signal contact is a thin Aluminum ring surrounding the active area. The minimum vertical dimensions are determined by the epitaxial growth of the layers, the lateral dimensions are not critical.

For a proper design of the devices, models are needed to simulate the behavior of the devices. An example of a small signal equivalent circuit used to simulate the SiGe pin-photodiode is shown in **(07)**.

The current source I_{ph} represents the conversion of the incoming photons to a photocurrent. The internal capacitance C_i is caused by the space charge region that depends on the applied external voltage. The differential resistance R_i is used to model the dark current in reverse bias. As the dark current depends on the bias voltage, the differential resistance R_i is voltage dependent, too. Those three elements form the inner or intrinsic diode. All other effects caused e.g. by interconnections and contact pads are represented by the series resistance R_S, the inductance L_d and the complex impedance Z_{open}, respectively.

The device is connected to a measurement system with an input impedance R_0 of typically 50 Ω. If too large, the junction capacitance C_i and the impedance R_0 are the reason for a severe RC limitation of the bandwidth. Most of all the voltage dependent capacitance C_i has to be as small as possible. The capacitance saturates at high reverse voltages at its minimum, given by the thickness of the intrinsic region and the diode area. On the other hand, high reverse voltages cause large dark currents, as explained before. Thus the saturation voltage of C_i has to be kept as small as possible by a low background doping level of the intrinsic material.

Another limitation is the time it takes the carriers to transit the intrinsic region. The minimum time is given by the saturation drift velocity, which is a material constant, and the thickness of the intrinsic region. Taking only the transit time into account, the absorber has to be as thin as possible – but this results in a large capacitance C_i. In an optimized structure a compromise of RC-limitation and transit time is found, when the transit time and the RC time constant are equal. The calculation is illustrated in **(08)** using the material parameters of Germanium and three different detector areas.

The RC-bandwidth f_{RC} increases linearly with the thickness of the intrinsic layer, assuming a constant detector area. The transit frequency f_T is independent of the area and decreases with thickness of the intrinsic layer. The intercept point of transit and RC frequency denotes the optimum thickness.

Both frequencies together define the total 3-dB-frequency f_{3dB} of the detector. As can be seen in **(08)**, a high bandwidth can only be obtained with very thin absorber regions and small detector areas. On

SUMMARY

One of the oldest methods to transmit information is using light signals. But the substantial break trough in optical data transmission was caused by the availability of optical fibers in the 1980ies. Then it was possible to connect countries and even continents by long distance optical transmission lines. The maximum data rate of these systems is mainly limited by the electronic circuits in the transmitter and receiver, not by the fiber itself. Therefore the main interest of researchers is to develop faster electronic components. To be competitive and to open new fields of applications e.g. in multimedia systems in upper class cars the components must be economically priced.

Thus it is important to realize sophisticated designs with standard technologies and not standard designs with expensive technologies, whenever it is possible. Unfortunately, most photodetectors suitable for the infrared wavelengths of fiber optical communication links are made of Gallium-Arsenide that requires an expensive technology.

In a joint project of the Institut für Halbleitertechnik and the Institut für Elektrische und Optische Nachrichtentechnik, both at Universität Stuttgart, structures and processes for the fabrication of fast photodetectors were developed that combine the well established Silicon-technology with the good infrared absorption properties of Germanium. The realized devices feature a bandwidth of 39 GHz, which is up to now the highest bandwidth reported for such structures.

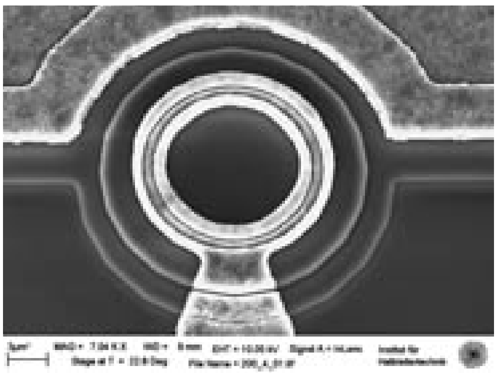

06

REM picture of a Germanium on Silicon pin photodiode.

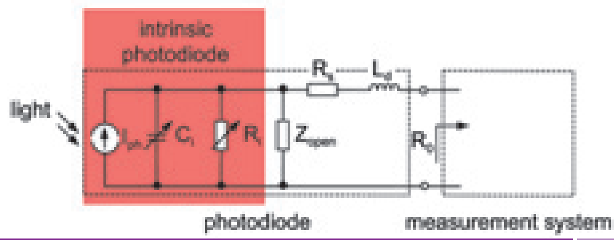

07

Small signal equivalent circuit of the SiGe pin-diode.

ZUSAMENFASSUNG

Eine der ältesten Methoden zur Informationsübertragung ist das Senden von Lichtsignalen. Der wirkliche Durchbruch der optischen Datenübertragung kam jedoch erst mit der Verfügbarkeit von Glasfasern in den 1980ern. Damit war es möglich, Länder und sogar Kontinente über optische Weitstreckenverbindungen zu verkabeln. Die maximale Datenrate dieser Systeme ist hauptsächlich durch die elektronischen Schaltkreise im Sender und Empfänger begrenzt, nicht so sehr durch die Faser selbst. Daher liegt das Hauptinteresse der Forscher in der Entwicklung immer schnellerer elektronischer Komponenten. Um wettbewerbsfähig zu bleiben und auch neue Anwendungsgebiete zu eröffnen, wie z.B. Multimedia-Systeme in Oberklasse-Wagen, müssen die Komponenten preiswert sein.
Daher ist es wichtig, wann immer möglich ausgeklügelte Entwürfe in Standard-Technologien zu realisieren anstatt in sehr teuren Technologien Standard-Entwürfe umzusetzen. Leider sind die meisten Photodetektoren, die sich für die infraroten Wellenlängen der faseroptischen Kommunikationsverbindungen eignen, aus Gallium-Arsenid gefertigt, was eine teure Technologie erfordert.
In einem Verbundprojekt des Instituts für Halbleitertechnik und dem Institut für Elektrische und Optische Nachrichtentechnik, beide Universität Stuttgart, wurden Strukturen und Prozesse zur Herstellung von schnellen Photodetektoren entwickelt, die die etablierte Silizium-Technologie mit den guten Absorptionseigenschaften des Germanium im Infraroten verbinden. Die gefertigten Bauelemente bieten eine Bandbreite von 39 GHz, was der derzeit höchste Wert ist, der berichtet wurde.

the other hand this results in reduced quantum efficiency and requires tighter tolerances for the alignment of the fiber. The detector shown in **(06)** has a diameter of 10 µm which results in an optimum thickness of 300 nm. The theoretical 3-dB frequency limit is then about 40 GHz.

3. State of the art

To get a real device with a bandwidth as close as possible to the theoretical limit, a sophisticated growth process and an optimized design of geometry and layout are necessary.
The main challenges are
- to grow a pure Germanium absorber layer with low defect density and optimum thickness on a Silicon substrate;
- to control the background doping of the intrinsic layer for a low reverse bias voltage;
- to reduce parasitic capacitances by an optimized layout.

(09) shows the measured results of the state of the art Germanium on Silicon pin-diode with a 3-dB frequency of 38.9 GHz at a modest reverse bias of -2 V [5]. The diameter of the device is 10 µm. For comparison, the data for devices of 20 µm and 30 µm diameter are also shown.
Even as important, high frequency limits (28 GHz) were also obtained with zero bias operation. The slight decrease in 3-dB frequency is caused by a higher internal capacitance.

4. The future

Germanium photodiodes monolithically integrated on Silicon substrates feature large bandwidth and a high potential for future optoelectronic systems based on Silicon. They can be used for long distance point to point transmission as well as for parallel data transfer in optical subsystems of computers or even for optical on-chip clock distribution.
For both fast, i.e. above 40 GHz, and highly efficient Ge-detectors new concepts have to be investigated. Some groups work with resonant structures, where the absorber is embedded between mirrors and the light is traveling several times through this layer. This extends the path, where the photons are absorbed without increasing the thickness of the absorbing layer. The quantum efficiency is several times better but the detector works well only at dedicated wavelengths because of the resonant structure.
Another idea is to combine the easy vertical coupling with the high efficiency of the waveguide detector by sophisticated coupling structures. The vertically incoming light perpendicular to the wafer's surface has to be forced to couple into a waveguide parallel to the wafer's surface. An approach for such a coupling structure

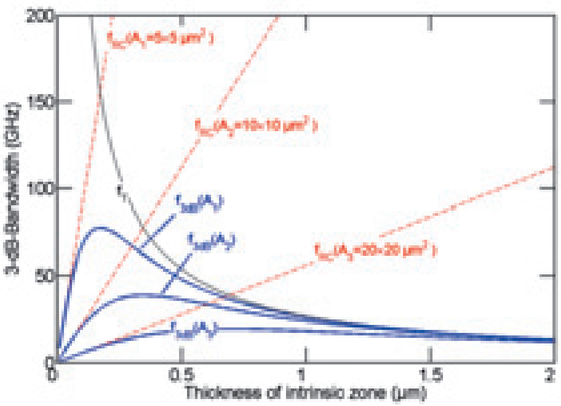

08

Theoretical 3-dB-frequency of an ideal pin photodetector.

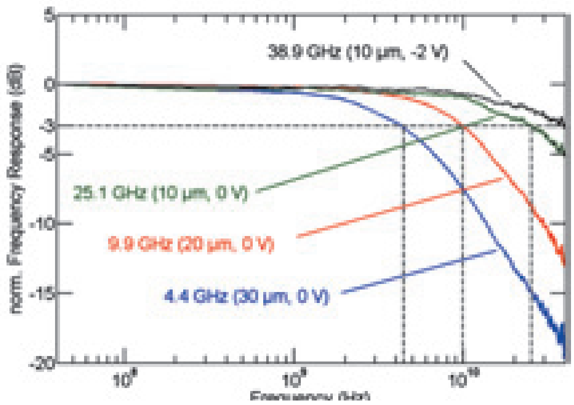

09

Measured frequency response of Germanium on Silicon pin-diodes with different diameters.

could be e.g. an integrated diffraction grating, which is investigated currently.

5. Acknowledgements

The presented article summarizes the results of a joint project of the Institut für Halbleitertechnik (IHT) and the Institut für Elektrische und Optische Nachrichtentechnik (INT), both at Universität Stuttgart, in the field of fast SiGe-photodetectors.

The vertical pin detector with a pure Germanium absorber on a Silicon substrate was designed and characterized at the INT; the processing was developed and performed by the IHT.

The authors would like to thank Wolfgang Vogel and Markus Grözing from INT and Michael Öhme, Gerd Wöhl and Klaus D. Matthies from IHT for their support and their work.

Manfred Berroth
Erich Kasper
Michael Jutzi

References

1 M. Jutzi, M. Grözing, E. Gaugler, W. Mazioschek, M. Berroth, 2-Gb/s CMOS Optical Integrated Receiver With a Spatially Modulated Photodetector, IEEE Photonics Technology Letters, Vol. 17, No. 6, 2005, pp. 1268–1270.

2 M. Bauer, C. Schöllhorn, K. Lyutovich, E. Kasper, M. Jutzi, M. Berroth, “High Ge Content Photodetectors on Thin SiGe Buffers”, Mater. Sci. Eng. B, Vol. 89, 2002, pp. 77–83.

3 See e.g. S. M. Sze, Semiconductor Devices Physics and Technology, John Wiley & Sons, 2001.

4 M. Jutzi, M. Berroth, G. Wöhl, M. Oehme, V. Stefani, E. Kasper, “Ge-on-Si Pin-Photodiodes for Vertical and In-Plane Detection of 1300 to 1580 nm Light”, 34th European Solid-State Device Research Conference, September 20–24, 2004, Leuven, Belgium, pp. 345–348.

5 M. Jutzi, M. Berroth, G. Wöhl, M. Oehme, E. Kasper, “Ge-on-Si Vertical Incidence Photodiodes with 39 GHz Bandwidth”, IEEE Photonics Technology Letters, Vol. 17, No. 7, 2005, pp. 1510–1512.

THE AUTHORS

Manfred Berroth

received the Ph.D. degree from the Ruhr-Universität Bochum in 1991 and became leader of the department “Devices and Circuits Development” at the Institute for Applied Solid State Physics in Freiburg, Germany, where he was engaged in the development of circuit simulation models for GaAs field-effect transistors and integrated-circuit design. Since 1996 he has been Professor and head of the Institute of Electrical and Optical Communication Engineering at the Universität Stuttgart. His research interests and activities are electronic and opto-electronic devices and circuits at high frequencies.

Contact *Institut für Elektrische und Optische Nachrichtentechnik*
Universität Stuttgart, Pfaffenwaldring 47, 70569 Stuttgart
Tel. +49 (0)711 685 67922
e-mail: berroth@int.uni-stuttgart.de, Internet: http://www.uni-stuttgart.de/int

Erich Kasper

received the Ph.D. degree in physics from the University of Graz, Graz, Austria, in 1971. He was active as a Scientist with the research laboratories of Telefunken, AEG and Daimler-Benz. Beginning in 1987, he was responsible for novel silicon devices and technology with Daimler-Benz Research, Ulm, Germany, with a main emphasis on SiGe/Si-based heterostructures for fast transistors (HBTs, MODFETs) and opto-electronic transceivers (ultra thin superlattices). Since 1993, he has been with the Universität Stuttgart, Germany, as Professor of Electrical Engineering and Head of the Institute of Semiconductor Engineering. His main interest is directed to silicon-based nanoelectronics, integration of millimeter-wave circuits, and SiGe/Si quantum-well devices.

Contact *Institut für Halbleitertechnik, Universität Stuttgart*
Pfaffenwaldring 47, 70569 Stuttgart
Tel. +49 (0)711 685 68003
e-mail: kasper@iht.uni-stuttgart.de, Internet: http://www.iht.uni-stuttgart.de

Michael Jutzi

studied electrical engineering in Lyon/France and Darmstadt and received his diploma from the TH Darmstadt in 1998. From 1999 to 2005 he worked as research assistant at the Institute of Electrical and Optical Communication Engineering at the UniversitätStuttgart, where he recently finished his Ph.D. thesis on Photodetectors on Silicon substrates. He is now with Tesat-Spacecom GmbH & Co. KG in Backnang, Germany.

Contact *Tesat-Spacecom GmbH & Co. KG*
Gerberstrasse 49, 71522 Backnang
Tel. +49 (0)7191 930 1305
e-mail: Michael.Jutzi@tesat.de, Internet: http://www.tesat.de

zurück zum Inhalt

Computer-generated holograms

A flexible way to control light

In most people's understanding, holograms are those marvelous pictures that, when illuminated properly, show three-dimensional objects as if they were really there. The perfect 3D-impression stems from the ability of holograms to reconstruct the very same light field that existed when the object was available. Thus, the eye that detects only the light field emitted from an object, cannot distinguish if the object is really present or not – if the light field is the same, it looks the same.

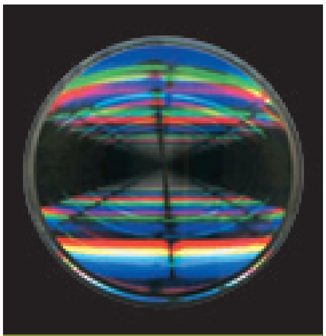

1. Introduction

Holography can do more than producing those decorative three-dimensional light fields. Since holograms give an exact optical replica of an object, they can be used as copies, e.g. of valuable, fragile, or historical objects. The holographic copy can be examined with optical methods just like the original, eliminating the need for having the original at hands.

The concept of reconstructing three-dimensional light fields with a flat element, the hologram, is very attractive for many applications. The working principle of holographic elements is diffraction on microscopically small structures created during the recording process. Other working principles in optics are refraction on smooth interfaces between two transparent media and reflection at mirror surfaces. Optical elements based on diffraction are often referred to as Diffractive Optical Elements (DOE).

Classical holograms can only record existing light fields, i.e. the objects that produce the light field must be physically existent. Computer generated holograms (CGHs) overcome this limitation. Here, the original object exists only in the computer. The light field that stems from the computer aided designed object can be computed and since the phenomenon of diffraction is well understood the microstructures forming the required hologram can be determined. With this data, the CGH is fabricated. Since the structure sizes are down to the order of a wavelength (e.g. 0.5 µm for green light), the fabrication process is quite challenging. The advances in semiconductor manufacturing such as optical lithography have helped a lot to produce such small structures with the required precision.

One of the first applications, where CGHs have been applied, is interferometric testing of aspherical surfaces. Here a CGH defines the ideal aspheric lens shape that is optically compared to the lenses that are actually polished. Section 2 gives more details.

The principle of creating a well defined light field with a computer generated hologram is not restricted to light fields generated by real or artificial objects. In fact, CGHs can manipulate light fields in a very general way. For instance, a CGH can be designed to focus an incoming plane wave. This kind of CGHs can be used instead of refractive lenses. They are called diffractive lenses, since their working principle, as of all holograms, is based on diffraction. Diffractive lenses are very sensitive to the illumination wavelength. This can be used to design systems that change their focal length according to the wavelength. In section 3, a topography measurement system based on this effect is described.

An even more general manipulation of light fields is necessary for pattern generation applications, where the light field needs to be designed such that a given intensity distribution appears in a certain distance. Typical useful intensity distributions can be squares, circles, bars, crosses, or even company logos. Also the creation of three-dimensional intensity distributions is possible. Section 4 describes an application where a pipe of light is required to confine very cold atoms.

In some cases it would be attractive to change the CGH in real-time, e.g. to create a varying light field. This is indeed possible using consumer digital light projection technology. In section 5 principles and components for realizing dynamic CGHs are explained. Applications for dynamic CGH are given in the subsequent sections, ranging from micro-material processing in section 6 over micro-manipulation with so called optical tweezers in section 7 to new approaches in wave front sensing in section 8.

2. Computer generated holograms in aspheric lens testing

One of the first applications of CGHs was in optical testing of aspheric lens surfaces. In 1970 the first CGH was proposed and only one year later it was suggested to use CGHs in interferometric testing of aspheric lenses [1][2]. Aspheric lenses are and have been very useful components for a lot of optical systems. They allow to improve the performance of a system while at the same time reducing the size and weight. A major drawback of aspheric lenses is that they cannot be tested as easily as the standard spherical surfaces. They need a so called null lens that optically exactly fits the asphere under test. In such a null test configuration, only the deviations of the asphere from its ideal shape are measured. This simplifies to measure very small deviations of the aspheric shape from its ideal shape down to a few nanometers or less.

The null lens defines the ideal shape of the asphere and therefore must be well known. For high precision measurements the whole setup must be calibrated. Here, CGH can be used. Since a CGH can be designed as the hologram of a perfect asphere, it can be placed at the position where the aspheric surface would be. It is then measured and since it represents an ideal aspheric surface, the measurement result should give zero. A non-null measurement result is due to imperfections in the interferometer or the null optic. So, for real measurements, we can subtract this calibration function.

This concept relies on a perfectly manufactured CGH. CGHs can be made with a very high precision, yet nothing is perfect, especially when a precision down to a few tens of nanometers is required. Therefore, calibration strategies have been developed that allow to determine the quality of the CGH also. For these methods the CGH is designed such that it can not only replace an aspherical surface but at the same time replace a spherical surface. For the measurement of spherical surfaces well known calibration methods exist, so the CGH can be calibrated using this auxiliary wave front.

3. Diffractive lenses for chromatic confocal microscopy

If we use a CGH in a wide, continuous spectrum of wavelengths, an intrinsic property of diffractive lenses shows up: Light of longer wavelength (e.g. red) is bent stronger than shorter wavelengths (e.g. blue). This property we have used to design a lens that varies its focal length depending on the wavelength. For many applications such as photography this so called longitu-

SUMMARY

Computer Generated Holograms (CGH) are a relatively new class of optical elements that allow a very general control of light fields not possible with conventional, refractive or reflective elements. We have shown a wide variety of applications that have been made possible with CGHs. A new and promising approach is the flexible generation of CGH with spatial light modulators (SLM). The possibility to change the holograms with video frequency or faster allows new applications such as one-shot micro material processing or flexible optical tweezers.

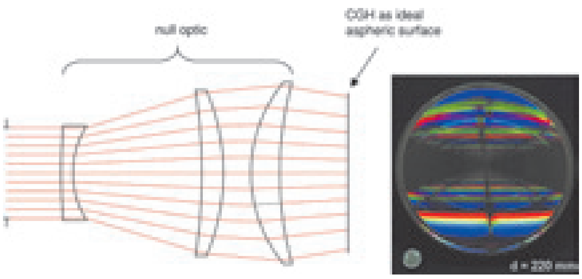

01

CGH replaces aspheric surface in the interferometric test setup. Left: test arm of the interferometer, right: CGH with a diameter of 220 mm and smallest structures below 1 µm.

dinal chromatic aberration is not desirable, since the image of say a white object gets blurred and shows colored edges. But imagine the object consists of blue parts and red parts and that the red parts are closer to the observer. This can be done by illuminating the white object on the far end with red and closer to the detector with blue light. In this case our specially designed CGH lens produces a sharp image of both parts of the object simultaneously. Although this does not really sound relevant for practical uses, it really is the basis for a very fast and robust measurement system: The chromatic confocal microscope. Here, the object is illuminated with a series of foci of different wavelengths at different focal lengths. A special aperture stop, the so called confocal pinhole, ensures, that only light from object parts that are in focus is reaching the observer. Therefore, one can see a colored image of the object, and the color in the image is directly proportional to the distance from the sensor. With a spectrometer, the color information is evaluated quantitatively. Altogether, this forms a flexible, robust, one shot height measurement system that can be miniaturized very well [4].

(02) shows a measurement example. CGH enable the wide measurement range and design flexibility of such systems. [5]

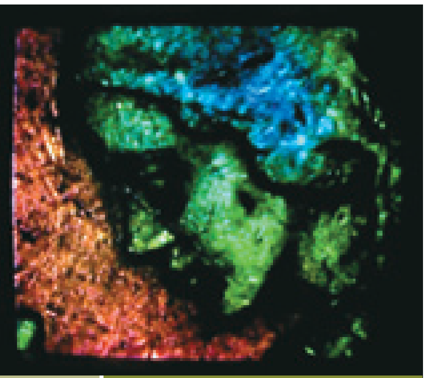

02

Detail of a coin, as seen by a chromatic confocal sensor. The height of the object is coded as color at each pixel. This allows one shot height measurements.

4. Manipulating matter with light: confining Bose-Einstein condensates

It is a fascinating effect, that microscopic particles feel a force in a light field with an intensity gradient. This effect can be used to trap matter in suitable light fields. Computer Generated Holograms are ideally suited to generate the necessary light fields. **(03)** shows the light field that is generated from a Gaussian laser beam with the help of a high efficiency CGH. In **(04)** experimental results of Bose-Einstein condensates travelling along the 1D path defined by the light pipe are shown. The condensate is trapped inside the dark area, which helps reducing the impact of the trapping light field on the condensate.

5. Dynamic computer generated holograms

We have so far only discussed applications that require static optical elements. By writing CGHs not permanently onto glass or other substrates but using a dynamic changeable medium of course a lot of new interesting applications become feasible.

Ideally one would like to have a modulator that can be used as a direct replacement for conventional DOEs written in glass. Unfortunately such devices are not available. Resolution is limited to about 10 microns, which is about a factor of ten worse than what one achieves with static DOEs, for all electrically addressable elements. Even worse, the number of addressable pixels lies in the range of only one to two million pixels. Compared to the billions of "pixels" that are stored on a conventional recorded hologram this is not very promising. Finally the light efficiency of the available modulators is quite bad (in the range of some ten percent). By using a dynamic DOE you are therefore losing a lot of light which is a problem for some applications.

In spite of these problems there are still applications where today's modulators are an interesting alternative to static systems. Before we show some of these applications we want to give an overview over the different types of modulator technology that are used for dynamic DOEs.

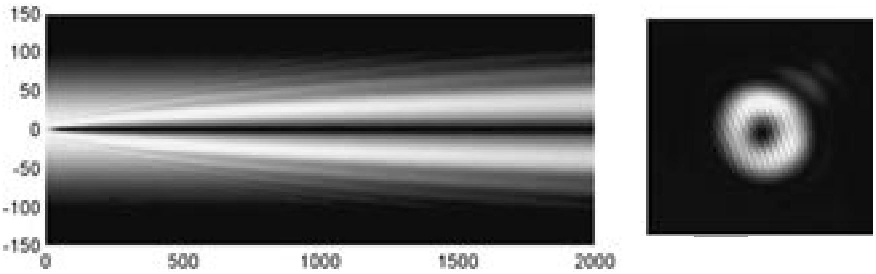

03

Light field generated with a CGH. The graph shows a cross-section of the light field immediately after the CGH, propagating from left to right. Well visible is the desired dark area on the optical axis. Right: Intensity in a plane parallel to the CGH.

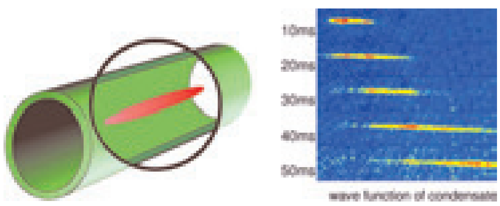

04

Bose-Einstein condensate trapped inside the light pipe. Left: schematic drawing of the geometry, right: Bose-Einstein condensate travelling along the light pipe.

Generally one has to distinguish between optically and electronically addressable elements. From the standpoint of usability of course electronic addressing is favorable. With a large (more than some hundred of thousands) number of pixels this unfortunately means that an active addressing matrix has to be used. For elements that work in transmission this results in a significant amount of space at the pixels that is used for the electronics and which results in an overall reduced transmission of the elements because at the position of the electronics (transistors, capacitors, and wiring) light transmission or modulation is not possible. The smaller the pixel size the more severe is the problem because one cannot shrink the addressing electronics below a certain limit of a few microns.

The solution to this problem is to use the light modulator in reflection. The addressing is done from behind so that a large effective area of the pixel really can be used optically. With liquid crystal displays these reflective elements today are mostly fabricated on a silicon basis. Therefore such elements are called LCoS (liquid crystal on silicon) displays.

Additionally it is often difficult (especially at long wavelengths) to achieve a full 2π phase modulation. This results in a reduced diffraction efficiency and the appearance of unwanted higher diffraction orders. In principle it is possible to design modulators that have a full 2π phase modulation but this is not advantageous for commercial amplitude modulating displays. Therefore if one wants to use consumer elements one has to live with an additional amplitude modulation and a reduced efficiency.

Another promising reflective modulation technology is based on micromechanical elements. Most noticeably are the so called digital micromirror devices sold by Texas Instruments. Unfortunately the Texas Instruments elements only modulate intensity. Therefore the diffraction efficiency is quite bad compared to – also available (but more expensive) – phase modulating devices.

Optical addressing completely circumvents the problem of the fill factor due to the electronics. On the other hand such elements somehow are exotic and are not manufactured for the mass market. Additionally the optical setup of a system is getting more complex and expensive since one needs an additional electronically addressable modulator for controlling the optically addressed modulator. A very rough comparison of the different available technologies is given in **(t01)**.

As is shown in **(05)** there are lots of disadvantages but only one advantage of modulator based DOEs compared to static DOEs. This advantage is of course the possibility to change the function of the DOE very fast (depending on the technology the maximum frequencies are between ten Hertz and a few thousand Hertz).

6. Dynamic CGH for micro material processing

(07) shows one example where this is employed. It is a setup for holographically writing structures on a microscopic scale into material. A laser is first expanded by a lens before it hits the modulator, in this case a 640 x 480 pixels Epson LCD panel.

After being modulated by the diffractive element written into the LCD the beam is Fourier transformed by the second lens. The Fourier transform of the light field behind the LCD is written into the material. By proper design of the DOE one can write more or less arbitrary patterns into the material. The pattern to be written is reconstructed by the lens. No mechanical scanning is necessary to change the patterns. All is done (even defocusing onto different depths) by electronic addressing of the LCD [7].

An example is shown in **(08)**. Compared with simple

ZUSAMMENFASSUNG

Computer-generierte Hologramme (CGH) werden heute in einer Vielzahl von Anwendungen als optische Elemente eingesetzt. Durch die Möglichkeit, Licht nahezu beliebig ablenken zu können, sind die Elemente sehr flexibel sowohl in Beleuchtungs- und Abbildungssystemen als auch in speziellen Messanwendungen einsetzbar.
Im Artikel werden verschiedene Spezialanwendungen von CGHs beschrieben. Insbesondere wird auf die Vermessung asphärischer optischer Flächen, die Vermessung von Wellenfronten und die konfokale Mikroskopie eingegangen. Ebenfalls besprochen wird die Möglichkeit, spezielle Lichtfelder zum Einfangen von Atomen, Zellen und mikromechanischen Teilen durch die CGHs zu generieren. Die CGHs können sowohl als statische Elemente (z.B. in Plastik oder in Quarz) als auch als frei programmierbare dynamische Elemente (basierend auf Flüssigkristalldisplays oder Mikro-elektromechanischen Systemen) realisiert werden.

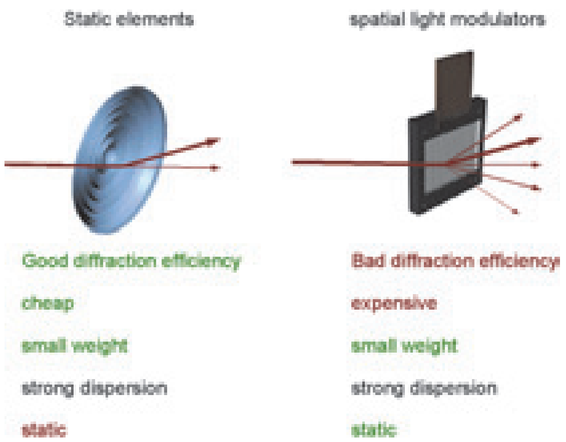

05

Static versus dynamic diffractive optical elements.

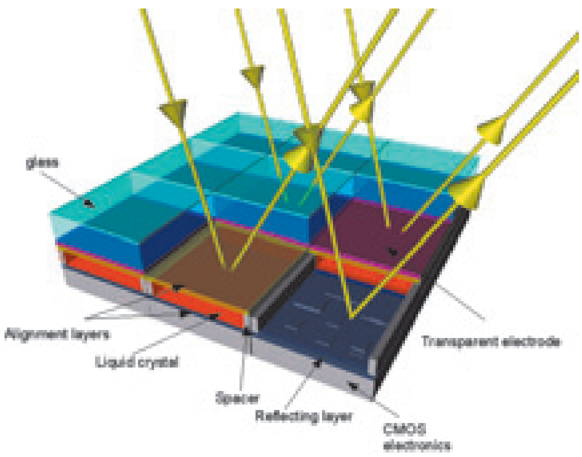

06

Liquid Crystal on Silicon (LCoS) reflective display.

Comparison of different SLM technologies

	OALCD	LCD in transmission	LCoS	DMD
Overall efficiency	30 … 40%	5 … 10%	5 … 20%	5.00%
Number of Pixels (Millions)	0.5...100	1 .. 2	1 .. 2	1 .. 2
Speed	30 Hz	50 Hz	200 Hz	10 kHz
Price (incl. addressing)	7000 EUR	1000 EUR	1000 EUR	2000 EUR

t01

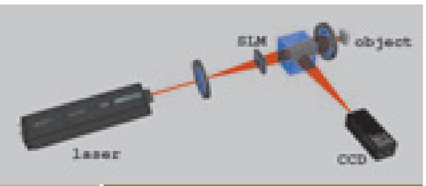

07

Holographic material processing with a dynamic hologram.

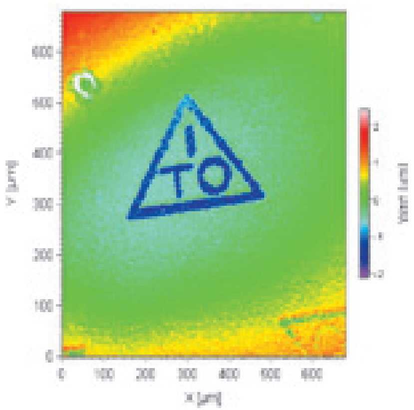

08

Holographic ablation of a pattern into Fe2O3 by a ruby laser.

imaging one saves a lot of energy because with pure imaging lots of the light (the black area of the pattern to be written) is lost because it will be filtered by the modulator. With the DOE approach this light is not lost. All the light falling onto the modulator is redirected (by diffraction) to the illuminated areas of the pattern. Still the efficiency is bad (only some ten percent) if we compare this with a mechanical scanning approach.

But getting rid of mechanical moving elements can be a great advantage especially if we work on the microscopic scale since precision and repeatability are greatly enhanced. An application where this turns out to be especially important are optical tweezers.

7. Dynamic optical tweezers

Again, a light modulator is used in the Fourier plane as shown in **(09)**. It is a setup for manipulating (trapping and moving) small particles like cells or microsystem parts. By changing the holograms (computation of the holograms is possible in video real-time) one can control a lot of traps, as shown for 7 particles in **(10)** (up to 100 is feasible) in three dimensions without mechanical motion and with high repeatability. Additionally by adapting the hologram it is possible to correct for aberrations caused by the optical system or the specimen [8].

8. Wavefront sensing with adaptive CGH

Another application of spatial light modulators lies in the field of wave front sensing. The Shack-Hartmann sensor is used to measure a wave front in a wide range of applications such as adaptive optics in astronomy, laser beam analyzers and non-contact measurements.

The conventional sensor consists of a static microlens array and a camera. In the adaptive sensor **(11)** the static microlens array is replaced by a spatial light modulator (2) that displays freely programmable diffractive microlenses. The wave front to be measured (1) is sampled by the array of microlenses (2) and brought to focus on the detector device (3). The displacements of the foci in comparison to the position of the focuses of a plane wave are proportional to the local wavefront tilts which are used to calculate the measured wavefront shape. In our example, beam (B) is clearly tilted because of the displacement of the focus (green arrow) on the detector device.

The use of an dynamic element makes the adaptive sensor very flexible. Sensor parameters such as focal length, aperture size and number of microlenses can be modified according to the measurement task. A long focal length of the microlenses, for example, favors measurement precision but limits the maximal measurable wave front slope [9].

In addition, the measurement restrictions of the conventional sensor concerning maximum measurement dynamic and accuracy can be overcome by adapting the microlenses to the wave front to be measured. It is, for example, possible to correct wave front aberrations which makes the determination of the exact focus position in the static sensor impossible.

Tobias Haist, Christof Pruss, Wolfgang Osten

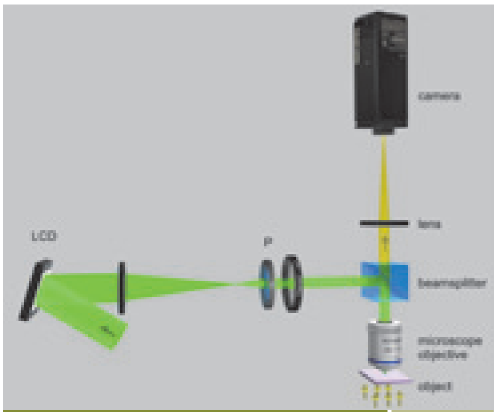

09

Setup for a holographic tweezers systems.

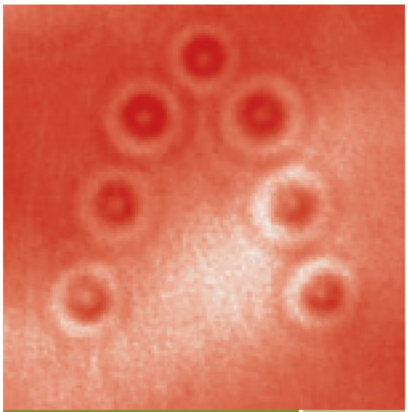

10

Trapping of seven particles by holographic tweezers.

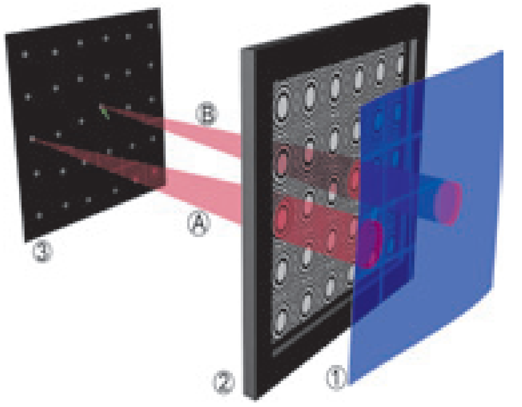

11

Adaptive Shack Hartmann sensor with exemplary beam propagation: 1) wave front, 2) transmissive SLM, 3) detector device with focuses from the microlens array, A) untilted beam of a single microlens, B) tilted beam of a single microlens.

References

1 J. MacGovern and J. C. Wyant, Applied Optics 10(3), 619 (1971).
2 F. Fercher and M. Kriese, Optik 35(2), 168 (1972).
3 S. Reichelt, C. Pruss, and H. J. Tiziani: *Absolute interferometric test of aspheres by use of twin computer-generated holograms.* Applied Optics, 42(22):4468–4479 (2003).
4 A. K. Ruprecht, C. Pruss, H. J. Tiziani, W. Osten, P. Lücke, A. Last, J. Mohr, P. H. Lehmann: *Confocal micro-optical distance sensor: principle and design*, Proc. SPIE, 5856–15 (2005).
5 C. Pruss, A. Ruprecht, K. Körner, W. Osten, P. Lücke: *Diffractive Elements for Chromatic Confocal Sensors*, in: DGAO-Proceedings, www.dgao-proceedings.de (2005).
6 M. Schiffer, M. Rauner, S. Kuppens, M. Zinner, K. Sengstock, W. Ertmer: *Guiding, focusing, and cooling of atoms in a strong dipole potential*. Applied Physics B67, 705–708, (1998).
7 T. Haist, E.U. Wagemann, H.J. Tiziani: *Pulsed-laser ablation using dynamic computer-generated holograms written into a liquid crystal display*. Journal of Optics A 1, 428–430, (1999).
8 M. Reicherter, M., Liesener, J., Haist, T., Tiziani, H. J.: *Advantages of holographic tweezers*. Proc. SPIE Vol. 5143, (2003).
9 L. Seifert, H.J. Tiziani, W. Osten: *Wavefront reconstruction algorithms for the adaptive Shack-Hartmann sensor*. Proc. SPIE 5856, 544–553, (2005).

Contact
Institut für Technische Optik, Universität Stuttgart
Pfaffenwaldring 9, 70569 Stuttgart
Tel. +49 711 685 6074, Fax +49 711 685 6586
E-mail: info@ito.uni-stuttgart.de
Internet: http://www.uni-stuttgart.de/ito/index.html

THE AUTHORS

Tobias Haist

studied physics and obtained his doctoral degree in engineering (Ph.D.) at the Universität Stuttgart. Currently he is leading the group "Active optical systems" at the Institut für Technische Optik where he is working on new applications for spatial light modulators. His main research interests are optical and digital image processing, computer-generated holography and optical measurement systems.

Christof Pruss

received his diploma in physics from the Universität Stuttgart, Germany, in 1999, and his MSc from the University of St. Louis in 1997. In 1999 he joined the Institut für Technische Optik, Universität Stuttgart. Since 2002, he leads the group "Interferometry and Diffractive Optics" at the institute. His main interest is in the field of aspheric testing and in the design and fabrication of diffractive optics.

Wolfgang Osten

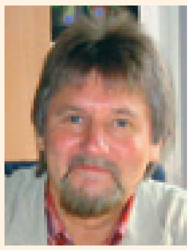

received his BSc from the University of Jena in 1979. From 1979 to 1984 he worked at the Institute of Mechanics in Berlin. In 1983 he received the PhD degree from the University of Halle in the field of holographic interferometry. From 1984 to 1991 he was employed at the Central Institute of Cybernetics and Information Processes, Berlin, making investigations in digital image processing and computer vision. Between 1991 and 2002 he was employed at the Bremen Institute of Applied Beam Technology (BIAS) as the head of the Department of Optical Metrology. Since September 2002 he has been a professor at the Universität Stuttgart and director of the Institut für Technische Optik. He is concerned with new concepts in industrial inspection by combining modern principles of optical metrology and image processing.

zurück zum Inhalt

Atom optics

Coherent atom sources and applications

Besides traditional light optics, matter-wave optics gains more and more importance. By means of appropriate optical elements (lenses, mirrors, etc.), researchers in this field influence and control the motion of particles, ranging from electrons, neutrons, neutral atoms, ions up to macroscopic bio-molecules. A well known example are

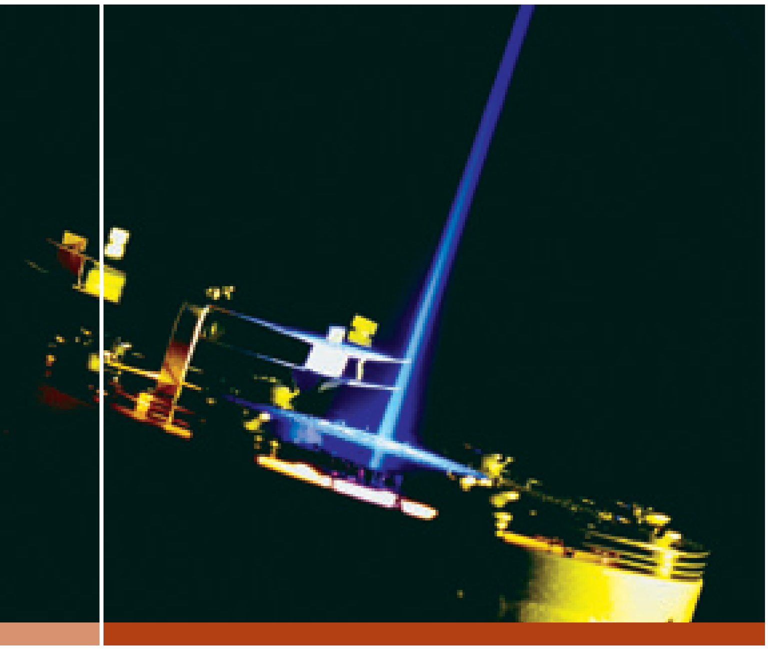

electron beams which are commonly used in electron microscopes to image sub-nanoscale structures, or in electron beam lithography to modify surfaces on an atomic scale. The concepts of light optics were recently transferred also to atom optics (see e.g. ref. 1). Mechanical gratings, conservative potentials generated by light, magnetic or electric fields are used to realize optical elements like lenses, mirrors, beam splitters, waveguides and atomic traps (atom resonators). The role of light and matter gets interchanged in atom optics. Light is used to manipulate matter, whereas in light optics, matter is used to manipulate light. Both photons and atoms, show particle- and wave-like properties. For an atom the wavelength is given by the de Broglie wavelength (λ_{dB}=h/(m v), where h, m and v are Planck's constant, the particle mass and the velocity) and for a photon the momentum is given by p=h/λ, where λ is the light wave length.

SUMMARY

In the past few years, atom optics has rapidly gained importance and belongs nowadays to the central topics of modern optics. Atom optics combines techniques, which allow to manipulate the trajectories of atoms. Hereby, potentials generated by light, magnetic or electric fields, provide optical elements like lenses, mirrors and beam splitters. In many cases, techniques known from classical light optics can be directly adopted to atom optics. Moreover, further properties of atoms including internal structure, mass and interaction between atoms lead to new optical elements that have no counterpart in light optics.

Dissipative elements allow slowing down, cooling and trapping of atoms. Advances in cooling techniques enable researchers to achieve Bose-Einstein condensation in trapped atomic gases. The phase transition from a thermal gas of identical bosonic atoms to a Bose-Einstein condensate occurs at very low temperatures ($T<1\mu K$) as soon as the extension of the quantum mechanical wave packet describing an individual atom, exceeds the interatomic separation. The gas becomes a macroscopic quantum object, which is characterized by a single wave function. A very similar behavior can be observed at the laser threshold in a light laser. According to a laser beam, a beam of coherent atoms coupled out of a Bose-Einstein condensate is called an atom laser beam.

Bose-Einstein condensates represent ideal and very flexible model systems which are used to study very diverse physical problems. Atomic quantum gases are well accessible since they can be observed by CCD-cameras besides being handled and controlled using atom optical elements. Interactions between the atoms lead to a Kerr-nonlinearity like it is known from nonlinear optics. Thus, e. g. four wave mixing and matter wave amplification can be observed in these gases. Whilst this article stresses analogies between light optics and atom optics, recent research on Bose-Einstein condensates goes beyond the scope of optics.
Measurements with condensates in periodic three-dimensional optical lattices are used to address solid state phenomena and problems. Recent studies of high-temperature superconductivity on the basis of data obtained from degenerated fermionic atomic quantum gases show that atom optics has developed to very interdisciplinary field of research.

1. Introduction

The field “atom optics” started in the early 1920s, when Stern and Gerlach showed that inhomogeneous magnetic fields exert a force on atomic magnetic moments. Already in 1927 Stern could demonstrate the reflection and diffraction of atoms from a metal and a crystal. In 1933, Frisch showed that an atomic beam can be deflected by light pressure. The first demonstration of a magnetic lens succeeded in 1951 by Friedburg and Paul. It took until 1978 when Bjorkholm and coworkers focused for the first time an atomic beam in a near-resonant co-propagating laser beam. Nowadays, atom beams and trapped atom clouds have become workhorses in modern atom optics. New cooling techniques involving light forces and atom evaporation enable researchers to obtain trapped atomic samples, with temperatures extremely close to zero Kelvin. It enables researchers to observe a phase transition to a new state of matter “Bose-Einstein condensate”, which occurs in bosonic gases in this temperature regime. This step which was awarded with a Nobel price in 2001 is comparable to the step from a thermal light source to a coherent laser source, in which a macroscopic number of bosonic photons occupy the same state. It made coherent atom sources and giant matter wave functions accessible for atom optics.

Despite of many common properties, there are lots of fundamental differences between atoms and photons. In contrast to photons, the atoms possess rest mass and have velocities well below the speed of light. These velocities are adjustable through atom optical methods. The quantum statistics of both, photons and atoms is determined by their spin. Photons have integer spin and thus obey the Bose-statistics. Unlike that, atoms (e.g. different isotope or different elements) have either integer or half-integer spin depending on the number of elementary particles of which they are composed, and thus obey either Bose- or Fermi-Dirac-statistics. By choosing fermionic isotopes measurements with degenerate fermionic quantum gases become possible. The internal structure of an atom enables to generate a huge variety of new tools, which are not known from light optics. Moreover the interaction between the atoms causes an additional nonlinear term in the wave equation, which is formally equivalent to the Kerr non-linearity in a non-linear material. Like in light optics, four wave mixing, solitons as well as up- and down conversion have been observed. Very exciting are experiments which combine Bose-Einstein condensates or degenerate Fermi gases with periodic optical lattices. Since in this model system both the periodic potential and the interaction of the gas can be easily adjusted, it is ideally suited to address basic solid state problems.

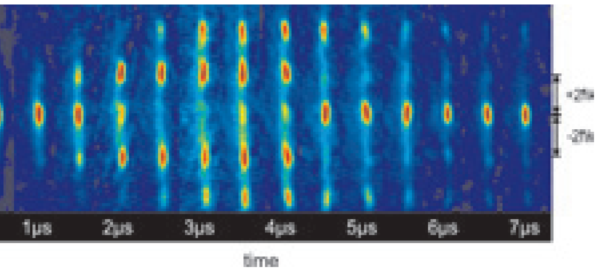

01

Diffraction of a rubidium matter wave in a one-dimensional optical lattice depending on the interaction time between lattice and matter wave.

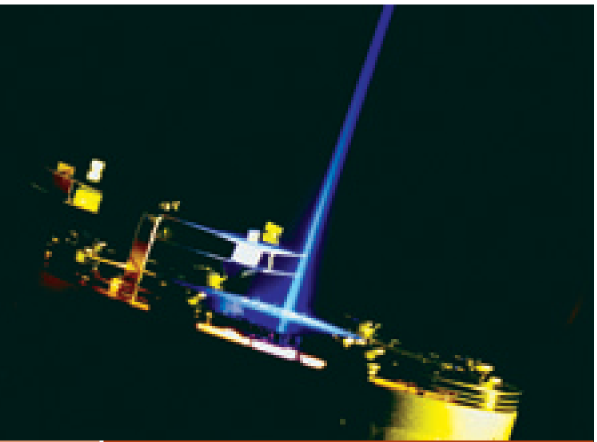

02

Thermal beam of chromium atoms illuminated by resonant laser light above a high temperature effusion cell.

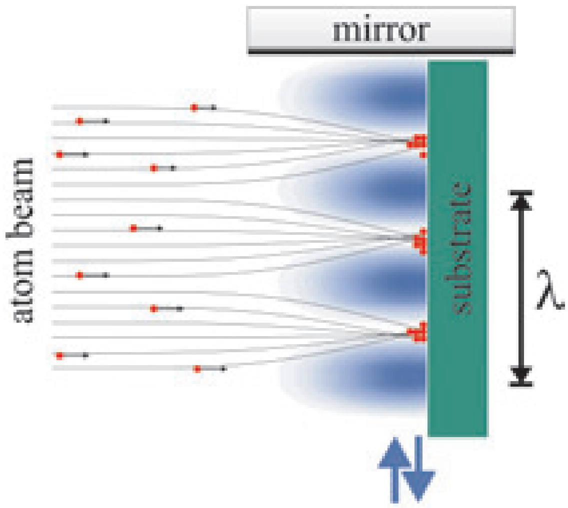

03

Principle of atom lithography: A standing blue detuned light wave created by a back reflected laser beam with the wavelength λ, focuses atoms of an atom beam onto lines on the substrate. The generated atom lines are separated by λ/2.

E.g. **(01)** depicts diffraction of a matter wave in a one-dimensional optical lattice. In the following we want to stress analogies and differences between light and atom optics and discuss exemplarily a few recent experiments of our group.

2. Atom lithography

The resolution of a far-field optical instrument is typically limited by refraction to half the wavelength of the applied light. Since the de Broglie wavelength of a thermal atom beam is typically only a few picometers and is thus comparable to x-ray radiation, one should in principle achieve resolutions well below the resolution limit of light optics. Lenses in atom lithography can be realized for instance by using the interaction of near resonant laser light and the light induced dipole moment of an atom. Depending on the laser frequency with respect to the atomic transition (detuning of the laser), the atoms are forced into high or low intensity regions of the light field. Many light field configurations result in approximately harmonic optical potentials that are ideally suited for atomic lenses. For instance, a standing optical light wave in front of a surface as depicted in **(03)** is a perfectly spaced array of cylinder lenses, which can be used to nano-structure the surface over a large area. In the experiment depicted in **(03)**, a collimated chromium atom beam of a thermal source **(02)** is directed onto a surface. The atoms are focused into the nodes of the blue detuned standing wave. If the substrate is placed in the focal point of the lenses, the atoms are deposited in lines on the surface with a line spacing of λ/2. We were able to structure the surface with a structure width of 50 nm in one and two **(04)** dimensions. The atomic lenses are extremely flexible and can be modified during the deposition. This method is especially applicable to periodic patterns. Non-periodic structures require more complex light masks and are harder to produce, but have been demonstrated by holographically generated light fields. Multilayer light masks which correspond to lens systems promise optimized atomic images.

In this respect, atom lithography is an example which shows a close analogy to the classical ray optics. However, light lenses for atoms possess unique properties, which lead to specific strengths of atom lithography in nanofabrication. Since the lenses rely on the resonant interaction between light field and the atoms, the lens is extremely element and even isotope selective. It becomes possible to produce different structures of different elements simultaneously. This property allows growing of materials that are nano-structured in three dimensions **(05)**. Hereby at least two materials – a light field sensitive dopant and a non-sensitive host material – are simultaneously deposited. During the deposition process, the light mask will only focus the dopant and leave the host material unaffected, which will lead to a homogenous growth of the host material. By moving or rotating the surface, nano-tailored matter can be produced which has been discussed in the context of photonic crystals. The interplay of the internal structure of the atoms and polarization gradients in the light field is another feature that can be used to modify the properties of the lenses and reduce the structure spacing below λ/2. A third aspect is the dissipative force arising from absorption and emission of photons. Atomic lenses cannot only focus atoms, they can at the same time cool their motional degree of freedom. A more detailed overview on the activities can be found in ref. 2.

3. Coherent atom sources

The experiments discussed up to here are carried out using thermal atomic beams. In conventional optics, the step from a light bulb to an optical laser in the 1960s enabled a huge technological progress and a variety of new, fascinating scientific experiments including most of the atom optics experiments. An equally important step in atom optics is the step from a thermal atom source to a coherent atom source. While an optical laser emits a beam of coherent electromagnetic waves, the output of an atom laser is a coherent, bright beam of matter waves.

The principle of such a coherent atom source is based on a postulation of Albert Einstein in 1925, who seized a suggestion of Satyendra Bose on the quantum statistics for identical particles with an integer spin quantum number (bosons). He stated that in an ideal gas bosons can macroscopically occupy the ground state, even if the thermal energy exceeds the level spacing. This occurs, if the thermal de Broglie wavelength becomes comparable to the mean particle separation, more precisely the phase space density rises above 2.6. The Bose-Einstein condensation (BEC) is a phase-transition which relies on pure quantum statistical effects and needs no particle interaction. For fermions (particles with half integer spin quantum numbers) a gradually transition from a classical gas to a degenerate Fermi gas can be observed if the above condition is fulfilled. The critical temperature depends on the density and particle mass. Thus, quantum effects for electrons, for phonons in solids or for liquid helium become significant at relatively high temperatures (in the order of 10^4 K, 100 K and 1 K, respectively). In bosonic atomic gases the phase transition can only be achieved in dilute systems ($n \sim 10^{13}$ atoms/cm^3) at temperatures below 1 µK (see e.g. ref. 3). Thus, it took 70 years until the required cooling methods and experimental techniques could be developed to realize a condensate in trapped atomic gas. However, the exciting point was not only the technical achievement of a theoretically predicted new state.

For the first time researchers had the unique opportunity to explore the nature of a well observable macroscopic quantum object with a size of up to 0.5 mm. Moreover, thanks to the low density, interactions are weak and the condensates can be well treated theoretically, which made the interplay between theory and experiment extremely fruitful. Therefore, already six years later (2001) Eric Cornell, Wolfgang Ketterle and Carl Wieman have been awarded the Noble Prize in physics "for the achievement of Bose-Einstein condensation in dilute gases of alkali atoms, and for early fundamental studies of the properties of the condensate".

Meanwhile condensates have been created in gases of nine different atomic elements. Due to the very different internal structures and collisional properties of the particles, the cooling techniques must be carefully designed for each atomic species. In our laboratory we recently succeeded to Bose-Einstein condense atomic chromium. This atomic species is especially interesting due to its high magnetic moment which triggers to novel questions in fundamental research, and also due to its technological relevance in atom lithography. Our experimental setup and an overview of the required and very complex experimental cooling strategy are shown in **(06)** and **(07)** and will be briefly discussed in the following.

To produce a BEC in a gas of chromium atoms, a beam of chromium atoms is generated by a high temperature effusion cell at 1600° C and directed to our science chamber. On their way up, the atoms are slowed down by a counter propagating laser beam in a Zeeman slower. In this way, they can be captured in a modified magneto-optical trap (CLIP trap) in the centre of the science chamber. With our cooling scheme we continuously accumulate 10^8 atoms in a magnetic trap. Another laser cooling sequence (Doppler cooling) is applied after the atoms have been compressed in the magnetic trap. However, due to the light momentum transfer, this laser cooling technique limits the achievable temperature of the cloud to 120 µK. Therefore, the near resonant cooling laser light is turned off and the trapped cloud is further cooled by forced radiofrequency (rf) induced evaporation in the magnetic trap. This technique is comparable to evaporation on a macroscopic scale. While hot atoms are removed from the trap, the temperature of the cloud decreases due to rethermalising elastic collisions of the remaining atoms. In a harmonic trapping potential, like it is used in our experiment, the density increases with decreasing temperature. The extraordinarily large magnetic dipole moment of chromium leads to an increasing twobody loss in the form of spin relaxation collisions with increasing spatial density of the cloud. This causes rf evaporation to become inefficient in the magnetic trap and the atoms have to be transferred to an optical dipole trap for the last cooling step. We use a horizontal aligned focused laser beam. To increase the

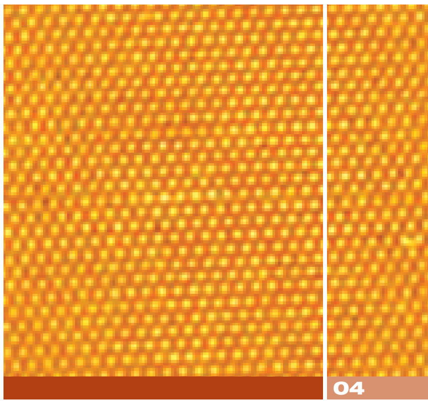

04

Two dimensional chromium nano-dots on a silicon surface. The pattern could be created using three interfering laser beams. The dots have a structure width of 120 nm and are separated by 2λ/3=284.

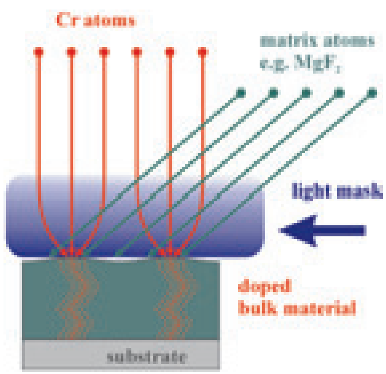

05

Structured doping: A light mask sensitive dopant (Cr atoms) and a light mask insensitive matrix material (MgF_2) are simultaneously deposited on a substrate. While the light mask focuses the dopant atoms, the matrix atoms are unaffected.

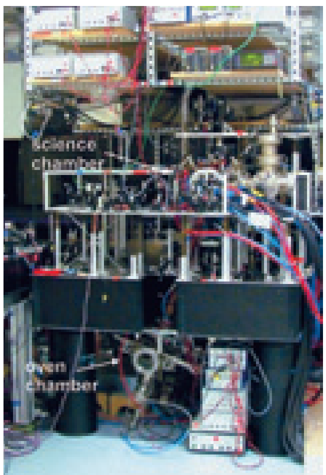

06

Experimental setup.

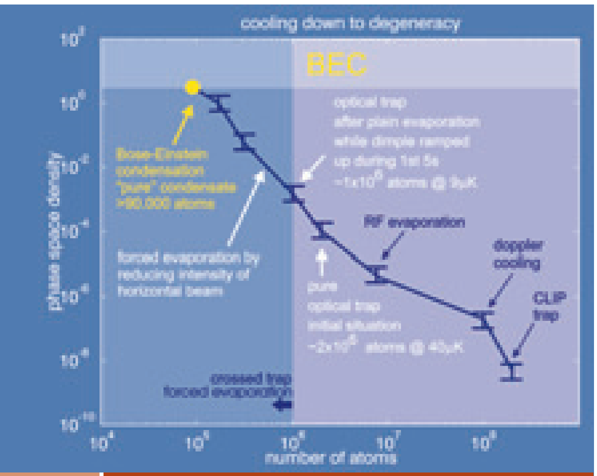

07

Required cooling steps to obtain a chromium BEC: Shown is the increase in phase space density vs. the trapped atom during the diverse cooling steps, where the phase space density compares the thermal de Broglie wavelength to the interparticle separation. For phase space densities > 1 a BEC forms up in the trapped cloud. During each cooling step atoms are lost, so that the initial atom number of 10^8 atoms drops to 10^5.

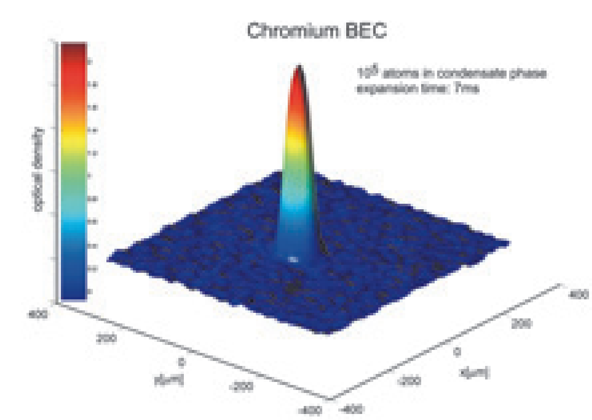

08

False color representation of an absorption image. Shown is the optical density of a chromium condensate consisting of 10^5 atoms after 7 ms of free expansion.

local density and the elastic collision rate during the following evaporative cooling stage, the trapping potential is modified by a second laser beam aligned in the vertical direction. Forced evaporation towards the critical temperature in order to achieve the condensation proceeds now by reducing the intensity of the horizontal beam. The cloud is then detected using a standard absorption imaging technique with a resonant probe beam propagating in the horizontal direction, perpendicular to both trapping beams. A typical image of the condensate containing about 10^5 atoms is shown in **(08)**. **(09)** depicts the typical critical behaviour of the condensate fraction (N_0/N) as the temperature of the sample is lowered.

In light optical terminology a BEC represents a resonant cavity highly excited in one mode which is the ground state of the trap. As elastic scattering of atoms is the corresponding process of spontaneous emission in the optical laser, stimulated emission is the scattering process into the ground state of the condensate. As soon as the critical temperature is reached, the atoms scatter predominantly into the ground state, if the sample is further cooled by evaporation. A crucial difference is that atoms cannot be created like photons. The atom number in the ground state can only be increased at the cost of atoms in other states. Phasecoherent matter-wave amplification, as it is known from a laser, could be demonstrated using a BEC of sodium atoms. An input wave generated by Bragg diffraction could be amplified by atoms of the condensate.

Atom traps with BECs were combined with controllable leaks to release a coherent beam of atoms from the trapped condensate. Pulsed atom lasers comparable to q-switched and mode-locked lasers were reported. A chromium atom laser is illustrated in **(10)**. Improving control over the leaks delivered atom laser beams for up to 100 ms from a single Rubidium condensate, until the last atom left the condensate. Up to now the production of a

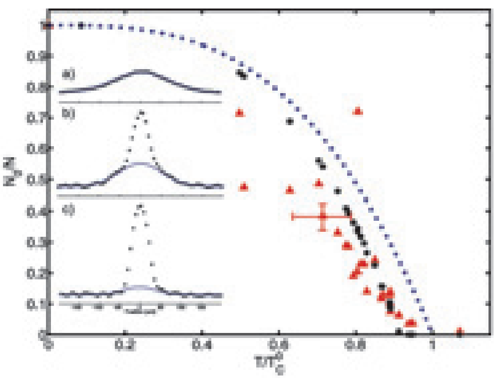

09

Dependence of the condensate fraction (N_0/N) on the temperature relative to the transition temperature of an ideal gas (T/T_C^0). Besides our measured data (triangles), calculated predictions are indicated by the dashed curve (ideal gas) and the solid circles (including finite atom number and interaction). Inset: Density profiles from absorption images of atom clouds taken after 5 ms of ballistic expansion: (a) thermal cloud at 1.1 µK; (b) two-component (BEC and thermal cloud) distribution at 600 nK, slightly below T_C; (c) nearly pure condensate with 50 000 atoms.

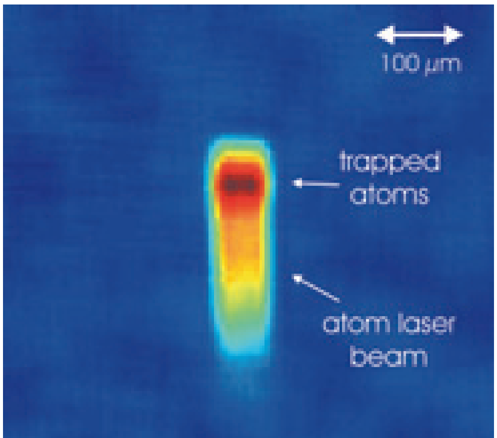

10

False colour representation of a chromium atom laser beam. Atoms leak out of a chromium BEC and form a coherent beam inside an optical wave guide. The atoms are accelerated by the gravity towards the bottom of the image.

condensate needs chronologically ordered cooling steps, which make a continuously pumping of the condensate difficult. Schemes, in which the condensate is prepared in a spatial separated trap and subsequently merged to the "lasing" condensate, are promising.

Again, there are significant differences between a photon and atom laser beam. Due to the very low velocities of the atoms, the propagation of an atom laser beam is

ZUSAMMENFASSUNG

In den vergangenen Jahren hat die Atomoptik eine explosionsartige Entwicklung durchlebt und gehört heute zu einem der zentralen Themen in der modernen Optik. Unter dem Stichwort Atomoptik werden Techniken zur Manipulation der Bewegung von Atomen zusammengefasst. Potentiale aus Licht, magnetischen oder elektrischen Feldern dienen in der Atomoptik als optische Elemente, mit denen beispielsweise Linsen, Spiegel oder Strahlteiler realisiert werden können. Wie Photonen in optischen Resonatoren können Atome in Atomfallen für eine gewisse Zeit gespeichert werden. Durch die Realisierung von Bose-Einstein Kondensaten und Atomlasern stehen Quellen kohärenter Materiewellen zur Verfügung. Wechselwirkungen zwischen Atomen ermöglichen nichtlineare optische Elemente. Durch die interne Struktur der Atome und die Wechselwirkung zwischen den Atomen können die Eigenschaften dieser optischen Elemente häufig wesentlich flexibler gestaltet werden, als dies in der klassischen Optik möglich ist.

Dissipative Elemente werden zum Abbremsen von Atomen und zur Kühlung von gespeicherten atomaren Gasen eingesetzt. Der Fortschritt in den Kühltechniken erlaubt es heutzutage, mit atomoptischen Mitteln Gase mit Temperaturen unter 1 nK zu erzeugen. Diese Gase gehören damit zur kältesten Materie im Universum. Quantenmechanisch stellen Atome Wellenpakete dar, deren Ausdehnung mit abnehmender Temperatur wächst. Übersteigt die Ausdehnung identischer, bosonischer Atome den mittleren Abstand zwischen den Atomen in einem gefangenen Gas, so ist es nicht mehr möglich zwischen den Atomen zu unterscheiden. Das Gas muss durch eine gemeinsame Wellenfunktion mit Amplitude und Phase beschrieben werden. Es kommt zu einem Phasenübergang von einem klassischen Gas zu einem sog. Bose-Einstein Kondensat, in dem ein Materiewellenzustand makroskopisch besetzt ist. Einen ähnlichen Übergang kann man an der Laserschwelle eines Lasers beobachten. Analog zum Laser ermöglicht auch hier ein geeigneter Auskoppler aus der Atomfalle einen kohärenten Atomlaserstrahl.

Bose-Einstein Kondensate stellen heute in der Physik ideale, sehr flexible, makroskopische Modellsysteme mit Ausdehnungen bis zu 100µm dar, die zur Untersuchung von unterschiedlichsten physikalischen Fragestellungen genutzt werden. Die Gase sind dabei sehr einfach zugänglich, d.h. sie können sehr gut mit einer CCD-Kamera beobacht und mit atomoptischen Elementen von außen manipuliert und kontrolliert werden. Die Wechselwirkung zwischen den Atomen führt zu einer Kerr-Nichtlinearität, wie sie aus der nichtlinearen Optik bekannt ist und erlaubt es beispielsweise, das Vierwellenmischen und die Materiewellenverstärkung in einem solchen Gas zu beobachten. Obwohl in diesem Artikel besonderes die Analogien zwischen Atomoptik und Lichtoptik hervorgehoben werden sollen, beschränken sich die möglichen Fragestellungen nicht nur auf diesen Bereich. So eignen sich Kondensate in periodischen dreidimensionalen optischen Gittern sehr gut zur Untersuchung von festkörperphysikalischen Problemen. Hochtemperatursupraleitung wird in letzter Zeit an Gasen aus fermionischen Atomen studiert und macht damit die Atomoptik zu einem interdisziplinären Forschungsfeld.

mainly determined by the gravity. The interaction between the atoms will spread the output beam and lead to collisions between two crossed atom beams.

4. Non-linear atom optics

Even though a BEC is a very dilute system, the interaction between the particles cannot be neglected compared to the kinetic energy. Even more, it is the interaction which adds zest to the system. Eric Cornell made the following statement shortly after the first realisation of a condensate in the following way: "…, if the system truly were an ideal gas, there would be little left to study at this point". Because of interparticle interactions in a condensate, the wave equation in the mean field description (Gross-Pitaevskii equation) contains an additional non-linear term, which is equivalent to the Kerr non-linearity in light optics. Thus, it is not surprising that the non-linear optics effects could also be observed in atom optics. However, unlike light optics, where this term arises from the interaction between light and matter, in atom optics the atoms themselves cause these effects.

As we will see in the following, this non-linear term can be easily manipulated over a wide range using external fields. By doing so, the nature of the quantum gas can be modified in a crucial way and different quantum regimes can be investigated.

In most of the quantum gases generated so far, the interaction between the atoms is given by the isotropic van der Waals-interaction and is characterized by the scattering length a, which corresponds to the $\chi^{(3)}$ non-linear coefficient in light optics. Using magnetic field dependent scattering resonances, so called Feshbach resonances, the scattering length can in principle be tuned to any arbitrary value. **(12)** depicts experimentally observed Feshbach resonances depending on the magnetic field in an ultra cold gas of chromium atoms. For example, changing the

11

Magnetic wave guide for the realisation of a continuously pumped high-flux atom laser with chromium atoms. Instead of cooling the atoms step by step at the same position, the cooling steps are separated in space.

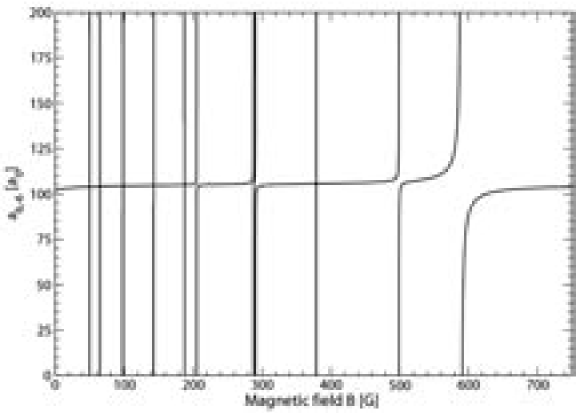

12

Theoretically predicted Feshbach resonances in gas of chromium atoms for magnetic fields ranging from 0 to 750 G. The scattering length a, which describes the van der Waals-interaction diverges in the neighbourhood of the scattering resonance. The scattering length corresponds to the $\chi^{(3)}$ non-linear coefficient in light optics.

scattering length from positive to negative values, i.e. changing the interaction from repulsion to attraction, leads, to a collapse of the condensate wave function. By tuning the scattering length to zero, the BEC behaves like an ideal quantum gas. In recent experiments, a slow sweep of the magnetic field across a resonance resulted in the adiabatic creation of molecules. An inverse sweep transfers the molecules back into atoms. The corresponding process in light optics is up- and down-conversion of light. In a degenerate fermionic quantum gas the quantum static changes during this process. The generated bosonic molecules, themselves can be Bose-Einstein condensed. Applying this technique to a system of fermionic atoms allowed one the investigation of the transition between a molecular BEC and strongly correlated Fermi gas (BCS) and turned out to be an ideal model system to study high temperature super conductivity.

Due to the high magnetic moment of chromium atoms, in a BEC of chromium the strength of the dipole-dipole interaction becomes comparable to the van der Waals-interaction. The two types of interactions differ significantly. While the van der Waals-interaction is isotropic and short-range, the dipole-dipole interaction is anisotropic and long-range. Hence, the properties of these gases are expected to differ significantly from those discussed so far. Because of the anisotropic nature of the interaction, the properties of the quantum gas depend on the direction of the external magnetic field and the shape of the trap. The sign and strength of the average interaction can be changed using rotating external magnetic fields. First experimental results show the dependence of the expansion dynamics of a chromium condensate on the external magnetic field direction **(13)**. The measurement represents not only the first manifestation of dipole-dipole interaction in a degenerate quantum gas but also the first observation of magnetostriction in an atomic gas. According to theoretical studies, this interaction should affect the basic properties of a condensate, including e.g. stability, low-lying excitations, roton excitations, Josephson junctions and solitons.

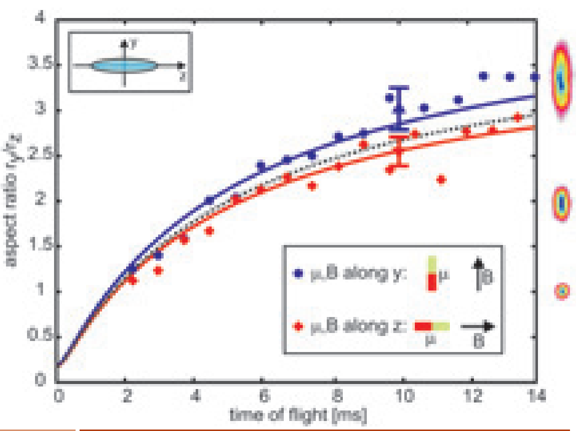

13

Aspect ratios of expanding chromium condensates. The anisotropic interaction induced by the dipole-dipole interaction leads to anisotropic Kerr non-linearity. Thus, depending on the external field direction, the expansion of the chromium condensate is affected.

The mass dependence of the non-linear term in the wave equation leads to a third approach, by which the non-linearity of the system can be tuned. According to the effective mass concept in solid state physics, optical lattices are used to obtain an effective negative mass. This approach allowed realising bright solitons with a repulsive interaction.

5. New technological interest

Up to now, we discussed experiments, where an ensemble of atoms is manipulated by classical atom optical tools, which are based mainly on the direct interaction between external fields and the atoms (e. g. atom-light interaction). Applying these techniques, it becomes also possible to individually trap and investigate single atoms. The intensive studies of coherent atom-atom interaction lead to new atom optical tools. For instance, in optical lattices this interaction allows one to purposely control more than 10^5 atoms as a collective. Hereby, a Bose-Einstein condensate is placed inside a shallow optical lattice. As the potential depth of the lattice is increased, the interaction energy of the atoms exceeds the kinetic energy and the atomic cloud undergoes a quantum phase transition from the superfluid to the Mott insulator phase. In the latter phase each lattice site can be occupied by exactly one atom with very small fluctuations in the atom number. Since number fluctuations are drastically reduced, the transition can be regarded analogue to the transition from a classical coherent state to a non-classical Fock state for atoms which find their counterpart in the respective quantum description of light fields. Using this model system, fundamental studies on the quantum phase transitions in lattices could be performed. Atom interferometers based on the phase transition have been proposed.

In our group, we intend to initiate this quantum phase transition close to a surface and deposit equally spaced single atoms on the surface by moving the lattice towards the surface. The scheme is depicted in **(14)**.

A condensate is prepared in an optical dipole trap and is transferred into a one dimensional standing wave, where it is distributed over several lattice sites. Subsequently, onedimensional lattice is moved towards a surface. Above the sur-face two additional, back reflected laser beams perpendicularly cross the transport wave and form a threedimensional optical lattice with an increasing potential depth. As the condensates traverse this lattice they undergo Mott-insulator transition. From this point on, each lattice site of the three dimensional lattice is populated with exactly one atom, which can be deposited onto surface with nm accuracy. Each atom layer deposited on the surface forms a regularly spaced two-dimensional lattice with a lattice constant $\lambda/2$. By moving the substrate after a layer had been deposited, complex periodic single atom structures can be written. The presented strategy describes a very robust method to periodically position single atoms on a surface and to gain technological relevance. E. g. in context of solid state based quantum computers single atom devices are discussed, where periodic arrays of single atoms located beneath an electrode, act as qubits. By applying voltage to the electrodes, the qubits may interact and carry out the desired operation. A further application perspective of this "bottom up" lithography technique might be the production of single atom contacts, which may lead to novel electronic, optical or magnetic devices.

6. Outlook

This short introduction to atom optics exhibits a very versatile and interdisciplinary field in modern optics. Various effects observed in atom optics correspond to the physics studied in light optics. However, due to specific properties of the atoms the atom optical tools exhibit novel features. Bose-Einstein condensates which represent the atom optical analogue to the light optical laser have revolutionized the classical atom optics. Many fundamental quantum effects which arise in very different fields of physics could be observed and discussed using this macroscopic quantum object, and will allow one to address further fundamental problems. Atom optics with weakly interacting, degenerate fermionic atoms opens up a novel field of modern optics, which has no counterpart in classical optic.

Technological application can be found in high precision atom interferometric measurements. Because of their mass and internal structure, atoms are very sensitive to gravitation and external fields. In future experiments, new intense atom laser sources may increase the already achieved enormous precision. Atom lithography allows nowadays creating atom structures on surfaces with a precision of a few tenths of nm. Including new technique as described before, the control of an atom cloud on the single atom basis becomes possible and will lead to new lithographic techniques and surface structures. •

Sven Hensler
Jürgen Stuhler
Tilman Pfau

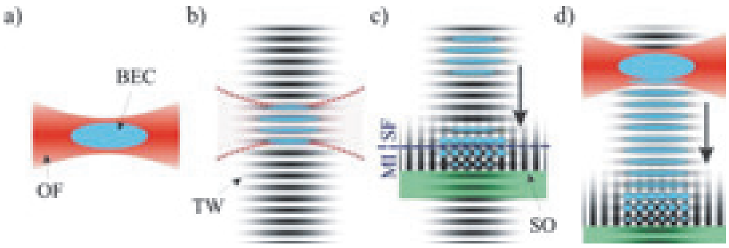

14

Single atom deposition scheme. (a) A BEC is prepared in an optical dipole trap. It is adiabatically transferred into a one-dimensional standing wave (transport wave) (b) and moved towards a substrate (c). Above the substrate the transport wave is perpendicularly crossed by two further standing waves. This light field configuration forms a three-dimensional optical lattice with an increasing potential depth. Thus, as the BEC traverses the optical lattice it undergoes a Mott-insulator phase transition and each lattice site is populated with exact one atom which can be deposited on the surface.

References

1 Bergmann Schaefer, *Optik*, (Walter de Gruyter & Co., Berlin, 10. Auflage, 2004)
2 M. Oberthaler and T. Pfau "One-, two- and three-dimensional nanostructures with atom lithography", J. Phys.: Condens. Matter 15, R233 (2003)
3 L. Pitaevskii and S. Stringari, Bose-Einstein Condensation, (Oxford University Press, Oxford, 2003)

THE AUTHORS

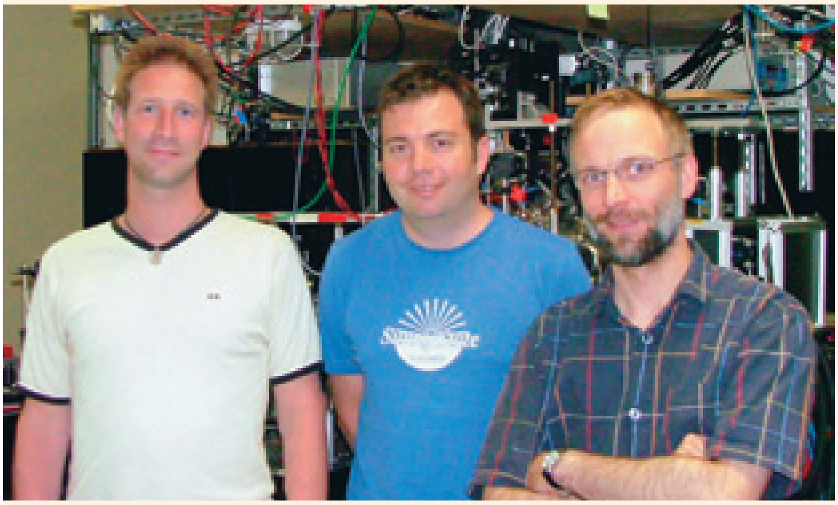

Dr. Sven Hensler (m.)

studied physics in Konstanz. He received his PhD degree in 2004 at the Universität Stuttgart on studies of interactions in ultracold dipolar gases. Since then he has been research associate at the 5th institute of physics. His current research interest is atom lithography and single atom deposition.

Dr. Jürgen Stuhler (l.)

graduated in physics at the University of Konstanz on laser cooling of chromium. As a Marie Curie fellow he spent two years at the LENS (Università di Firenze, Firenze, Italy) building a gravitometer based on atom interferometry. Since 2003 he has been research associate at the Universität Stuttgart his main interests are atom and quantum optics and degenerate quantum gases. He is supported by the Eliteförderprogramm of the Landesstiftung Baden-Württemberg.

Prof. Dr Tilman Pfau (r.)

has been head of the 5th institute of physics in Stuttgart since 2000. He habilitated at the University of Konstanz in 1999. During the last years he was guest scientist in the groups of Prof. C. Cohen-Tannoudji (ENS, France) and Prof. W. Ketterle (MIT, USA). His research interest is atom and quantum optics and basic research on optical technologies and materials including non-classical light sources and detectors and nano-structured optical materials.

Contact
5. Physikalisches Institut, Universität Stuttgart
Pfaffenwaldring 57, 70569 Stuttgart
Tel. +49 (0)711 685 4820
Fax +49 (0)711 685 3810
E-mail: t.pfau@physik.uni-stuttgart.de
Internet: http://www.physik.uni-stuttgart.de/institute/pi/5/

zurück zum Inhalt

Semiconductor single-photon sources

A single photon source, which is able to generate photons on demand allows the ultimate quantum control of the photon generation process, i.e., single photons can be generated within short time intervals with a deterministic dwell time between successive photon generation events. Such a source has the potential of enabling many new applications in the field of photonics and quantum information technology. This is in particular true for quantum cryptography, which exploits the fundamental principles of quantum mechanics to provide unconditional security for communication. An essential element of secure key distribution in quantum cryptography is an optical source emitting a train of pulses that each contain one and only one photon. Because measurements unavoidably modify the state of a single quantum system, an eavesdropper cannot gather information about the secret key without being noticed, provided that the pulses used in transmission do not contain two or more photons. Recently, it has also been shown that the availability of a single-photon source which is able to generate indistinguishable photons enables the implementation of quantum computation using only linear optical elements and single photon detectors. Possible other applications are imaging and lithography beyond the diffraction limit as well as quantum teleportation.

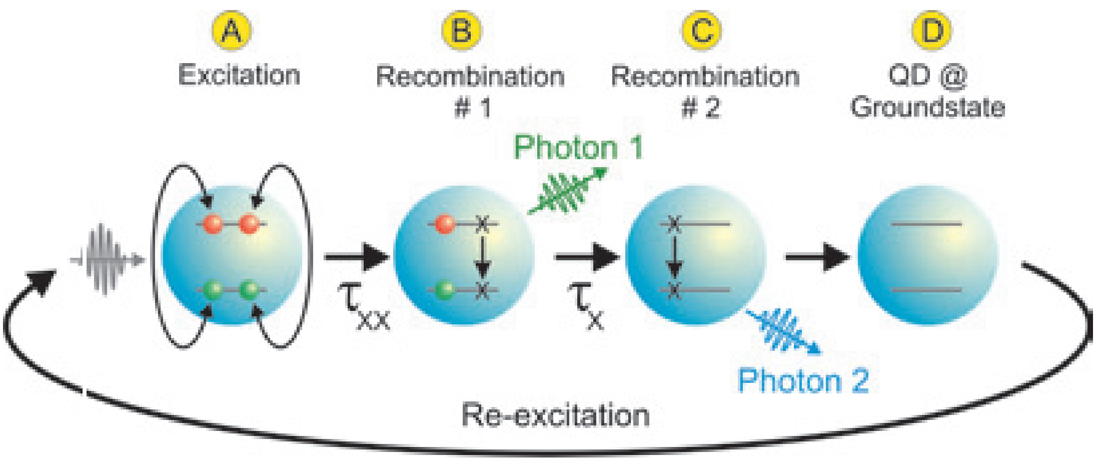

1. Introduction

The single-photon sources used today either employ highly attenuated laser pulses or rely on parametric down-conversion. Both schemes possess a serious disadvantage since photons are created randomly, i.e., with a Poissonian photon statistics. In order to maintain a low multi-photon emission probability the average photon number per pulse has to be kept as low as ~ 0.1. The realization of a practical single photon source requires three main elements: a single quantum emitter, regulation of the excitation and/or the recombination process and an efficient output coupling of the single photons. The active emitter should possess a short radiative recombination time to allow operation at high repetition rates. Furthermore, the possibility of electrical pumping is desirable with respect to a compact and robust source.

Though working until now at low temperature, epitaxially self-assembled InAs quantum dots (QDs) are ideal candidates since they offer several advantages, including high quantum efficiencies of $\eta \sim 1$, large dipole moments, narrow linewidths that can be close to the Fourier-transform limit, and the option of electrical pumping. The triggered single-photon emission at the single exciton ground state transition of a self-assembled QD is ensured by a *pulsed excitation*, the *anharmonicity* of the multi-exciton spectrum in combination with *slow relaxation* of highly excited QD states. Spontaneous emission of a quantum emitter is generally emitted in all directions (full solid angle) and therefore hard to capture efficiently. For a practical use, however, the emitter should be coupled to a cavity mode with a directional field profile. Self-assembled QDs can be easily embedded into an appropriate microcavity, e.g., into a micro-pillar. This allows an efficient collection of the single photons thus enabling their use for external applications.

In the following, we will first give an introduction to the physics of quantum dots and the concept of photon statistics measurements. Second, we will discuss recent experimental results where resonant coupling of the QD transitions to a cavity mode has been achieved. Efficient triggered generation of single and photon-pair emission is demonstrated. Finally, the remaining challenges for the use of QD pillar cavities as single photon sources will be discussed.

2. Quantum Dots

Semiconductor-based QDs typically contain only a few 10^4–10^5 atoms of a material *A* (e.g., indium arsenide *InAs*) providing a smaller band gap energy than the surrounding semiconductor matrix material *B* (e.g., (aluminium) gallium arsenide *(Al)GaAs*). During the last two decades, various sophisticated semiconductor growth methods have been developed and refined in order to gain a high degree of control on the exact size and composition of these nanostructures which allows for an application-oriented design. One of the well established methods for self-assembled growth is e.g., the strain-induced Stranskii-Krastanov growth mode in which the formation of islands is achieved via surface energy minimization of droplets of a low band gap material *A* on top of material *B*. Finally, the islands are overgrown by material *B* thus generating a fully embedded QD in the host material *B*.

From a basic energetic view, carriers inside a QD will therefore be subject to a full three-dimensional barrier potential thus trapping these particles. The strong three dimensional confinement leads to quantization effects on the eigenstates of electrons and holes. As a result, a few discrete bound energy eigenstates with limited degeneracy are available for occupation by carriers – which reflects itself in the sharp emission spectra of *single* QDs by a pairwise radiative recombination of electrons and holes from conduction and valence band states, respectively.

SUMMARY

Exploiting the quantum properties of the light which is emitted from semiconductor nano-structures has the potential of enabling many new applications in the field of photonics and quantum information technology, such as secure communication, imaging and lithography techniques beyond the diffraction limit, as well as photonic quantum computing. Many of these applications require a single-photon source, which is able to generate photons on demand. A single semiconductor quantum dot embedded into a microcavity is able to deliver triggered single photons with ultra-high repetition rates of ~ 1 GHz.

This contribution gives an introduction into the exciting physics of single semiconductor nanostructures and their use as non-classical light sources. The efficient triggered generation of single photons and photon pairs by placing an individual quantum dot into a micropillar cavity is demonstrated. Furthermore, the remaining challenges for the application of quantum dots in pillar cavities as practical single-photon sources will be discussed.

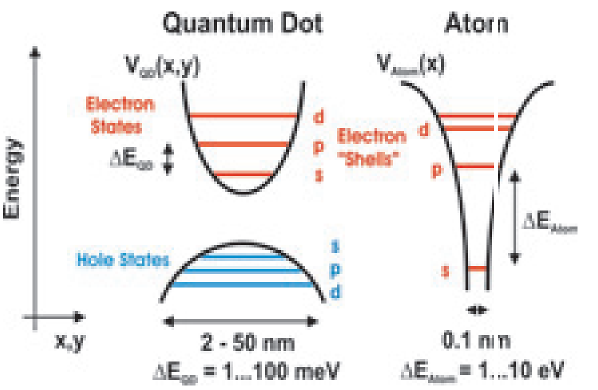

01

Comparison between basic properties of quantum dots ("artificial atoms") and real atoms. Both model systems provide discrete bound eigenstates for electrons (atom) or electrons and holes (QD). Due to the significant differences in size, the quasi-harmonic energy splittings between QD shells are on the meV scale (~ 100 times less than for real atoms).

Even though QDs are often referred to as "artificial atoms" due to these unique characteristics similar to "real" atoms, one should note the differences between these two model systems **(01)**: Due to the small size of real atoms (~ 0.1 nm), the anharmonic *s*-, *p*-, *d*-shell structure of eigenstates reveals a high energetic splitting ΔE in the 1–10 eV range whereas the quasi-equidistant splitting of QD shells is significantly lower (< 100 meV) due to their comparably large extent (see above). As a direct consequence of this, the emission properties of QDs are sensitive to the lattice temperature in a sense that bound carriers might be thermally activated into unbound states of the barrier material. Experiments on these structures are therefore mainly done at cryogenic temperatures (T < 100 K). However, progress in high temperature operation of QDs has been already achieved [1] and room temperature operation seems to be possible with specially designed QDs in the near future.

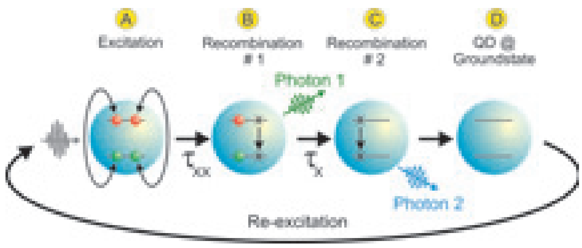

02

Simplified scenario for the sequential decay of different (s-shell) electron-hole pair configurations within a single QD forming a photon cascade. After initial excitation of the biexcitonic state XX, radiative recombination of the first e-h pair emits a specific photon (#1) thus leaving the QD in its excitonic s-state (i.e., one e-h pair in the lowest shell). A second photon (#2) is the result of the sequential decay of the remaining state. τ_{XX} (τ_X) represent the radiative lifetimes of the corresponding QD carrier configurations.

For the generation of radiative quantum cascades, the QDs are excited with short optical or electrical pulses to generate the electron-hole pairs in the barriers (material *B*) of the QDs. The carriers are subsequently captured by the QDs and relax to the lowest energy levels (s-shell) within a few tens of picoseconds. Inside a QD, Coulomb interaction between a captured s-shell electron-hole pair naturally forms the lowest-energy *exciton* (*X*) state of an excited QD. The scenario of fully occupied s-shells by two electrons and holes, respectively, represents a *biexcitonic* (*XX*) configuration. The radiative recombination of this multiexcitonic state occurs in cascaded processes **(02)**, i.e., in sequential optical transitions of the biexciton (*XX*) and the exciton state (*X*). Due to Coulomb interactions enhanced by strong carrier confinement, the energy of the emitted photons depends sensitively on the number of e-h pairs that exist inside the QD. If the recombination times of the multiexcitonic states are longer than the recombination time of the free electron-hole pairs in the barriers, each excitation pulse can lead to at most one photon emission event at the corresponding dot transition. Therefore, a regulation of photon emission processes can be achieved due to a combination of Coulomb interactions creating an anharmonic multiexciton spectrum and vanishing re-excitation probability on short time scales after the corresponding photon emission event at the *XX* or *X* transitions. Thus, specific photons from the cascade process, e.g., the *XX* and *X*, can be spectrally filtered out and used to generate single photons or correlated photon pairs. Even the generation of polarization-entangled photons is expected.

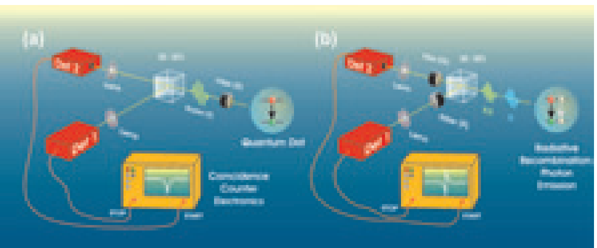

03

Photon correlation setup scheme: (a) Auto-correlation: *Light collected from the sample* **(02)** *is spectrally pre-filtered to select a single narrow QD luminescence decay line. Dividing this photon stream into two 50:50 single-photon detection paths, the statistics of two-photon coincidences separated by a delay $\tau = t_{Stop} - t_{Start}$ between both detections is investigated. The characteristic behaviour of a single photon source is the so-called "anti-bunching" reflected by a significant dip in the statistics at zero delay ($\tau = 0$);* (b) Cross-correlation: *Photonic cascades are verified by use of consecutive photons (e.g. XX→X→0) which – due to their different energy – are spectrally separated within the START and STOP detection arms of the setup. Photonic cascades reflect in a significant antibunching-bunching correlation trace asymmetry (see schematic trace).*

3. Photon statistics measurements

To get insight into the statistical nature of light emitted by the single QD a *Hanbury-Brown & Twiss* photon-correlation setup was used as is depicted schematically in **(03)**. The basic version (a) of such an experiment consists of two orthogonal detector arms on which the collected photon stream is divided by a 50/50 beam splitter: A narrow band spectral filter is used in front of the HBT setup to select the desired recombination line (e.g., excitonic *X* or biexcitonic *XX*) and to reject background light. Due to the quantum mechanical picture of a single photon as an indivisible "wave packet", each photon can either be detected on one of the two high-sensitivity avalanche photo diodes (Det 1 + Det 2).

If we recall the simple atomistic picture explained in the preceding paragraphs **(02)**, it becomes obvious that immediately after recombination of an e-h pair (i.e., the emission of a photon of equivalent energy) it is impossible to detect a second identical photon from the same decay process as the initial configuration of e-h pairs within the QD needs to be re-established first. This argument holds for both continuous wave (cw) and pulsed excitation of the QD. In the case of an ideal single-photon emitter (a single QD) the auto-correlation statistics **(03a)** reveals full suppression of photon pair coincidence events with *zero* delay, thus reflecting in either (a) correlation trace "dip" at τ=0 (cw) or (b) the suppression of only the τ=0 correlation peak within a train of coincidence peaks at integer multiples of the laser pulse period (see also next chapter). In other words, the probability to simultaneously detect two photons from the same decay channel on both detector arms completely vanishes. This *non-classical* behaviour of emission is known as "*photon anti-bunching*" which allows for a clear identification of an atom-like photon source.

(03b) displays the experimental scheme for the identification of temporally correlated two-colour photon pairs from consecutive e-h recombination within a single QD. The basic idea of this *cross-correlation* type of experiment is to prove the *temporal interconnection* between different recombination channels which can be spectrally distinguished. **(02)** sketches the main sequence of recombination processes which form such a two-photon cascade. Assuming the lowest energy levels of electrons and holes (s-shell) to be initially occupied by two carriers each, the QD is in its "biexcitonic" (*XX*) configuration (*A*). The spontaneous radiative decay of one of the two e-h pairs (transition $B \rightarrow C$) leads to the emission of a characteristic single *XX* photon which is spectrally selected for detection by only one arm (START) of the correlation setup. Due to the Coulomb interaction (attractive or repulsive, depending on the microscopic conditions of the 3-D carrier confinement of the QD) the decay of the remaining excitonic (*X*) dot configuration ($C \rightarrow D$) deviates in energy. If the excitation conditions are carefully chosen such that re-excitation in between *XX* and *X* decays can be neglected, each spontaneous biexciton recombination should involve the subsequent decay of a remaining exciton thus leaving the QD in its empty state (*D*). Therefore, in cross-correlation experiments, the second detection arm (STOP channel) of the setup is energetically tuned to the *X* transition so that in total the distribution $g^{(2)}(\tau)$ ("second-order correlation function") of coincidence events between both channels reflects their probability as a function of delay $\tau = t_{Start}(XX) - t_{Stop}(X)$. As one expects an enhanced probability to find an *X* photon at short time scales after an *XX* decay but *not* for the inversed scenario, the fingerprint of such a photon cascade should be a significant correlation trace asymmetry of anti-bunching (suppressed signal) and bunching (increased signal; see sketched trace in **(03b)** in the vicinity of zero delay. This behaviour is indeed observable under the conditions of continuous wave optical excitation, as will be discussed in detail in the following paragraphs.

4. Efficient generation of triggered single photons and photon pairs

With respect to future applications in the fields of quantum information technology, there is an important requirement to be fulfilled for an effective use of single-photon emitters: As the spontaneous emission of photons is randomly distributed over the full solid angle 4π of space and is therefore subject to photon losses by total internal reflections on the semiconductor-vacuum surface, this reduces the photon-capture efficiency for any optically coupled devices (e.g., fibers for collection of the emission). It is therefore desirable to channel the stream of emitted photons which can be achieved by embedding QDs into micro-resonator structures. These resonator structures are characterized by well defined spectral and spatial mode profiles as a consequence of a strong lateral and vertical confinement of the light field.

The use of semiconductor microcavities leads to a drastic increase of the light emission efficiency of devices. A vertical pillar microcavity is formed by a pair of bottom/top distributed-Bragg reflectors (DBRs) separated by a cavity region containing an active material layer in the center. Inside the λ-cavity the optical field is trap-

ZUSAMMENFASSUNG

Die gezielte Ausnutzung der quantenmechanischen Eigenschaften von Licht (Photonen), welche insbesondere auf Basis von Halbleiter-Nanostrukturen erzeugt werden, eröffnet zahlreiche neue Möglichkeiten für Anwendungen auf dem Gebiet der Photonik bzw. Quanten-Informationstechnologie. Dazu zählen insbesondere die Entwicklung abhörsicherer Datennetze sowie verschiedene Konzepte für das optische Quantencomputing. Weitere viel versprechende Einsatzgebiete ergeben sich im Bereich der bildgebenden Verfahren (Imaging) sowie der Mikrostrukturierung (Lithographie) durch die Möglichkeit, eine Auflösungsgrenze unterhalb des beugungsbedingten Limits zu erreichen. Grundvoraussetzung für eine Vielzahl derartiger Anwendungen ist die Verfügbarkeit von deterministischen Photonenquellen, welche in der Lage sind, "Einzelphotonen auf Bestellung" zu erzeugen. Einzelne Halbleiter-Quantenpunkte in Mikroresonatoren eröffnen diese Möglichkeit, wobei ultra-hohe Wiederholraten von bis zu 1 GHz erreicht werden.

Dieses Kapitel gibt einen Einblick in die spannende Physik von Halbleiter-Nanostrukturen, insbesondere ihre Anwendung als nicht-klassische Lichtquellen. Basierend auf Quantenpunkten, eingebettet in eine Mikroresonator-Struktur, wird die effiziente Erzeugung einzelner Photonen sowie von Photonenpaaren demonstriert. In diesem Zusammenhang sollen ebenfalls die augenblicklichen physikalischen Grenzen dieser Technologie diskutiert werden.

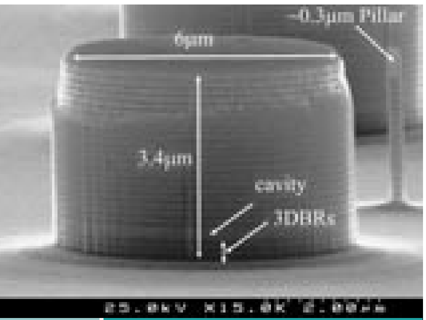

04

Scanning-electron microscope (SEM) micrograph of AlAs/GaAs pillars fabricated by electron beam lithography and dry etching.

ped, where λ/n is the wavelength of the light in the material. The DBRs are formed by alternating epitaxial growth of λ/4n layers of semiconductor or dielectric materials of different refractive indices. As DBR semiconductor materials being lattice matched to the substrate material typically have a small refractive index contrast (e.g., $n_{AlAs} = 2.92$ and $n_{GaAs} = 3.52$), several mirror periods are required to reach a sufficient reflectivity of more than 99.9 percent. The almost total internal reflection in the microcavity leads to the formation of cavity modes. By embedding QDs as the active layer in semiconductor microcavities, one can (a) guide the light emission in a desired direction, (b) control the emission wavelength and (c) also the emission patterns. In practice, the emission energy of a QD should be in resonance with the mode of the microcavity to achieve high collection efficiency. In this study, 23- and 20-period bottom and top DBRs of AlAs/GaAs layers, respectively, were used. Each DBR period consists of a 79 nm AlAs/67 nm GaAs layer pair. A 1.4 nm thick single layer of self-assembled QDs is used as the active region at the centre of a GaAs cavity. **(04)** illustrates a scanning electron microscope (SEM) micrograph of such typical AlAs/GaAs microcavity pillars [2].

In this picture two different pillar sizes are visible. The larger structure has a nominal diameter of 6 μm and the smaller one has a diameter of 0.3 μm with a height of 3.4 μm (only three layers of the bottom DBR have been etched away). The pillar sidewalls are nearly vertical with only small damages appearing next to the top surface.

To characterize the investigated system, photoluminescence emission spectra of (In,Ga)As QDs in pillar microcavities of decreasing diameter have been studied. Since larger-diameter pillars typically contain a huge number of QDs, the inhomogeneously broadened ensemble PL (due to the QD size distribution) can be used as an internal light source to reveal the pillar mode structure. For instance, the charge-coupled device (CCD) image in **(05a)** provides a one-dimensional cross section through the emitted intensity pattern of the 6 μm pillar in the plane parallel to the mirror layers as a function of the emission wavelength. This CCD image experimentally accesses the transverse mode structure: the outermost right peak is identified as the fundamental mode (having a field maximum in the center and a simple Gaussian-like shape); other peaks correspond to higher-order modes. A quality factor Q (λ/Δλ) of ~10 000 is estimated for the fundamental mode. **(05b)**, **(05c)** and **(05d)** display the measured PL spectra of 6, 5 and 4 μm diameter pillars, respectively. For decreasing pillar diameter, these spectra show characteristic properties: (i) The wavelength of the fundamental mode decreases with diameter (*D*) and (ii) the spacing between resonant wavelengths increases monotonically for decreasing diameter (approximately as D^{-2}).

To access individual QD emission, PL measurements were performed on small diameter pillars. Since a single layer of QDs is positioned between the cavity mirrors, microstructuring with decreasing circular pillar cross section cuts out an area with a reduced number of QDs. For a diameter of 0.3 μm the pillars contain about 21 QDs and since the linewidth of the QD ensemble is considerably larger than the linewidth of a mode, only very few QDs will therefore fit energetically to a certain cavity mode. As a consequence, the emission spectra of **(06a)** and **(06b)** do not reflect the cavity mode structure but sharp emission lines of individual QDs. From our mode calculations (not shown here) we conclude that the observed lines shown in the respective figures appear within the same cavity mode.

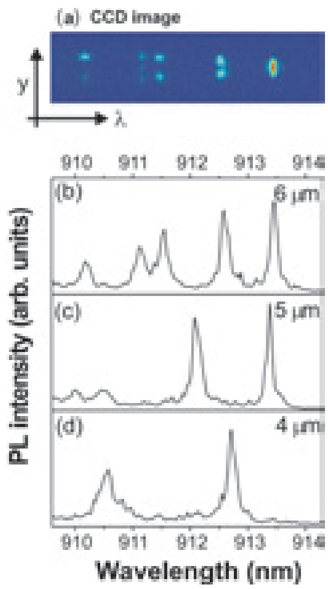

05

(a): Spectrally resolved charge-coupled device image as a cross-section of the 6 μm pillar mode structures; (b), (c), and (d): measured cavity spectra for decreasing pillar diameters of 6, 5 and 4 μm, respectively.

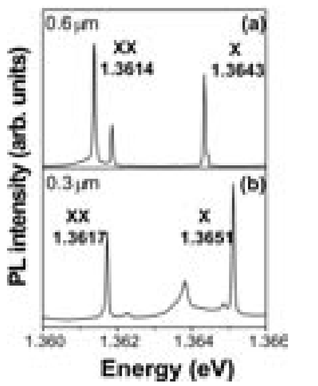

06

Photoluminescence spectra from pillars with diameters of (a) 0.6 μm and (b) 0.3 μm observed under pulsed laser excitation.

In each case the spectra are dominated by a pair of PL lines which were assigned to excitonic (X) [1.3643 eV (a) /1.3651 eV (b)] and biexcitonic (XX) emission [1.3614 eV (a) /1.3617 eV (b)] due to their linear and superlinear dependence on excitation power, respectively. As will be shown in the following, in either case these line pairs originate from the same single quantum dot. The appearance of additional PL lines between X and XX is not fully clarified, but could result from a charged exciton transition of the same QD or a further excitonic transition from a different QD.

(07) shows the cw laser power dependence of the X (closed triangles) and the XX (squares) intensities from the 0.6 µm pillar microcavity as well as, for comparison, the typical X (open triangles) intensity observed from a QD in a bulk semiconductor. The X line in the pillar cavity shows an approximately linear power dependence, therefore reflecting a QD configuration containing only a single photo-excited electron-hole pair. In contrast to this, the XX line reveals a superlinear increase with a slope of 1.7 which is attributed to emission from the QD containing two photo-excited electron-hole pairs. At high cw excitation powers a saturation behaviour is observed for both lines. An enhancement of the PL intensity by a factor of ~ 40 was found for X in a pillar microcavity when compared to the PL intensity of X in bulk semiconductor. The following two effects contribute to this observation: (1) the exciton transition being mainly coupled into the cavity mode by the Purcell effect and/or (2) the enhanced photon collection efficiency due to channeled emission out of the cavity structure. The enhancement of the spontaneous emission rate in the cavity resonance is given by the Purcell factor which is proportional to the Q-factor of the mode and inversely proportional to the mode volume. Purcell factors up to 10 have already been realised in QD pillar cavities. Due to this cavity effect, the lifetime of the photon emission is dramatically reduced with respect to its value in bulk semiconductors, hence also allowing high repetition rates (~ 1 GHz) of these kinds of single photon sources.

Autocorrelation measurements have been performed to demonstrate single-photon generation under pulsed excitation of QDs in pillar microcavities with different pillar diameters. For instance, **(08)** shows the measured unnormalized correlation function n(τ) of the fundamental mode of the 6 µm pillar **(08a)** and of the XX QD emission from the 0.3 µm pillar **(08b)**. The corresponding PL spectra are given in **(05b)** and **(06b)**, respectively. The measured n(τ) of both pillars exhibit peaks at integer multiples of the laser pulse repetition period T_{rep} = 13.12 ns, indicating a locking of the photon emission to the pulsed excitation. The correlation peak areas are related to the conditional probability to detect a second photon (on the stop) after the first photon has already been detected during the excitation cycle. As expected, for the 6 µm pillar diameter all correlation peaks have the same areas which is expected for a Poissonian light source.

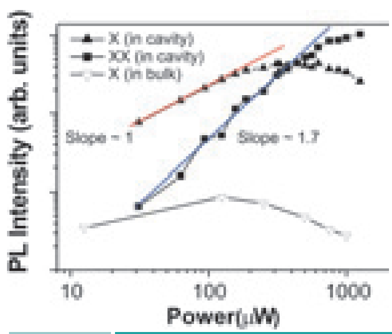

07

Continuous-wave laser power dependence of the X (closed triangles) and XX (squares) intensities from a QD located in a 0.6 µm diameter pillar microcavity in comparison to excitonic emission from a QD in a bulk semiconductor (open triangles).

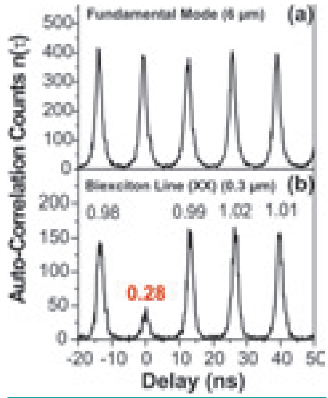

08

Autocorrelation measurements under pulsed laser excitation obtained from (a) a fundamental mode of a 6 µm diameter pillar (PL spectrum in **(05b)** *and (b) the XX photon of a 0.3 µm diameter pillar (PL spectrum in* **(06b)**).

This is due to the fact that many QDs contribute independently to the mode emission. In contrast to the 6 µm pillar, the central peak at τ = 0 ns of the 0.3 µm pillar is significantly suppressed, demonstrating the single-photon nature of the emitted light. However, for a perfect single-photon emitter one expects $g^{(2)}(0) = 0$. For the 0.3 µm pillar, $g^{(2)}(0) = 0.28$ is observed for the central correlation peak which does not reach its theoretical value of zero. This is attributed to the presence of a weak uncorrelated background originating mainly from the wetting layer and leaky modes.

In order to prove the cascaded nature of XX and X emission, cross-correlation mea-

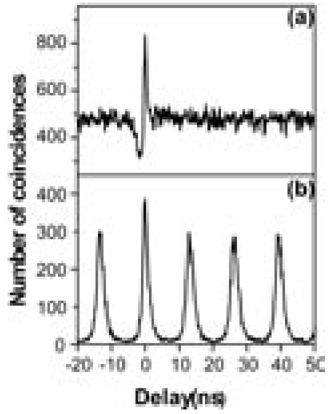

09

Cross-correlation measurements of X (stop) and XX (start) photons from a 0.6 µm diameter pillar recorded under (a) cw laser excitation and (b) pulsed excitation, respectively.

THE AUTHORS

Dr. Mohamed Benyoucef (l.)

received his Ph.D. degree from the department of physics, University of Bristol (UK) in Febraury 2002. Having worked as a research associate at the Institute of Solid State Physics (University of Bremen) and the 5th Institute of Physics (University of Stuttgart), he started in August 2005 in the MBE group at the Max-Planck-Institute for solid state research, Stuttgart. His current research interests include self-assembled quantum dots, quantum dots in microcavities, microcavity lasers, semiconductor nanostructures, and development of single photon sources.

Prof. Dr. Peter Michler (m.)

is the head of the department "Neue optische Materialien und Technologien" at the 5th Physics Institute of the Universität Stuttgart. His group studies the fundamental electronic and quantum optical properties of semiconductor nanostructures with respect to applications in photonics and quantum information technology.

Sven Marcus Ulrich (r.)

studied physics at the University of Bremen (Germany) where he received his diploma degree on "Optical Spectroscopy of Donor-Acceptor Pair Recombinations in GaN:Mg" in 2001. His current Ph.D. work as a scientist at the 5th Institute of Physics (Universität Stuttgart) focuses on the generation of non-classical light states from individual semiconductors quantum dots, with particular interest in single and cascaded photons, as well as QDs in microcavity laser structures.

Contact

5. Physikalisches Institut, Universität Stuttgart, Pfaffenwaldring 57, 70550 Stuttgart
Tel. +49 (0)711 685 4660
Fax +49 (0)711 685 3810
E-mail: p.michler@physik.uni-stuttgart.de

surements were performed on the 0.6 µm diameter pillar. The PL spectrum is depicted in **(06a)**. **(09a)** shows the cross correlation measured by using the XX transition to trigger the start channel and the X to supply the stop, recorded under cw laser excitation. The cross correlation reveals asymmetric features, i.e., bunching ($\tau > 0$) and antibunching ($\tau < 0$) due to cascaded emission. In detail, there is a suppressed probability to detect an exciton photon before the biexciton which leads to the observed antibunching behaviour. The dip in the cross correlation in the vicinity of $\tau = 0$ again does not reach its theoretical value of zero due to the presence of an uncorrelated background. For $\tau > 0$ the enhanced probability to observe an X decay following an XX photon gives rise to the bunching behaviour. We have repeated the same cross-correlation experiments under pulsed excitation, the histogram of which is shown in **(09b)**. Again the cross-correlation displays a series of peaks separated by the laser period of 13.12 ns. The zero delay peak integral appears larger than the other peaks ("bunching"), which again reflects the cascaded nature of subsequent X photon-XX photon decay processes. This bunching effect is the signature for the generation of triggered photon pairs. Note that similar results were found for the 0.3 µm diameter pillar.

In conclusion, we have demonstrated the possibility of using the biexciton-exciton radiative cascade of a single quantum dot (QD) in a pillar microcavity to efficiently generate triggered photon pairs. Due to the enhanced photon collection efficiency out of the cavity structure an increase of the photoluminescence intensity by a factor of ~ 40 was found as compared to the corresponding QD PL intensity in bulk semiconductor material.

5. Outlook

The presented experimental results have demonstrated the high potential of semiconductor nanostructures for the realization of single-photon sources and photon pair emitters. However, a few technological challenges remain for practical devices. The currently investigated QDs emit in the near infrared spectral region (0.85 µm – 1 µm) and possess shallow electronic confinement potentials which prevents a high quantum efficiency of the emission at temperatures above ~ 50 K. CdSe/Zn(S,Se) or (In,GaN)/GaN QDs with higher electronic confinement potentials and higher biexciton binding energies may provide a solution for room temperature operation in the blue-green spectral region. Promising results from CdSe/Zn(S,Se) QDs have been recently reported by us [1]. We observed the generation of triggered single-photons with epitaxially grown self-assembled CdSe/Zn(S,Se) QDs for temperatures up to 200 K. For fiber-optical communications one would prefer to use the dispersion and absorption minima of the optical fiber at ~ 1.3 µm and ~ 1.55 µm, respectively.

Very recently, first results for the 1.3 µm telecom fiber range have been reported from the group of A. Shields from Toshiba [3]. They reported on-demand single photon emission from a microcavity sample with a low density of large InAs/GaAs self-assembled quantum dots into the fiber-optic transmission band at 1.3 µm.

A precondition for mass production of devices is the *controlled* coupling of the QD emission to a cavity mode with directional field profile in order to achieve a high photon collection efficiency. For this task the spatial position of the QD and the energy of its transition has to be adjusted with respect to the maximum of the mode profile and the energy of the cavity mode, respectively. The former task is still a challenge although considerable progress has been made on pre-patterning of MBE samples to create nucleation spots on which QD growth takes place. Together with our colleagues from the Max-Planck-Institut für Festkörperforschung, Stuttgart (Group of O.G. Schmidt), we are planning to tackle this challenging task in the near future. The energetic resonance condition can be achieved by temperature tuning or by electric field tuning via the quantum-confined Stark effect. However, the QD transition energies are only defined within a relatively broad inhomogeneous linewidth (~ 10 – 30 meV) of the corresponding QD ensemble. That implies that several QDs have to be placed inside a cavity so that one can be tuned into resonance. Therefore, control of QD exciton energies during or after growth by e.g., an annealing technique would certainly constitute a breakthrough for numerous applications.

In summary, the ongoing progress on the fabrication procedure of pillar cavities and quantum dots opens the way to highly-efficient single-photon sources and new types of applications in the field of quantum information technology.

Mohamed Benyoucef
Sven Marcus Ulrich
Peter Michler

References

1 K. Sebald *et al.*, Appl. Phys. Lett. **81**, 16, 2920 (2002).
2 M. Benyoucef *et al.*, New Journal of Physics **6**, 91 (2004).
3 M. B. Ward *et al.*, Appl. Phys. Lett. **86**, 201111 (2005).

zurück zum Inhalt

THz radiation: The no-man's-land between optics and electronics

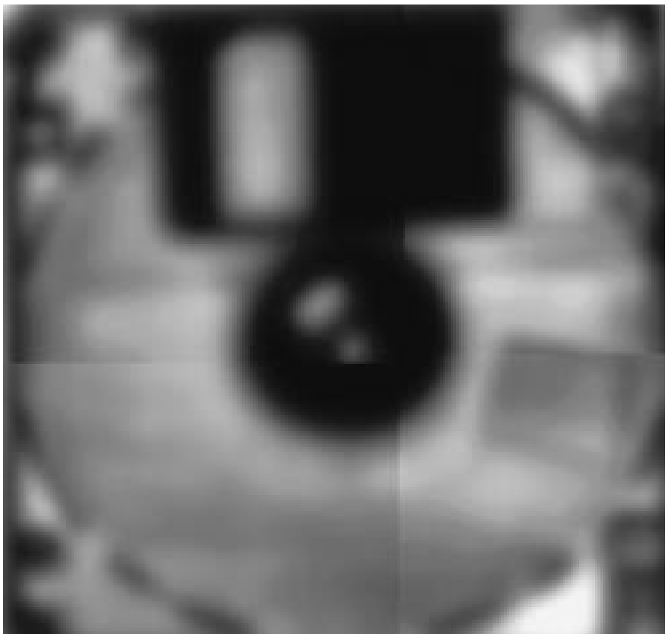

After James Clerk Maxwell had developed his famous equations in 1864, which predicted the existence of propagating electromagnetic waves, scientists started to explore the areas beyond the small spectral region humans can detect with their bare eyes. Heinrich Hertz was the first who demonstrated that radio-waves and light are the same kind of radiation only at different frequencies. And Heinrich Rubens wrote in a famous article about 'Heat rays of great wave length' in 1897: "since we become accustomed to think of electrical energy and light waves as forming component parts of a common spectrum, the attempt has often been made to extend our knowledge over the wide region that separates the two phenomena, and bring them closer together". More than hundred years later, heat rays are called infrared radiation and electrical energy can be produced up to frequencies of several hundred GHz employing semiconductor devices; but still there is a small nearly untouched region between optics and electronics, the so called THz gap, sketched in **(01)**.

SUMMARY

Between the highest frequencies which can be generated by electronic devices and the lowest which can be handled with optics, there is a nearly untouched region, the so called THz-gap (300 GHz to 10 THz). Despite this problems of generating and detecting radiation at these frequencies, the THz range is rich in interesting scientific questions and potential applications for example in material science and medicine. THz-rays can penetrate matter similar to x-rays, but they are non-ionizing and therefore assumed to be harmless and they give specific spectroscopic information not accessible with other optical techniques in the visible or infrared, with x-rays or nuclear magnetic resonance. But broader applications and the development of new techniques in this interesting frequency range are hindered by the lack of compact, cheap and easy to handle THz-sources. Additionally for most imaging applications a good resolution is required. Unfortunately THz-radiation has a very long wavelength (1mm – 30 µm). Therefore the maximum resolution in the far-field is strongly limited by diffraction. Here we want to give on the one hand a short overview over the interesting scientific questions which can be investigated in the THz-range, on the other hand we want to show same application from material science and medicine.

1. Introduction

In our days the limits of this THz range are generally taken to be 300 GHz – 10 THz or in wavelength between 1mm – 30 µm. On the low energy side (microwaves) of this region, cables and hollow metallic waveguides are utilized to transport the energy, but it is hard to built circuits capable to handle higher frequencies. On the high energy side (infrared) one has normal optics with lenses and mirrors to guide the freely traveling waves, but new optical components and sources have to be developed for larger wavelength. Experiments in the THz-region are still challenging largely due to a lack of compact and easy to handle sources and detectors.

Despite these problems, the THz range is rich in interesting scientific questions and potential applications. THz-rays can penetrate matter similar to x-rays, but they are non-ionizing and therefore assumed to be harmless and they give specific spectroscopic information not accessible with other optical techniques in the visible or infrared, with x-rays or nuclear magnetic resonance. For example, THz-rays penetrate many visually opaque materials such as paper, plastics and clothes but are strongly absorbed by water and metals. Many specific excitations lie in the THz-range, like molecular vibrations and librations, or low-energy excitations in solids. The role of protein structure on molecular recognition had been investigated by X-rays and NMR spectroscopy since long. However, only recently the role of protein dynamics had been recognized. Due to the large 3-dimensional structure of proteins this dynamics lies mainly in the THz-range.

Even the echo of the Big Bang, the cosmic background radiation, peaks in the THz-region as displayed in **(02)**. Since the photon energy of a few meV is comparable to a few Kelvin in temperature and a few Tesla in magnetic field, the THz spectral range is ideally suited to study superconductivity and similar collective phenomena. Fundamental concepts of solid state physics can be tested, new states of matter can be investigated, and the scaling laws close to quantum phase transitions. As a consequence of the confinement also in Nanoscience many excitations lie in the THz-range.

Based on decades of experience and strong efforts, the 1. Physikalisches Institut at the Universität Stuttgart became a center of THz research on solids well recognized throughout the world. Using Fourier transform spectrometers with Helium cooled bolometers as detectors in the far infrared and coherent source THz spectrometers based on backward wave oscillators a huge variety of new materials can be investigated. Also novel approaches are surveyed to create tunable continuous-wave THz radiation, for instance by mixing two solid state lasers with the help of non-linear devices in order to obtain the difference frequency which is chosen to lie in the THz range. These compact and easy-to-use THz sources might become the heart of future spectrometers to discover the *terra incognita*. But also small parts, like lenses, beam splitters, polarizers, attenuators, etc. have to be developed and optimized. To this end, material properties have to be investigated, design studies to be made, numerous tests to be conducted. Photonic crystals and even materials with negative refractive index are among the possible novelties which are discussed for this particular spectral range. Only slowly a network of competent laboratories is

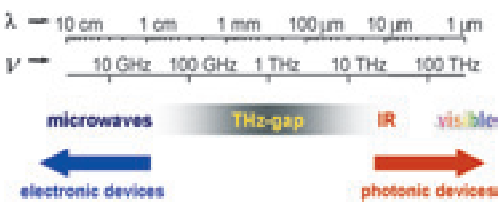

01

The electromagnetic spectrum still includes a gap between microwaves and infrared region which contains a wealth of interesting phenomena and potential applications, but which is explored only to a very small extend.

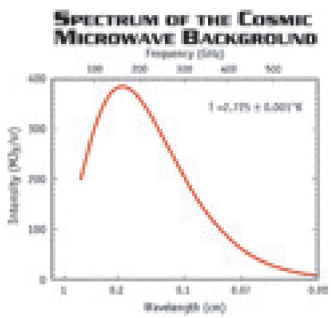

02

Spectral intensity of the cosmic background radiation. Tiny deviations from Planck's radiation law yield information on the origin of the universe.

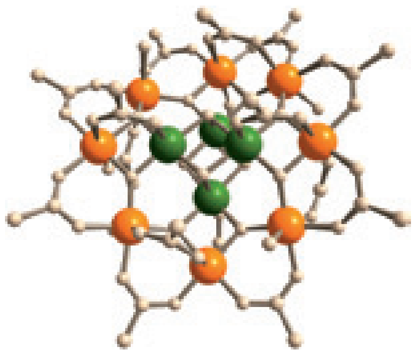

03a

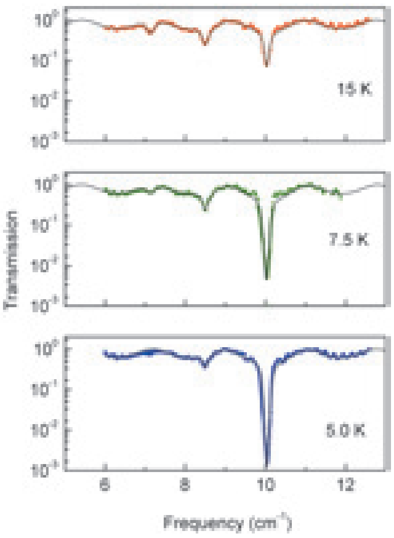

03b

03c

a *Nanomagnets are the smallest possible magnetic structures. $Mn_{12}ac$ is considered the prime example of this class of novel materials.*
b *Due to the coupling of the magnetic atoms in the molecule characteristic low energy excitations in the THz-range can be observed.*
c *The photograph shows the THz-spectrometer at the 1. Physikalisches Institut at the Universität Stuttgart.*

formed to enable the exchange of experience and know-how between the different scientific communities which participate in this unique endeavor.

2. Basic research

Nanosized materials can be achieved by either structuring large samples for example by lithography (top-down approach) or by assembling small nanometer-sized building blocks, as single atoms or molecules, to larger units (bottom-up approach).

A new bottom-up approach in the design of magnetic materials for high-density data storage and quantum computation goes in the direction of single molecule magnets. They are exchange coupled clusters of four to about thirty paramagnetic ions, usually from the first period of the transition metals, that have large spin ground states, for example S = 10. They do not interact with each other. Some of these molecular magnets can be magnetized at low temperatures, and will remain magnetized even after removal of the external field. For this reason these systems have been dubbed “single molecule magnets”. Applications in data storage devices have been proposed. The maximum theoretical data density would be up to 10 000 times what is possible today, since every molecule can be considered as a bit of data. Beyond that even applications in spintronics and quantum computers could be possible. Apart from these promising perspectives, their physical properties are also hugely interesting, due to their mesoscopic size of the systems. Molecular magnets show many distinct quantum properties like quantum tunneling of the magnetization. In order to optimize these macromolecules and tailor the physical properties, a close collaboration between chemists, material scientists and physicists is required. To investigate the material parameter, we have developed a novel spectroscopic technique in the THz range of frequency, which can be described as Frequency Domain Magnetic Resonance Spectroscopy. As an example the spectrum of a nanomagnet recorded at our institute is shown in **(03)**. We nicely observe the transitions between the magnetic sublevels split by the crystal field.

Superconductivity is one of the most fascinating phenomena in solid state physics which did not lose any of its challenge and attraction to theory and experiment. Although we have a rough understanding how superconductivity works in most conventional metals, high-temperature superconductivity still remains a mystery. The superconducting electrons form pairs due some attractive interaction, usually lattice vibrations, but also magnetic interaction is discussed as a possibility. For typical superconductors like niobium it takes the energy of a few milli-electron-volts (1 meV corresponds to 8 cm^{-1} which corresponds to 240 GHz) to break up this pair and this can best be investigated by THz spectroscopy. In **(04)** the electrodynamic response is displayed in the real and imaginary parts of the conductivity. Clearly seen is the development of the gap-like feature around 20 cm^{-1} as the temperature drops below $T_c = 8.31$ K.

Due to the severe experimental constrains and non-availability of commercial instruments, only very few laboratories worldwide are capable of performing these com-

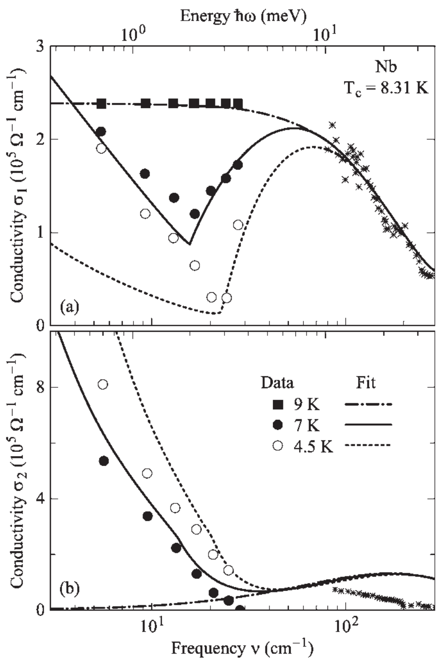

04

Frequency dependence of the real and imaginary parts of the conductivity in niobium at various temperatures. The transmission through a 150 Å thick film on sapphire was measured by a Mach-Zehnder interferometer; the stars were obtained by reflection measurements. The solid lines correspond to the theoretical prediction. The inset shows basically shows the fraction of condensed charge carriers.

plicated experiments by now, Stuttgart certainly is among the leading ones.

3. Potential applications

Beside fundamental research there are also a large number of potential applications in the THz range ranging from so different fields as non-destructive testing and quality control, over homeland security to new medical imaging techniques and rapid screening for the development of new drugs. None of them is thoroughly explored nor well established, let alone commercially available. However, even if only a fraction of them materialize, the financial implications would be tremendous. All this gives strong motivation to develop new systems for generating, detecting and manipulating radiation at THz frequencies.

During the last five years worldwide activities in THz research can be observed and, in particular in the United States, the funding has multiplied and numerous laboratories and companies mushroomed.

Most real samples, biological as well as artificial, are spatial inhomogeneous. For their characterization imaging techniques and microspectroscopy are very important. Unfortunately the extremely long wavelengths of up to a millimeter in the THz range cause severe problems in the optical design due to diffraction and unintended interference (standing waves). In principle near-field techniques can overcome this problem. But sub-wavelength pinholes with radius r reduce the intensity proportional to r^6 and they show exponential signal decay with the probe-sample distance. Therefore it is often hard to find a good compromise between intensity and resolution and the probe-sample distance had to be controlled accurately. This is in principle also true for apertureless methods using small tips as near-field probes. With these methods superior resolution can be achieved, but they image only the sample surface, which especially in the field of life science is often not the relevant information. Another complication is, that in the THz-range biological samples show only little differences in their overall optical properties. On one side this requires a large dynamic range (high S/N ratio) on the other side the interpretation of the observed image contrast calls for additional spectroscopic information.

In the visible the development of solid-immersion lens (SIL) techniques has dramatically increased the capacity of optical memories. Due to the ionic polarisation the refractive index of all mate-

05

A silicon hemisphere serves as a solid immersion lens for the THz spectral range in order to increase the spatial resolution of imaging applications by n = 3.5.

06

Custom-designed and special-made hyperbolic lens of polyethylene suitable for the THz range of frequency.

ZUSAMMENFASSUNG

Zwischen den höchsten Frequenzen, die elektronisch erzeugt werden können und den tiefsten, die optisch nutzbar sind, befindet sich ein bis jetzt wenig erforschter Bereich des elektromagnetischen Spektrums, der THz-Bereich (etwa 300 GHz bis 10 THz). Obwohl technologisch schwer zugänglich, ist dieser Frequenzbereich doch reich an interessanten wissenschaftlichen Fragestellungen und es wird ein großes Anwendungspotenzial in der Medizin, Pharmazie und in den Materialwissenschaften gesehen. THz-Strahlen durchdringen Materie ähnlich wie Röntgenstrahlen. Sie sind aber nicht-ionisierend und liefern spezifische spektroskopische Informationen, die mit anderen Techniken im Sichtbaren, mit Röntgenstrahlen oder NMR nicht zugänglich sind. Einer breiteren Anwendung und der Entwicklung neuer Messverfahren in diesem interessanten Frequenzbereich steht aber ein Mangel an kompakten, billigen und leicht zu handhabenden Quellen entgegen. Außerdem benötigt man für alle Abbildungsverfahren eine gute Auflösung. Die Wellenlänge von THz-Strahlung ist aber sehr lang (1mm – 30 µm). Deshalb ist die maximal erzielbare Auflösung im Fernfeld stark beugungsbegrenzt. Der Artikel soll auf der einen Seite einen kurzen Überblick geben über die wissenschaftlichen Fragestellungen, die mit THz-Strahlung bearbeitet werden können, und auf der anderen Seite einen Einblick in Anwendungsmöglichkeiten in der Materialprüfung und der Medizin geben.

07

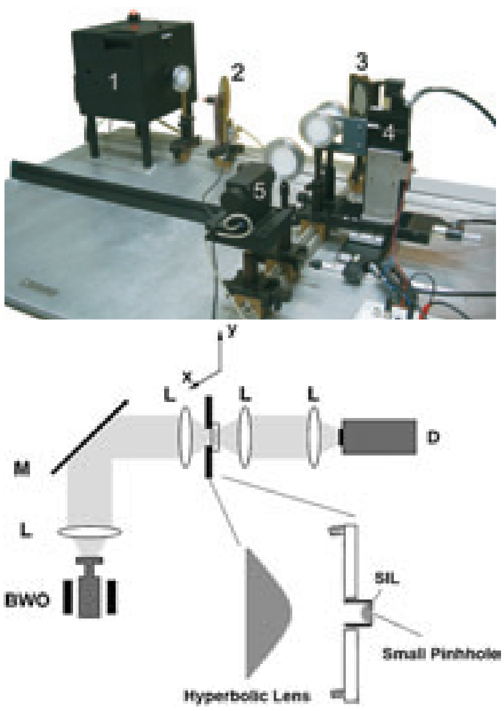

Simple setup utilized to obtain THz images in transmission geometry: (1) Backward wave oscillators in a permanent magnet serve as powerful, tunable and coherent radiation sources; (2) chopper connected to lock-in amplifier enables the operating even at low signal-to-noise ratio; (3) mirror or beamsplitter to guide, polarize and attenuate the radiation; (4) computer-controlled xyz-translation unit; (5) Golay cell radiation detector. The optical layout is sketched in the lower part. SIL: Solid immersion lens.

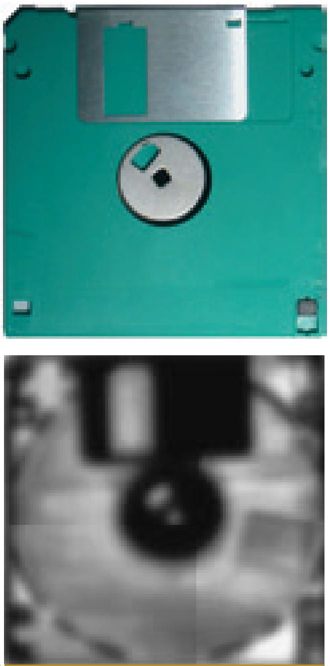

08

Floppy disk non-destructively tested by THz radiation. The THz image was taken at $\lambda = 1$ mm corresponding to 290 GHz. The plastic parts are more or less transparent for THz-rays, whereas metal is opaque.

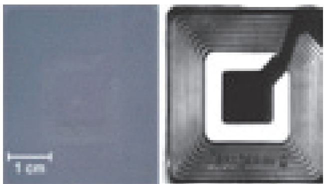

09

Electronic security tag with fine antenna structure. Only the THz radiation can penetrate the plastic housing and reveal the interior. Solid immersion lenses allow a resolution well below the used wavelength.

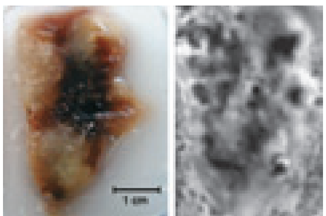

10

Photograph and THz image of cancer cells: oesophagus (gullet) carcinoma of a horse embedded in paraffin. Taking THz spectra of the bright spots reveals distinct differences between healthy and cancerous tissue which go beyond the water content.

rials is much lower in the visible than in the THz-range, where values of up to 10 are possible. Recently we have shown that THz-radiation can be focused beyond the Abbe diffraction limit with a hemispherical SIL **(05)**. A photograph of the THz micro-spectrometer using a solid immersion lens for resolution enhancement is reproduced in **(07)**; also shown is a sketch of the optical layout. As THz-sources we use backward-wave oscillators (BWO), which supply highly monochromatic ($\Delta\nu/\nu \approx 10^{-6}$) and coherent radiation with an output power of up to 300 mW. The emitted radiation is collimated by a plan/convex polyethylene (PE) lens to a parallel beam with a diameter of about 23mm and afterwards focused to a diffraction limited spot on the microscope stage by a hyperbolic lens. The advantage of plano/hyperbolic PE lenses **(06)** is, that they produce, comparable to mirrors, aberration-free foci but allow much higher numerical apertures. In this frequency range they show no dispersion and can be easily produced by a computer-controlled lathe with high optical quality (roughness better than $\lambda/10$). The microscope stage (enlarged drawing in **(07)**) consists of a hemispherical silicon SIL ($n = 3.5$) with 8mm diameter clued on a thin (80µm) copper foil with a pinhole in the diameter of the reduced wavelength (λ/n). The sample is scanned in close contact to the pinhole and the transmitted intensity is collected by a confocal arrangement and than focused on the detector. SIL imaging is not really a near-field technique, which means, that beside the possibility to improve the resolution without cost of intensity, the probe-sample distance can be much larger than in normal near-field setups without a significant decrease of resolution.

As an example of non-destructive testing in **(08)** a Floppy disk is imaged by THz radiation. The image was taken at $\lambda = 1$mm (290 GHz) with low resolution in the far field. The plastic parts are more or less transparent for THz-rays, whereas metal is opaque. In **(09)** as an example of a high resolution image recorded with a SIL a security tag encapsulated in a plastic housing is shown; the THz transmission image clearly shows the fine antenna structure with subwavelength resolution.

(10) represents a photograph and a THz-image recorded at 0.48 THz cm^{-1} of oesophagus cancer from a horse. To stabilize the tissue it was embedded in wax. Whereas in the photograph the metastases are bright they appear as dark regions in the THz-image. Due to the fact that THz-radiation can penetrate tissue up to several millimetres, the THz-image shows much more details of the metastases than the photo. Details form inside the sample down to about 100µm can be resolved.

In order to go further beyond the Abbe's diffraction limit real near-field techniques had to be used. Although no radiation can propagate through an aperture considerably smaller than the wavelength, it is possible to utilize the evanescent waves to probe matter which is placed very closely behind the pinhole. This so-called near-field approach is well established for imaging in the near-infrared and visible spectral range. Very recently we were able to realize a near-field spectrometer in the THz range of frequency which allows us to take images with a spatial resolution of $\lambda/10$ or even $\lambda/100$ and at the same time obtain complete spectral information at each pixel in a reasonable period of time.

Although many visions might not be realistic and things are more complicated than anticipated, for sure the THz gap is about to be closed even when it always remains a difficult territory to work in. For basic solid state research this spectral range is already indispensable, and now more and more scientist form other disciplines, as biology, chemistry, geology, medicine, pharmacy, just to name a few, step into this unknown region and find new and exiting questions and applications in their fields. • *Martin Dressel, Bruno Gompf*

THE AUTHORS

Martin Dressel (r.)

received his doctor of science degree in 1989 form the Universität Göttingen where he subsequently worked as a postdoctoral research fellow. Since then he has held positions in the University of British Columbia at Vancouver; the University of California, Los Angeles; the Technische Universität Darmstadt; and the Center for Electronic Correlations and Magnetism at the Univerisität Augsburg; Prof. Dressel is now head of the 1. Physikalisches Institut at the Universität Stuttgart.

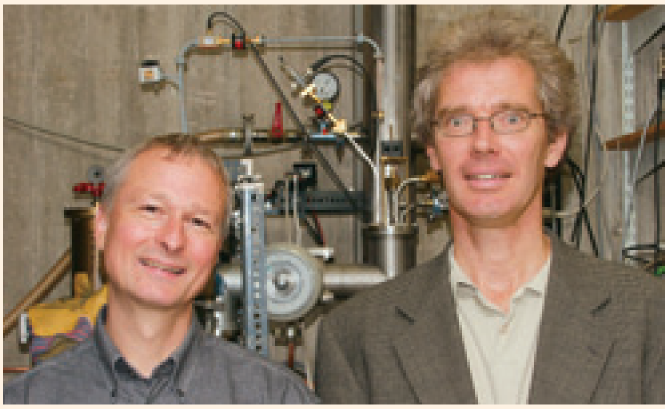

Bruno Gompf (l.)

received his doctor of science degree from the Universität of Tübingen in 1990. Since then he is at the 1.Physikalisches Institut at the Universität Stuttgart.

Contact
1. Physikalisches Institut, Universität Stuttgart, Pfaffenwaldring 57
Tel. +49 (0)711 685 4949, Fax +49 (0)711 685 4886
E-mail: gompf@pi1.physik.uni-stuttgart.de

zurück zum Inhalt

White light lasers and their applications

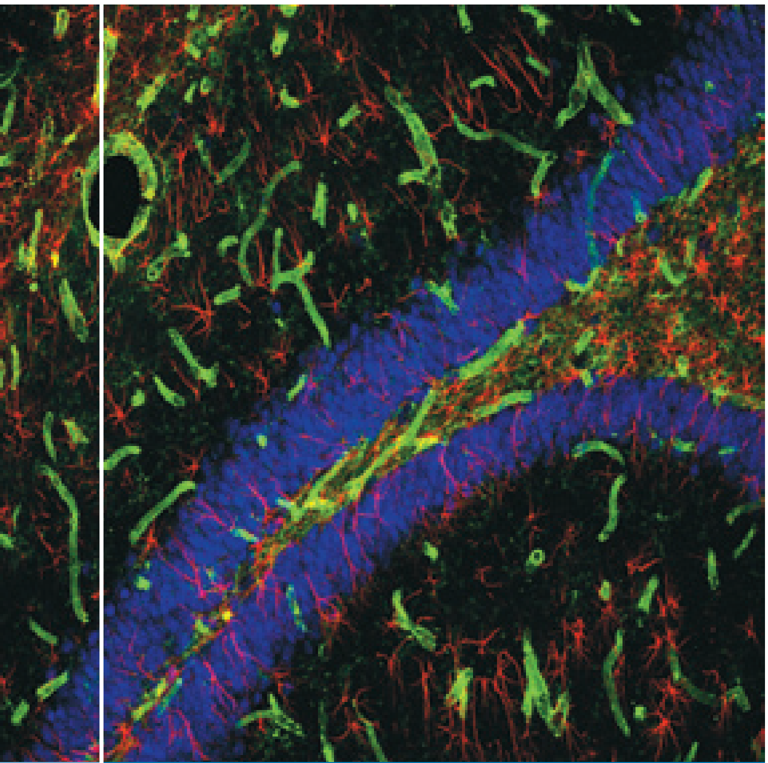

The generation of white laser light has been a very hot topic of research within the last five years. The term “white laser light” implies a continuous spectrum, including all wavelengths from blue to red and all the way into the infrared spectral range. An incandescent light bulb will also generate such a broad white light spectrum, however, its fundamental properties are completely different. Excellent focusing properties, high spectral density, and a small divergence of the white laser light are some of the unique advantages. Additionally, spectral, temporal, and spatial coherence are especially beneficial properties of the white laser light. Coherence means that two different parts of the laser light have a certain fixed phase relationship with respect to each other.

1. Basics

Generating such white laser light requires very high optical power densities (Gigawatts/cm^2), as the physical mechanism is based on highly nonlinear optical processes. This means that the effects depend on the square, the third, or even higher powers of the electric field of the light. In order to achieve such high power densities, pulsed ultrashort laser sources are being focused into small areas, preferentially into glass fibers with a core diameter of only a few µm. Typically so-called photonic crystal fibers and tapered glass fibers are being used. Pulsed lasers can achieve extreme peak powers of several kilowatts per pulse. As pump sources, typically femtosecond lasers are utilized, however, picosecond and nanosecond pump sources have also been demonstrated to be useful for white light continuum generation.

The major physical processes involved in converting the spectrally narrow pump light into the broad spectrum include self-phase modulation due to Kerr-nonlinearities, soliton formation due to the interplay between anomalous dispersion and self-phase modulation, soliton break-up due to higher order dispersion, and Raman shifting of the solitons, leading to nonsolitonic radiation in the short wavelength regime.

The glass fibers possess a certain dispersion characteristics, i.e., light of different colors travels at different speed inside the fiber. Additionally, the fiber core diameter should be quite small in order to concentrate the light in a small area to increase the power density.

The fiber core diameter also influences the dispersion properties of the fiber, hence, optimizing the white light generation requires a specific fiber design, taking parameters such as group velocity dispersion and power density into account.

In order to achieve a small and rather flat anomalous group velocity dispersion characteristics, the right choice of refractive indices for the different glasses of fiber core and cladding and the optimum dimensions have to be calculated for a given pump wavelength, pump pulse duration, and pump power.

Tapered fibers are manufactured from standard fibers, which are pulled over a gas flame into several centimeter long strands. The diameter of the tapered fiber shrinks from 125 µm to only about 2 µm, and lengths of more than 20 centimeter are attainable. 2 µm is only one fifth of the diameter of a spider web, and only one fifteenth of the diameter of a blonde human hair!

Such a tapered fiber consists after flame-drawing of two untapered parts which resemble a standard single mode fiber, two taper transition regions where the light is being confined, and the waist region where the highly nonlinear processes take place. Its intrinsic advantage over photonic crystal fibers is the convenient, stable, and easy input and output coupling. This is an important prerequisite for possible applications of such fibers.

Astonishingly, tapered fibers are quite robust when encapsulated in an appropriate holder, and even dropping them onto the floor does not necessarily destroy them. This is due to the fact that the weight of the extremely thin waist is much smaller than a hair or a spider yarn – therefore its own inertia cannot destroy it.

Pumping the fiber with pico- or nanosecond pulses requires interaction lengths between the light and the fiber waist of several centimeters – therefore longer tapered fiber waists are required in order to generate white laser light in combination with such cheap, simple, and robust laser systems.

2. Applications: general

Possible applications for white light lasers include optical coherence tomography, frequency metrology, spectroscopy, and linear / nonlinear microscopy. Usually, ultrashort laser pulses are generated by a titanium-sapphire laser, which is pumped by a frequency-doubled diode-pumped solid state laser, using $Nd:YVO_4$ as laser crystal. This laser light is coupled into the tapered fiber, and the resulting white light can have output powers up to 400 mW at a repetition rate of 80 MHz. The spectrum stretches from 400 to 1400 nm. Such a white light system, however, has a price tag of more than 100.000 EUR. This number limits the possible applications.

New and modern solid state laser sources with ultrashort pulse durations have become available over the last few years. Combining these sources with tapered fibers results in novel compact and relatively inexpensive white light lasers. An example for such a combination consists of a diode-pumped Yb:glass femtosecond oscillator in combination with a tapered fiber. Size and price of this system are drastically reduced due to the convenient absorption properties of the Yb crystal (at 980 nm, where cheap and high-brightness laser diodes from telecom applications are available) and the SESAM-modelocking technology, which was recently awarded the Leibinger-prize.

The laser emits 200 fs pulses at 20 MHz repetition rate and at a wavelength of 1040 nm. Its output power can reach 1 Watt. The resulting white light continuum has an average power of about 200 mW and stretches from 500 nm to beyond 1700 nm.

A different pump technology utilizes a passively modelocked $Nd:YVO_4$ oscillator, which is diode-pumped at 808 nm. This system, emitting at 1064 nm, offers repetition rates up to 120 MHz and pulse durations of about 8 ps. An amplified version at 80 MHz reaches even average power levels of 30 W. Successful white light generation using three similar tapered fibers that

SUMMARY

White light lasers are a new class of lasers, emitting not just a single color, but rather covering a wide range of the wavelength spectrum. White light lasers, covering the whole visible range from blue, green, yellow, red, into the infrared, have been developed. Until recently, such lasers were not available, and only ultrashort laser pulse technology paved the way towards their realization. However, commercial applications were scarce due to their high prize tag. Over the last couple of years, diode pumped ultrashort solid state laser technology together with tapered glass fibers allowed the fabrication of compact, cost-effective white light lasers. We are going to describe the key developments of this field and present a number of applications.

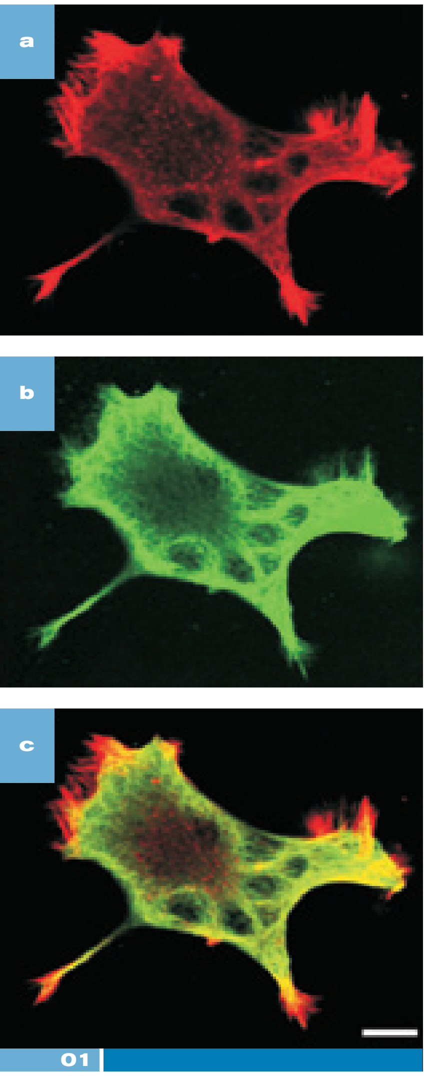

(01 a) *shows the actine cytoskeleton of a neuroblastoma cell which was stained with TRITC-phalloidine dye.* **(01 b)** *shows the microtubuli cytoskeleton, which was stained using Alexa-488 dye.* **(01 c)** *is the overlay of* **(01 a)** *and* **(01 b)**. *The white laser light was generated in a tapered fiber with 2.1 µm diameter, using 650 mW of titanium-sapphire laser light at 803 nm and 76 MHz repetition rate. The generated white light had an output power of 280 mW, which was coupled into a commercial Leica CLSM microscope – instead of the standard cw lasers. The scale bar corresponds to 10 µm.*

were spliced together resulted in 5.6 W of white light, with a spectrum from 460 nm to 1600 nm. These kinds of power levels enable the user of this white light system for 3-dimensional measurements of objects of several decimeters diameter.

3. Application: Nonlinear microscopy

Possible applications usually require a continuous spectrum with a high spectral power density. One example of such an application is microscopy. Different regions of biological cells are being stained with a variety of fluorescent dyes, allowing

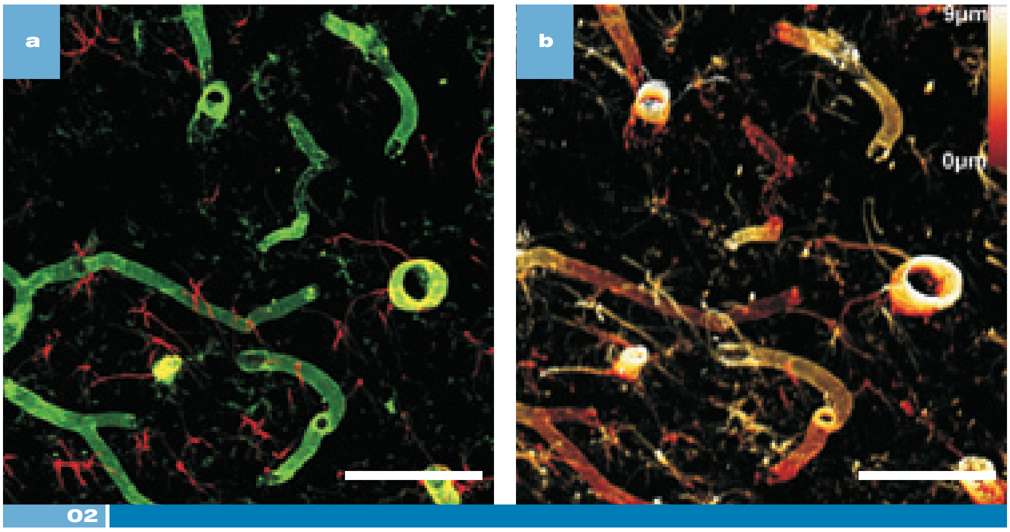

3D image of astrocytes of a rat brain, stained with Cy3 (depicted in red) and blood vessels of the brain (depicted in green), stained with Cy2. The scale bar corrsepsonds to 50 µm. The color coding in **(02b)** *contains the information about the third dimension of the tissue structure.*

the observer to distinguish between the alternating functional units. Each of such dyes absorbs light of a different spectral region and emits a new color. In order to excite the dyes, a finite number of continuous lasers is usually used. Typically three to four lasers are integrated in a fluorescence microscope. This means that, in principle, up to four different species within biological tissue can be distinguished by the different fluorescent colors.

Using a white light laser, basically hundreds of different colors are possible. Recently, quantum dots have become available for dye-staining of biological samples, and in combination with the white light laser, distinguishing between a large number of different species comes into reach.

As an example, we conducted an experiment together with Prof. Käs, Timo Betz, and Daniel Koch at the University of Leipzig, using neuroblastoma cells. **(01)** demonstrates a multi-color fluorescence confocal microscopy image of these cells, differentiating between the actine cytoskeleton, using the dye TRITC-phalloidine **(01 a)**, and the microtubuli cytoskeleton, stained with the dye Alexa-488 **(01 b)**. **(01 c)** demonstrates nicely how the overlay of the two previous image with different colors gives a 3D impression of the cell.

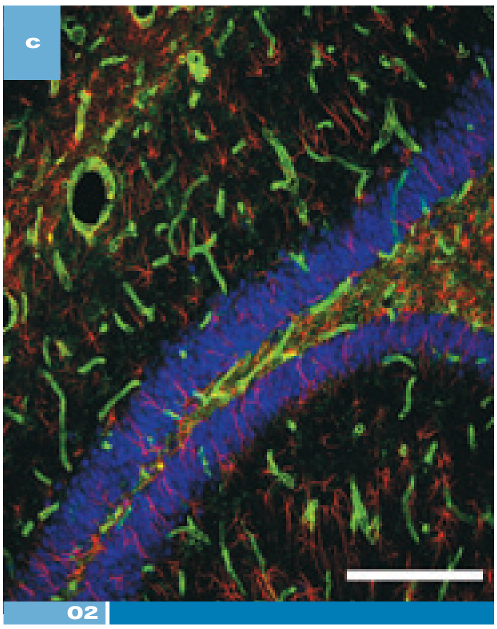

Same as **(02a)** *and* **(02b)**, *but using a third dye (Cy6) to stain the neuronal cell bodies. The scale bar is 100 µm.*

The output spectrum of the tapered fiber was optimized in a way to generate most spectral intensity in the blue and green wavelength region, where the two dyes absorb most light. Using filters (for example a combination of acousto-optical beam splitters), the optimum excitation and detection wavelengths could be selected.

(02) demonstrates the use of this method to look into the functional structure of a rat brain. Astrocytes and blood vessels can nicely be distinguished **(02a)**, and with the aid of the confocal microscope, even height information can be retrieved **(02b)**. The dyes for staining in this case were Cy3 for the astrocytes and Cy2 for the blood vessels.

When extending the staining to even three dyes (including Cy6 for the neuronal cell bodies, depicted in blue), the images become even more impressive **(02c)**.

A different way for obtaining height information and slicing the sample optically is multi-photon microscopy. The biological sample absorbs two pump photons only within the laser focus volume, which is about 1 μm^3 in size, and emits at a longer wavelength. The advantage of the white light laser source is besides its large spectral tunability also the short pulse duration and the high spectral power of the laser pulses. Therefore, multiphoton microscopy is possible, even for different pump laser wavelengths.

We have demonstrated this simultaneous possibility for the first time, as can be seen in **(03)**. The neuroblastoma cells are being exposed to the spectral region from 700–1300 nm of the ultrashort white light.

4. Application: Laser microdissectioning

The short laser pulses of the white light are also useful for laser dissectioning of cells. The company PALM Microlaser Technologies AG produces systems for microdissection and micromanipulation in cells. They can cut out for example cell nuclei and manipulate them out of the cell framework. The applied method is called LMPC (laser microdissection and pressure catapulting). Conventionally, they focus a nanosecond nitrogen laser onto the cell and cut right through it, for example in order to separate a cell from adjacent tissue. Subsequently, the laser beam is defocused and the water below the cell is instantaneously vaporized. This catapults the individual cell from the microscope slide to a nutrient medium above. Together with PALM we were able to demonstrate the usefulness of the blue part of the white light laser spectrum for cutting of subcellular structures. Cutting widths of around 1.5 µm were obtained **(04)**. The perfect TEM_{00} beam profile of our white light laser allows diffraction-limited laser spots with very small diameters.

5. Application: Surface metrology

Not only precise cutting, but also micrometer precision in surface measurements was demonstrated using the white light laser source. In collaboration with Precitec Optronik GmbH, noncontact measurements of different samples (ranging from metallic parts, sheet metal, glass, to rubber and teflon) were performed. The technology uses a lens with a strong chromatic aberration **(05)** which gives a series of different longitudinal foci for different colors. The reflection of the laser light is sent back through the lens and imaged onto a pinhole. Only the wavelength that has its focus exactly at the sample surface can pass this pinhole. The reflected light analyzed in a spectrometer, relating different wavelengths to varying sample heights. **(06)** demonstrates the height dependence of the reflected wavelength on a galvanized sheet metal sample, which is usually a tough material to test the setup. The white light laser provides enough spectral power and spectral width to easily pass that test, demonstrating its profound capability for this task. It should even be possible to use the powerful multi-Watt white light laser beam to perform in-situ height measurements

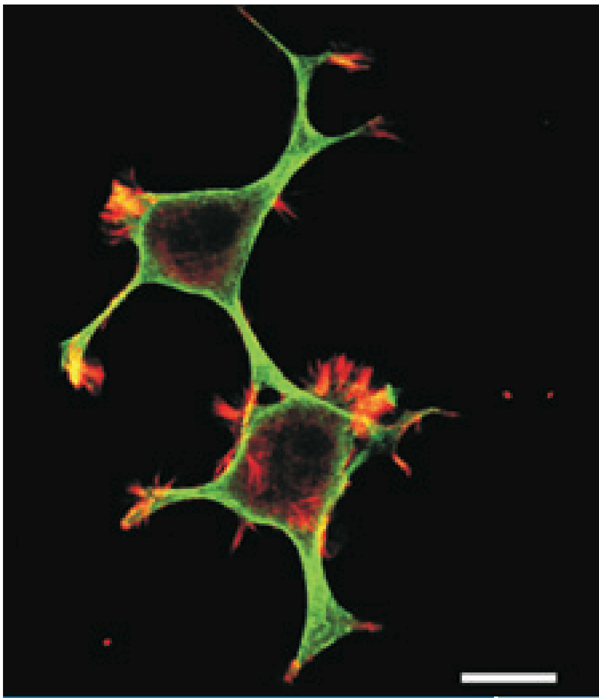

03

Multiphoton image of the same neuroblast cell as in **(01)**. *The same details as in multicolor confocal linear miscropscopy are visible.* **(01)–(03)** *result from a fruitful collaboration with Prof. J. Käs, University of Leipzig.*

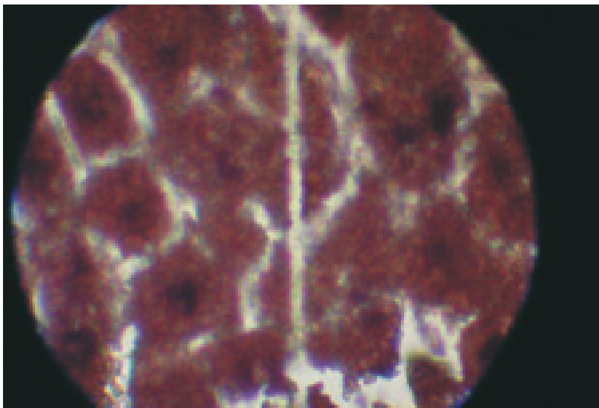

04

White light was generated in a 2,0 µm diameter tapered fiber with an average power of 330 mW. It was collimated using a 10x microscope objective and sent through a 40 nm wide interference filter at 450 nm. The remaining 8 mW of blue light are being focused through a 40x microscope objective onto a piece of rat liver. Moving the sample led to a vertical cut with a width of 1.5 µm. The images result from a collaboration with P.A.L.M. Microlaser Technologies AG, Bernried.

ZUSAMMENFASSUNG

Weißlichtlaser sind eine neue Klasse von Lasern, die nicht nur einfarbiges Licht aussenden, sondern einen weiten Bereich des Lichtspektrums abdecken. Es gibt bereits Weißlichtlaser, deren Spektrum vom Blauen über das Grüne, das Gelbe, das Rote bis in den Infraroten Spektralbereich reicht. Bis vor kurzem waren solche Laser noch undenkbar, und erst die Technologie der Ultrakurzzeitpulse hat solche Laser ermöglicht. Ihre kommerzielle Verwendung wurde bisher durch hohe Anschaffungskosten verhindert. Seit kurzem erlaubt diodengepumpte Festkörper-Lasertechnologie in Verbindung mit gezogenen Glasfasern, solche Weißlichtlaser kompakt und kostengünstig herzustellen. Wir stellen die wesentlichen Entwicklungen und eine Reihe praktischer Anwendungen vor.

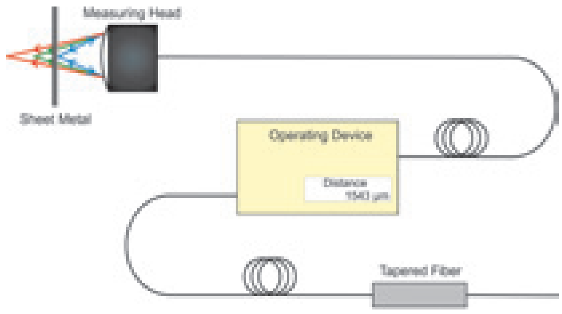

05

Working scheme of the distance measurement: A 2.5 µm thick tapered fiber was pumped with 550 mW of Ti:sapphire light at 800 nm. The generated white light was reduced to 5 mW and sent into the operating device, which contains a beamsplitter. The white light is sent through a fiber to a chromatic lens, causing longitudinal chromatic aberration with a series of different colored foci. Reflected light is sent back into the operating device, being focused onto a pinhole and analyzed by a spectrometer. The measurements are the result of a collaboration with Precitec Optronik, Rodgau.

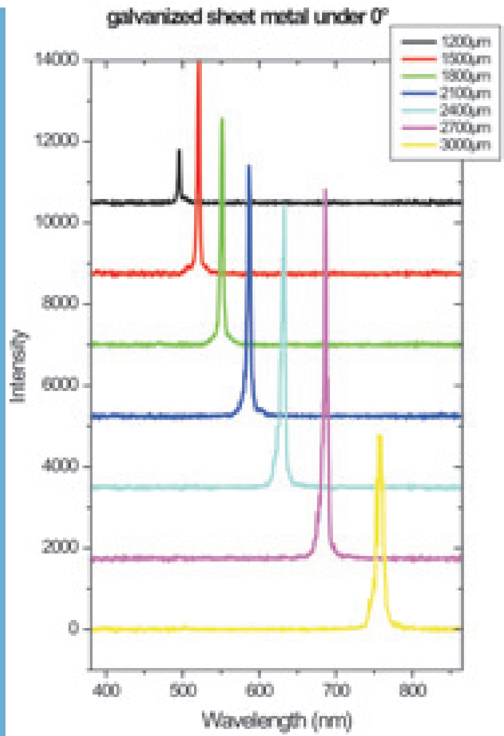

06

Distance measurement using galvanized sheet metal. The curves show the reflected spectra for different sample-measurement head distances. The signal-to-noise ratio is quite large.

directly in a laser welding arc, giving micrometer accuracy. We have also demonstrated that this method works at large angles up to 75° as well. A high signal-to-noise ratio is still achievable in this case. Once more, the superb white light laser beam allows high input coupling efficiency (especially when compared with a light bulb) and high spectral intensity in this difficult measurement environment. Also, the large spectral width of the white light allows for a superior distance range.

6. Application: Coherence radar

Coherence radar is a white-light Michelson interferometer technique, which allows the determination of the surface structure of objects which are several decimeters in diameter. Professor Häusler from Erlangen is specialized in this field and collaborated with us for these experiments.

The white light laser beam is split into two parts using a beam splitter. One part is reflected off a reference mirror, and the second part is sent to the object under investigation. The reflected light interferes with the reference light, and the resulting fringe pattern is evaluated as a function of distance of the reference mirror to the beam splitter. Equaling reference distance with measurement distance gives rise to strong interference effects, which in turn allow the surface relief measurement with submicron accuracy. This coherence radar technology had been demonstrated for centimeter sized objects, however, measuring objects from the automotive sector or turbine blades was out of reach up to now. The biggest obstacle was low light intensity, as the laser beam had to be expanded to decimeters in diameter.

The compact white light laser source with multi-Watt output power would be able to circumvent this problem. Record object diameters with submicron resolution were achieved. **(07)** shows an engine block which was measured using this method in a single scan.

7. Conclusion

Compact and reliable white light lasers have become available over the last few years, using diode pumped solid state laser technology in combination with tapered fibers. We have constructed such relatively inexpensive systems and demonstrated a variety of applications, ranging from biology (microscopy, laser cell cutting) to surface metrology (optical coherence radar). In the future, such sources will certainly gain spectral width, become more compact and even cheaper, and will find their way into a plethora of scientific and industrial implementations. •

Harald Giessen
Felix Hoos
Jörn Teipel

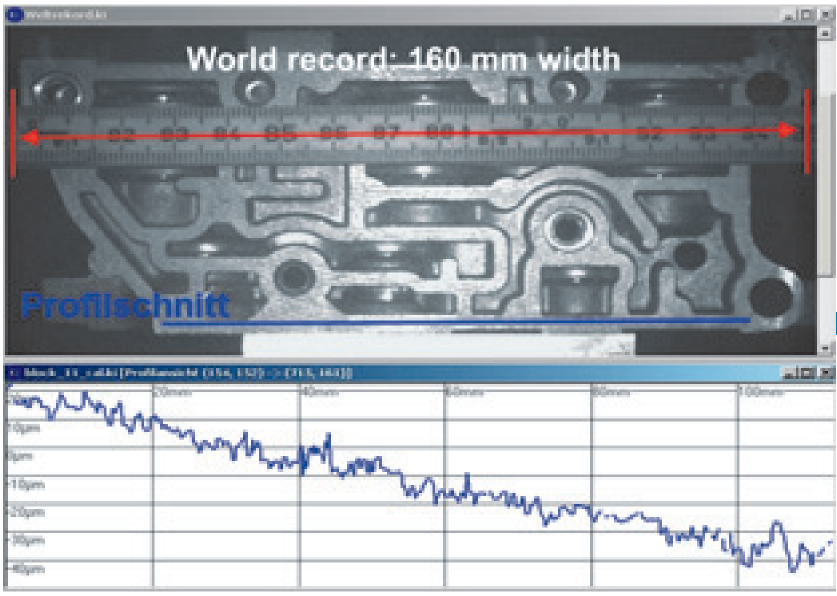

07

Three-dimensional coherence radar measurement of an engine. We used a white light fiber with 2.5 µm diameter and an output power of 375 mW. The width of the engine is 13 cm. The image is a result of a collaboration with Prof. Dr. Gerd Häusler of the University Erlangen-Nürnberg.

THE AUTHORS

Harald Giessen

got his Physics Diploma in Technical Physics from Kaiserslautern University (1992), working on optical properties of II–VI semiconductors. He was a J.W. Fulbright scholar at the Optical Sciences Center of the University of Arizona and obtained his M.S. and Ph.D. degrees in Optical Sciences in 1994 and 1995, respectively, working on ultrafast optical properties of semiconductor quantum dots. He was a post-doc at the Max-Planck-Institute for Solid State Physics in Stuttgart in 1995 and 1996, discovering coherent Rabi flopping in semiconductors. From 1997 to 2000, he held a C1 position at the University of Marburg, working on submicron spatial optical resolution and ultrafast photoionization dynamics of noble gases. In 2001, he became a C3 professor at the University of Bonn, focusing on ultrafast white light lasers and plasmonics. Since 2004, he has been head of the 4. Physikalisches Institut at the Universität Stuttgart, concentrating research on metallic optical metamaterials and applications of compact white light lasers.

Felix Hoos

is a Ph.D. student, building compact ultrafast diode-pumped solid state laser systems. He got his Diploma in Electrical Engineering from the University of Karlsruhe in 2004, utilizing white light from tapered fibers in ultrafast pump-probe spectroscopy.

Jörn Teipel

is a Ph.D. student, working towards his degree investigating applications of compact white light lasers. He got his Physics Diploma in 2002 from the University of Bonn, working on tapered fibers and their optical properties.

Jörn Teipel *(left) and* Felix Hoos *(right) at Hannover Messe 2005, presenting the compact white light laser.*

Contact
4. Physikalisches Institut, Universität Stuttgart, Pfaffenwaldring 57, 70569 Stuttgart
Tel. +49 (0)711 685 5111 (office), +49 (0)711 685 5110 (secretary)
Fax +49 (0)711 685 5097
E-mail: giessen@physik.uni-stuttgart.de, Internet: http://www.physik.uni-stuttgart.de/nano

zurück zum Inhalt

Photons and photonics in solar cells and photodiodes

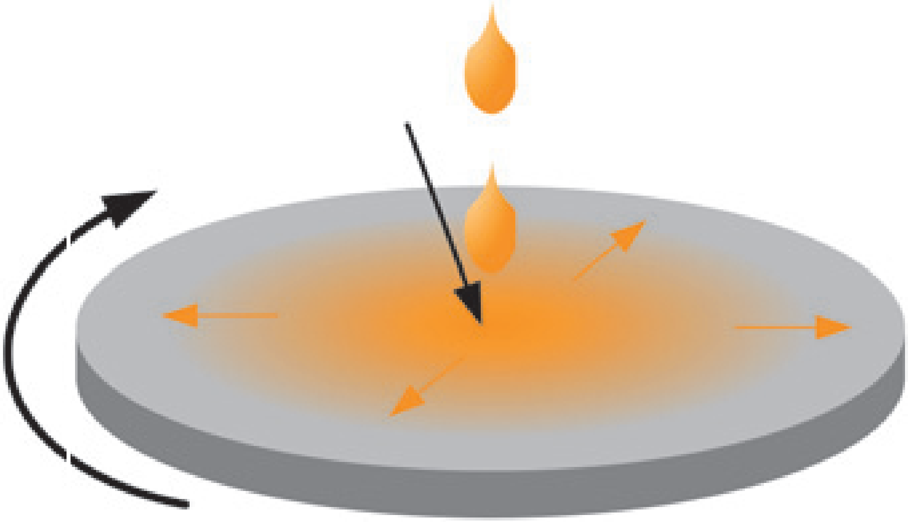

Solar cells and photodiodes rely on the interaction of photons with the electron/hole system of semiconductors. After the absorption of photons, transport of excess electrons and holes results in the observation of an electrical signal at the contacts of the diodes. However, the fabrication of high efficiency solar cells or photodetectors requires far more than the seemingly simply physics and technology of fabricating "just a large area diode". Instead, sophisticated theoretical and practical concepts are necessary for such high efficiency devices.

1. Photovoltaic fluorescent collectors combined with photonic filters

The concept of photonic crystals, three-dimensional periodic dielectric structures that allow for the complete control over the propagation of electromagnetic waves, was introduced by Yablonovitch in 1987 [1]. Since then, photonic crystals entered in a wealth of implementations in opto-electronics, laser optics, and photonics. Surprisingly, photonic crystals have not found any application in photovoltaics up to the present. In fact, the usefulness of this concept for improving solar cells has been disputed even in the original publication [1]. The difficulty to combine photonic crystals with solar cells lies in the fact that photonic crystals can manage electromagnetic waves in an arbitrary, but relatively narrow, range of wavelengths. In contrast, solar cells have to handle the complete band of the solar spectrum. However, the recently reinforced effort to overcome classical limits of photovoltaic power conversion [2] has also brought the use of advanced optical nanostructures (among them: photonic crystals) for solar cells under reconsideration.

Here we briefly sketch a combination of photonic nano-structures with the classical concept of fluorescent collectors (FCs). Classical FCs, as already intensely investigated during the 1980s [3,4], use organic dyes or inorganic fluorescent molecules embedded in a dielectric material to collect and concentrate solar light. As sketched in **(01)**, the incoming light is first absorbed by the dye in the collector and then re-emitted at a lower photon energy. This re-emission serves also for the randomization of the light. As a consequence, the classical concentration effect of FCs results from the total internal reflection of the randomized light. However, only photons with a direction outside of the critical angle of internal reflection are kept in the system and the collection efficiency of such a system will be *always* considerably below unity.

(01) also features the possibility to put a photonic band stop (PBS) filter at the top of the collector. This PBS should be designed to be transparent for the incoming light above a certain threshold photon energy E_{th} but should provide a reflectance of unity for those photons that are re-emitted from the dye. In this way, 100% of those photons are kept within the system. Note that practical means to realize PBS with omnidirectional optical reflection in specific wavelength ranges are readily available using technologies that are able to cover large areas, e.g., by one-dimensional periodic dielectric structures [5], i.e., thin film interference filters.

(02) shows the results of a recent Monte-Carlo analysis of the collection properties of FCs with and without PBS [6]. Here we consider the situation where only radiative losses, as required by the principle of detailed balance, are allowed within the FC *and* the solar cells at its bottom. The coverage fraction *f* is defined by the portion of the FC's backside that is covered by the solar cells. We see that the system *with* a PBS has a maximum efficiency of η = 33% at *f* = 1. Interestingly this maximum equals the maximum conversion efficiency of a solar cell having a band gap energy E_g that equals the threshold energy E_{th} of the FC. Thus, even with PBS, FCs cannot overcome the classical Shockley-Queisser limit [7] for photovoltaic energy conversion. However, almost the same efficiency is maintained at a coverage fraction *f* = 0.01, i.e., with a 99% saving of solar cell material. In contrast, the system *without* PBS has a maximum efficiency of only η = 29% at *f* = 1 due to the losses discussed above. Furthermore, with decreasing *f*, the available η drops sharply such that any saving of solar cell material has to be paid by losses in output power.

The benefit from the use of photonic band structures for this idealized system is obvious. However, more realistic configurations that include also non-radiative losses in the collector as well as in the solar cells exhibit similar efficiency gains by using the spectral selectivity of photonic band structures [6]. Experimental and technological work is in progress in order to demonstrate this effects also in practical systems.

SUMMARY

This contribution gives three examples for the research on photonics and optoelectronics at the Institute of Physical Electronics (ipe). Part 1 decribes our work on fluorescence converters for solar cells. The combination of these converters with photonic crystals opens a new way to boost the efficiency of classic solar cells. Part 2 presents the application of amorphous silicon photodiodes as large area light sensors in modern digital cameras. The combination of our technology with high dynamic range cameras (HDRC) has the potential of constructing future cameras with a much higher resolution and sensitivity. Finally, part 3 reports on the laser as a tool in the preparation of solar cells. Here, the laser replaces the classic furnace diffusion of a pn-junction. In fact, this process seems to be simple. However, at present we are the only group in the world that is able to fabricate an emitter for a solar cell in a such well defined way with the help of a scanned laser.

2. Thin-Film-on-CMOS camera technology

Hydrogenated amorphous silicon (a-Si:H) and its alloys with carbon (a-SiC:H) or germanium (a-SiGe:H) open new possibilities of constructing photodetectors with a superior performance over their crystalline silicon counterparts. Thin film photodiodes greatly enhance the capabilities of modern CMOS (complementary metal oxide semiconduc-

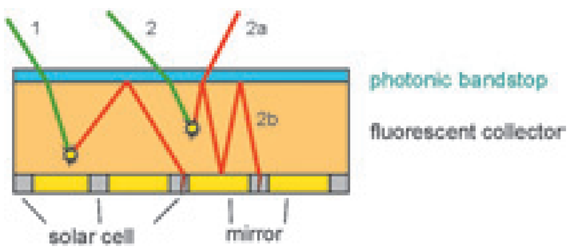

01

Schematic drawing of a fluorescent collector with solar cells at its bottom. The fluorescent layer absorbs incoming photons (1) and emits them at lower photon energy. Without photonic band stop (PBS) some of these photons leave the collector (2a). The PBS reflects these photons back into the collector (2b).

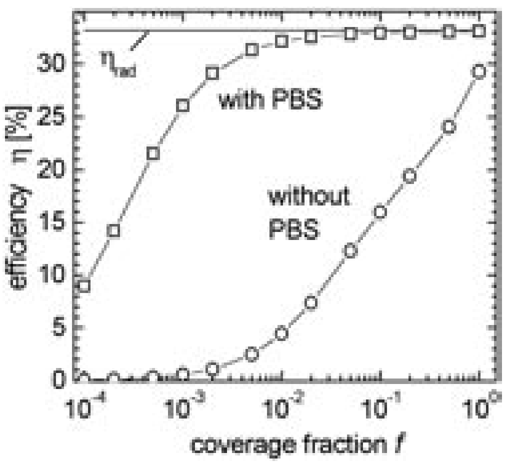

02

Efficiencies for band gap energy Eg = 1.12eV and thresholf energy Eth = 1.32eV for ideal solar cells. Without photonic band stop (PBS) the efficiencies degrade rapidly with decreasing coverage fraction f (circles). With PBS the systems efficiency drops much slower with decreasing f (squares) almost maintaining the optimum efficiency down to f = 10-2.

tor) cameras by the so-called “Thin-Film-on-CMOS (TFC)” technology.

Modern CMOS image sensors, also often addressed as “Active Pixel Sensors” (APS), are successfully competing with CCDs (charge-coupled devices) in volume as well as high definition applications [8]. Cost, system integration, and manufacturing issues clearly favour CMOS cameras, whereas CCDs still feature the smallest pixels and ultimate sensitivity. Standard CMOS camera design faces an inherent dilemma: The very same pixel area, which ought to be as small as possible, hosts a diode as photodetector and all readout and signal conditioning circuits at the same time. If sophisticated readout electronics for correlated double sampling, adaptable integration time, or application specific pre-processing is needed, very little space is left for the photodiode. Hence the “eye” of the CMOS camera will be almost blind. On the contrary, photodiodes with a large area fill factor limit the number of transistors inside the pixel, and hence the chance for hardware-based signal processing.

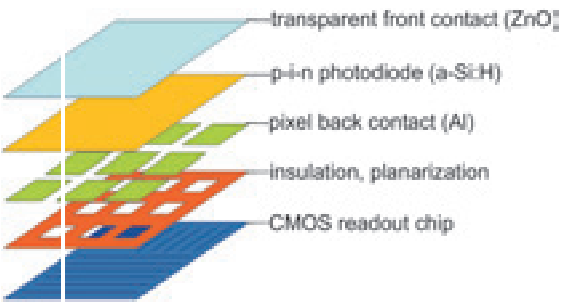

03

Schematic representation of a Thin-Film-on-CMOS layer system. Three-dimensional integration of amorphous silicon based thin film photodiodes enhances the functionality of an underlying CMOS camera chip. Wafer production ends with an open pixel contact in the top metallization layer. After planarization of the interconnect stack and pixel back contact formation, plasma enhanced chemical vapour deposition grows a p-i-n type thin film photodiode which needs no patterning into single pixels. Finally, aluminium doped zinc oxide forms the transparent front contact.

Current and future semiconductor technology lends an additional argument to enhancing CMOS cameras by the three-dimensional addition of a-Si:H based photodiodes. As the standard feature size is shrinking according to Moore’s law, *pn*-junctions become very shallow, resulting in a very low and blue-shifted spectral sensitivity. Moreover, interconnect and passivation layers pile up to several micrometers height. The viewing angle of the wafer-based photodiodes consequently shrinks into a “chimney view” through a tiny hole in the interconnect stacks.

04

The impressively high dynamic range of 120 dB in this photograph results from both, a sophisticated logarithmic input stage in the underlying HDRC readout chip, and the six orders of magnitude in light-to-dark conductivity ratio of the a-Si:H based photodiodes on top of the TFC camera. The inset in the lower right corner presents a microscopic top view of one pixel.

Thin-Film-on-CMOS resolves all these limitations, and adds even more benefits to the novel hybrid CMOS camera system [9].

(03) sketches the general layout of a TFC camera pixel. The bottom readout and signal processing circuit is manufactured in state-of-the-art CMOS technology, making best use of optimized mixed-signal design and wafer processing. No photodiode is present in the pixel on the wafer, but integrated on top of the interconnect and planarization layers. Manufacturing of the readout electronics provides one top contact per pixel, which later connects to the back contact of the thin film photodiode.

Due to the short diffusion length L_D of charge carriers in the a-Si:H based semiconductors of typically L_D = 100 to 150 nm, no pixel separation is needed in the upper photodiode layers. Down to a back contact spacing of 1.5 µm, the cross-talk between adjacent pixels outperforms CCDs by a factor of 5 to 10. Moreover, the small diffusion length determines the layer structure of the thin film photodiodes. Contrary to crystalline semiconductors, diffusion based carrier collection is almost impossible in these amorphous materials. Therefore a built-in electric field must serve for separating the photogenerated charge carriers. The typical *p-i-n* layer structure of such amorphous silicon based photodiodes mainly consists of an undoped absorber layer sandwiched between very thin doped layers which generate the necessary electric field across the intrinsic *i*-layer. Plasma enhanced chemical vapour deposition (PECVD) of a-Si:H proceeds at low temperature between 100 °C and 150 °C. The thin film photodiodes can therefore easily add upon the CMOS chips after all standard semiconductor processing is finished at a silicon foundry, or at the Institute of Microelectronics Stuttgart (IMS-CHIPS), respectively.

The Thin-Film-on-CMOS technology jointly developed by *ipe* and IMS-CHIPS presents a number of advantages over standard APS or CMOS cameras. The three-dimensional integration of photodiodes on top of the readout electronics implements almost 100 percent area fill factor for the pixel photodiode, and for the underlying electronics as well. Consequently, sensitivity and modulation transfer function of TFC systems clearly outperform those of standard active pixel sensors. Modern CMOS cameras with pixel sizes of a few micrometers are limited to fill area factors below 30 to 40 percent. Amorphous silicon itself adds an additional gain in sensitivity, since its optical bandgap $E_g \approx 1.8$ eV is substantially higher than $E_g = 1.1$ eV of crystalline silicon. Hence the detection limit of TFC cameras is only restricted by leakage due to back contact patterning and by readout noise, rather than by the thermally generated dark current of standard devices. Our photodiodes present typical values of dark current density j_d as low as $j_d = 10^{-10}$ A/cm².

Many applications ask for a spectral sensitivity which is similar to that of the human eye. Thin film a-Si:H photodiodes perfectly match this requirement. Moreover, the hydrogen content of a-Si:H, layer thicknesses and the alloys a-SiGe:H and a-SiC:H provide easy means of continuously adjusting the spectral response of the TFC photodiodes to various fields of application [10].

Manufacturing of complete TFC camera chips is performed in a close cooperation between IMS-CHIPS and our institute. Customer and application specific requirements control the design of the readout electronics at IMS-CHIPS. The readout characteristics of the photodiode signals can be logarithmic as well as linear, with various options of noise reduction, signal pre-processing etc. Highly miniaturized endoscope camera chips contain pixels as small as 4 x 4 µm² but provide a full color resolution, as it is mandatory for medical applications.

(04) presents an impressive example of high dynamic range imaging. The HDRC camera chip in Thin-Film-on-CMOS technology displays details of the glowing filament, and of the imprint on the light bulb in the very same image frame, with a dynamic range up to 120 dB. Proper readout electronics could enable even higer values, due to the very low dark current of a-Si:H or a-SiC:H photodiodes. Similar logarithmic readout is useful for the control of automated welding or laser cutting machines, and for various automotive applications as well.

Highly sophisticated readout electronics in conjunction with well adapted thin film photodiodes allow for ultimate sensitivity in TFC star sensors. Comparatively large pixel sizes of 20 x 20 µm² accommodate the long focal length of star tracking systems which ensure the precise positioning of every satellite in orbit. Due to their high sensitivity, low power consumption and rather simple system integration, TFC star sensors are now challenging the well established technology of CCD and CMOS-APS based star trackers.

The key to high performance of TFC photodetectors is the interplay between the layout of the thin film photodiode and the input of the pixel amplifier or readout circuitry. Depending on the target application, different photodiode structures are needed. **(05a)** demonstrates significant differences in sensitivity, as measured by the external quantum efficiency of different photodiode structures. The layer sequence with the light entering from the p-side of the pin photodiode performs much better due to the difference in charge carrier transport in a-Si:H based materials. Since their effective electron mobility is a factor of 10 to 100 higher than the respective hole mobility, the collection of electrons succeeds across the whole i-layer thickness whereas hole collection is rather limited to the vicinity of the *p*/*I* interface. Consequently, most photogenerated holes recombine on their way to the p-type back contact of the structure depicted at the bottom of **(05a)**. As expected, hole collection can be slightly improved by raising the readout voltage from V = -2 V to V = -3 V which is however the limit set by the supply voltage of the current CMOS technology.

Some applications, for example incorporating radiation hard readout circuits, enforce the use of a *p*-type back contact, and hence a structure with light unfavorably entering from the *n*-side. For such configurations, **(05b)** evaluates the amount of improvement attainable by careful tuning of the *i*-layer thickness. Due to readout noise considerations, the capacitance of

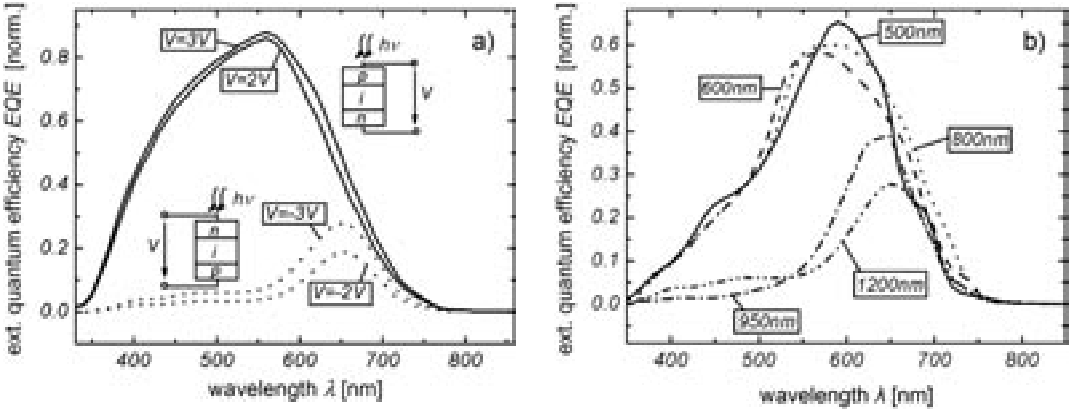

05

(a) *External quantum efficiency* EQE *measurements on comparatively thick TFC diodes reveal the breakdown of charge carrier collection in* n-i-p *structures where the light enters through the* n*-type doped layer. In contrast, the response of* p-i-n *diodes nicely resembles the spectral sensitivity of the human eye, and peaks at values above 80 %. The* i*-layer thicknesses of the* n-i-p *and* p-i-n *diodes amount to 1.2 µm, and 1.5 µm, respectively.*
(b) *The thickness dependence of* EQE *in* n-i-p *photodiodes proves that an optimum thickness of 700 nm can indeed be used for* n-i-p *TFC layer stacks. Larger* i*-layer thickness clearly hinders hole collection in those structures.*

the thin film photodiode should be as high as possible, asking for thick *i*-layers. **(05b)** demonstrates a significant enhancement of carrier collection if the *i*-layer is kept thin enough to allow for successful extraction of photogenerated holes, and thereby presents a viable compromise in the optimization of sensitivity versus noise reduction. Future applications of TFC technology will further exploit the ease of tuning the spectral response of a-Si:H based thin film photodiodes. **(06)** visualizes the bandgap change by alloying a-Si:H with germanium or carbon. All samples shown have an equal thickness of 1 µm, their colors hence directly indicate the respective optical bandgap E_g. Alloying with Ge enables 1.0 eV < E_g < 1.7 eV, alloying with C raises E_g above 1.8 eV. Reasonable electronic quality can be maintained in a range of 1.4 eV < E_g < 2.1 eV. Interesting applications, e.g. in bioanalytics, arise if the simple *p-i-n* type photodiodes evolve into more sophisticated structures like *n-i-p-i-n* or *p-i-i-n* with varying E_g and layer thickness of the single *i*-layers [10,11]. Such structures open the possibility of dynamically adjusting the spectral response by the variation of the applied readout voltage, and moreover realizing steep gradients of the spectral sensitivity which are useful for discriminating different fluorescence markers or spectroscopic signals in a narrow range of photon energies.

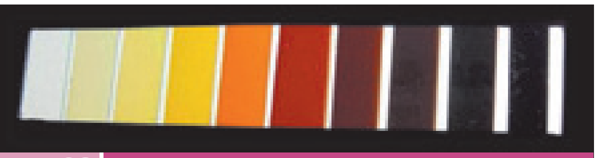

06

Due to the amorphous structure of the a-Si:H based alloys, truly continuous adjustment of the optical bandgap is possible, in contrast to crystalline semiconductors with their well-defined bandgaps. The photograph presents 1 µm thick films with varying alloy composition from a-SiC:H at the left hand side, over a-Si:H in the middle, to a-SiGe:H at the right hand side. Since the film thickness is similar for all films, their color directly visualizes the change in optical bandgap.

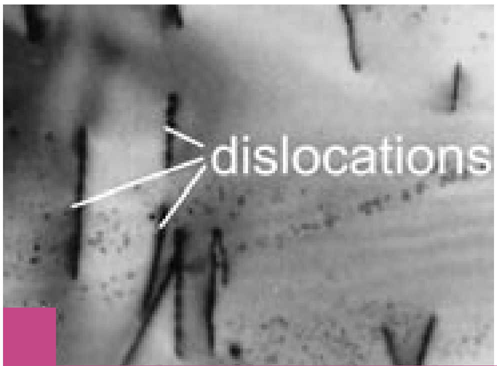

07 a) b)

Cross section TEM pictures of laser processed silicon wafers. **(a)** *Laser processing with 50 µm circular laser focus results in high defect density.* **(b)** *Line beam shaped laser focus enables recrystallization without any defects.*

3. Room temperature doping of crystalline silicon using pulsed laser radiation

Significant cost reduction in silicon wafer processing for large area electronic devices such as solar cells requires new processing techniques avoiding the most cost intensive steps like wafer handling for batch processing or time and clean room area consuming furnace processing. Our laser doping technology aims at replacing costly high-temperature and vacuum processing steps by low-temperature processing in air.

First papers in the field of laser processing of semiconductors were published in the mid 1970s. Dopant activation of implantation doped silicon and germanium layers was demonstrated for the first time, using laser annealing [12]. Here, the pulse of a Q-switched Nd:glass-laser annealed radiation defects, recrystallized the disordered structure of implantation doped layers, and also stimulated the process of electrical activation of the implanted impurities. Re-crystallization of polycrystalline silicon films on silica and on silicon nitride layers deposited on crystalline silicon wafers also was first achieved using cw-lasers. Yamada et. al. [13] demonstrated the crystallization of sputtered amorphous silicon on sapphire substrates also using a cw-laser. The rapid development of semiconductor laser processing goes hand in hand with the development and availability of new laser sources. Problems with thermal stress cracking of cheap glass substrates during cw-laser crystallization were eliminated by using pulsed lasers, like frequency doubled Nd:YAG and other solid state lasers, as well as gas lasers like excimer-lasers.

More recently, the development and availability of highpower pulsed gas lasers and diode laser pumped solid state lasers with high pulse repetition rates and high average power in the 100 W range made it possible to increase the processing speed and throughput of large area laser processing considerably. The first industrial application of large area laser processing was laser crystallization of amorphous silicon for active matrix liquid crystal displays. Here, laser processing is performed in air, with a throughput of several 10 cm²/s.

In contrast to laser crystallization, existing laser doping techniques use vacuum or a protecting atmosphere during irradiation of the samples, which decrease the overall throughput and increase cost. An additional problem of existing laser doping techniques is the high concentration of defects, mainly dislocations, within the recrystallized layer, which leads to a significantly lower open circuit voltage compared to furnace diffusion if laser doping is applied to crystalline silicon solar cells.

Our laser doping process uses a line-beam shaped laser focus with very narrow, below 10 µm, short axis focus. The result is a completely different melting and recrystallization behavior of crystalline silicon compared to laser processing which uses a circular laser focus. The difference between laser crystallization using a circular laser beam focus and a line beam shaped laser beam focus is depicted by the transmission electron microscope images of **(07)**. Our laser processed emitters of monocrystalline silicon solar cells contain no defects. First solar cells processed with this technique achieve open circuit voltages higher than V_{oc} = 620 mV and efficiencies of $\eta > 14\%$ [14]. In fact, the "secret" of our process lies just in the shape of the laser focus on the sample. Without the well-defined shape it would not be possible to obtain large-area, spatially homogeneous pn-junctions with a low saturation current density.

In our experiments, spin coating of phosphorous containing liquid and subsequent drying on a hotplate results in a 400 nm thick solid doping precursor on the surface of a boron doped, *p*-type <100> oriented wafer with thickness $w = 375 \pm 25$ µm and resistivity $\rho = 0.35$ Ωcm. **(08)** shows spin coating of a rotating wafer, which leads to a homogeneous distribution of a thin layer of the liquid dopant on the wafer surface.

A lens system consisting of cylindrical and spherical lenses focuses the beam of a 15 ns pulsed frequency doubled Nd:YVO_4 laser onto the surface of the wafer. The laser emits light at a wavelength $\lambda = 532$ nm with a tunable repetition frequency $f <$ 100 kHz and power $P < 1$ W. The size of the line beam shaped laser focus is 5 µm wide in y-direction and 200 µm in the perpendicular x-direction. The intensity distribution is Gaussian in both x and y directions. An automatic focusing system controls the focus size and keeps the pulse energy density at a constant value during wafer processing. An *xy*-translation stage fixes and moves the wafer in *y*-direction with a scanning speed v_y. After each laser pulse the sample is translated by a distance $\Delta y = v_y / f$. We tune the repetition frequency f according to the scanning speed v_y to obtain a translation 0.3 µm $< \Delta y <$ 3 µm, which corresponds to an overlap $95\% > O_y > 40\%$ between the laser pulses. The next column of pulses is then shifted by a distance Δx with respect to the previous column. **(09)** schematically displays the principle of the scanning process. The laser beam scans the surface and creates the emitter by locally melting the silicon and allowing the dopant to diffuse into the wafer. We process different samples varying the energy density D_{pulse} of the laser pulses, the overlap O_x in x- and O_y in y-direction between the pulses.

ZUSAMMENFASSUNG

Die Wirkung von Solarzellen und Photodioden beruht auf der Wechselwirkung von Licht, der Photonen, mit dem elektronischen System, den Elektronen und Löchern eines Halbleiters. Nach der Absorption der Photonen führt der Transport von Elektronen und Löchern zu einem elektrischen Signal an den Kontakten dieser Bauelemente. Für die Herstellung von hocheffizienten Solarzellen und Photodioden benötigt man jedoch bei weitem mehr als die scheinbar einfache Physik und Technologie einer Diode, die 'halt ein bisschen größer ist als üblicherweise'. Die Herausforderung besteht darin, komplexe Konzepte und Technologien zu entwickeln, die zuverlässig und reproduzierbar zu hochwertigen, großflächigen Bauelementen führen.

Dieser Beitrag stellt drei Beispiele der Forschung am Institut für Physikalische Elektronik (ipe) im Bereiche der Photonik und Optoelektronik vor. Teil 1 beschreibt unsere Arbeiten an Fluoreszenzkonvertern für photovoltaische Anwendungen. Die Kombination dieser Konverter mit nano-optischen Strukturen (z.B. photonischen Kristallen) eröffnet neue Möglichkeiten, Licht einfach und effizient zu konzentrieren und somit Solarzellenmaterial zu sparen. Teil 2 demonstriert die Anwendung von amorphem Silizium für großflächige Photodetektoren in modernen digitalen Kameras. Die Kombination unserer Technologie mit so genannten high dynamic range cameras (HDRC) erlaubt in Zukunft die Herstellung von Kameras mit einer viel größeren Auflösung und Empfindlichkeit. Schließlich berichtet Teil 3 über die Verwendung von Lasern für die Dotierung von Solarzellen. Mit dieser Technologie kann die energieaufwändige Diffusion eines pn-Übergangs durch einen schnellen, energie- und kosteneffizienten Prozess ersetzt werden. Obwohl die Idee einfach klingt, sind wir derzeit die einzige Forschungsgruppe in der Welt, die diesen Prozess reproduzierbar und auf hohem Niveau beherrscht.

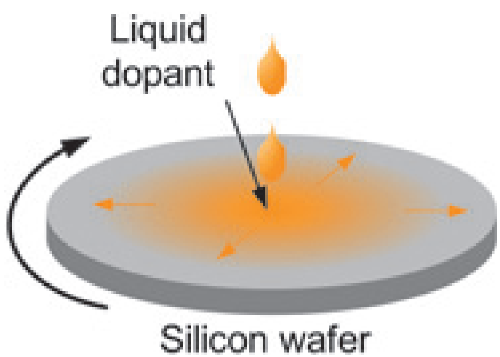

08

Spin coating covers the silicon wafer with a thin layer of a dopant containing liquid.

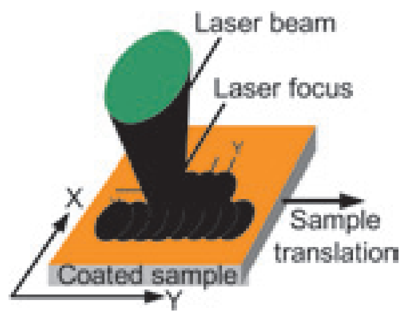

09

Sketch of the LD process. Each pulse melts a several hundred nanometer thick layer of silicon under the phosphorous containing paste and phosphorous atoms diffuse into the molten layer. The laser scans the wafer with a shift 0.3 µm < Dy < 3 µm in Δy-direction and 100 µm < Dx < 200 µm in Δx-direction between the laser pulses.

10

Finished solar cell with antireflection layer and contacts.

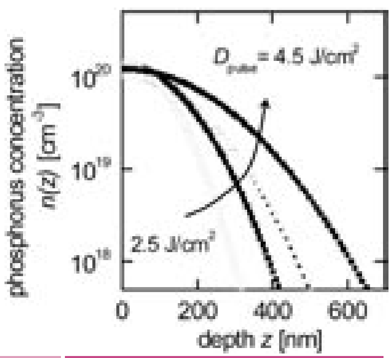

11

Phosphorus depth profile measured by SIMS of four solar cells processed with pulse energy densities D_{pulse} = 2.5, 3.2, 3.8 and 4.5 J/cm². The effective depth z of the emitter increases with the pulse energy density D_{pulse}.

After laser processing of the samples, the front contacts are formed by vacuum evaporation of 2 µm thick Ti/Pd/Ag fingers using a mask. The back contact consists of an evaporated 1.5 µm thick aluminum layer. A 75 nm thick SiN_x layer with a refractive index n_r = 1.9 additionally serves as anti-reflection layer. Contacts are annealed in forming gas at 420 °C for 10 minutes in order to improve the electronic contact properties. Finally a mesa structure is formed by CF_4 plasma-etching to define the cell area. **(10)** depicts the completion of the solar cell by adding an antireflective coating as well as front and back contacts.

We use different analyzing techniques to investigate the influence of the laser doping process on the performance of the solar cells. Secondary ion mass spectroscopy determines the depth and lateral distribution of the dopant concentration. **(11)** shows the phosphorous depth profile of four cells processed with pulse energy densities D_{pulse} = 2.5, 3.2, 3.8 and 4.5 J/cm². The LD process creates a shallow highly doped emitter. The emitter depth increases with the pulse energy density D_{pulse}. **(T.01)** shows the parameters of a solar cell under 100mW/cm² intensity AM1.5 irradiation, independently confirmed by FhG-ISE, Freiburg. This solar cell is irradiated with a pulse energy density D_{pulse} = 2.5 J/cm², shifted by Δx = 100 µm in x- and Δy = 0.5 µm in y-direction.

J_{sc} [mA/cm²]	V_{oc} [mV]	*FF* [%]	η [%]
31.07	612.3	74.6	14.2

(T.01): Photovoltaic output parameters short circuit current density J_{sc}, open circuit voltage V_{oc}, fill factor *FF*, and efficiency η under 100mW/cm² intensity AM1.5 irradiation. The data are independently confirmed by FhG-ISE, Freiburg. During laser processing, the cell is irradiated with a pulse energy density D_{pulse} = 2.5 J/cm², shifted by Δx = 100 µm in x- and Δy = 0.5 µm in y-direction.

The laser doping process offers a simple manufacturing method of solar cells where diffusion in a clean room environment is superfluous. Solar cells made with the method described above show a high efficiency of η = 14.2% even without photolithographic steps or texture on the front side. At present we study several simplifications of the laser doping process and investigate scaling up to the size of industrial solar cells of 15 x 15 cm². If that stage is reached, the process will be transferred into an industrial environment of solar cell production.

Jürgen R. Köhler
Uwe Rau
Markus B. Schubert
Jürgen H. Werner

References

1 E. Yablonovitch, Phys. Rev. Lett. **58**, 2059 (1987).
2 M. A. Green, Progr. Photov.: Res. Appl. **9**, 123 (2001).
3 E. Yablonovitch, J. Opt. Soc. Am. **70**, 1362 (1980).
4 A. Goetzberger and V. Wittwer, Solar Cells **4**, 3 (1988).
5 D. N. Chigrin and C. M. Sotomayor Torres, Optics and Spectroscopy **91**, 484 (2001).
6 G. C. Glaeser, F. Einsele, and U. Rau, in *Techn. Digest 15th Photovoltaic Science and Engineering Conference* (in print).
7 W. Shockley and H. J. Queisser, J. Appl. Phys. **32**, 510 (1961).
8 E. Fossum, IEEE Transact. Electron Devices **44**, 1689 (1997).
9 H. Fischer, J. Schulte, J. Giehl, M. Böhm, and J. P. M. Schmitt, Mat. Res. Soc. Symp. Proc. **258**, 1139 (1992).
10 K. Eberhardt, T. Neidlinger, and M. B. Schubert, IEEE Trans. Electron. Dev. **ED-42**, 1763 (1995).
11 R. Brüggemann, T. Neidlinger, and M. B. Schubert, J. Appl. Phys. **81**, 7666 (1997).
12 E. I. Shtyrkov, I. B. Khaibullin, M. M. Zarpov, M. F. Galyatudinov, and R. M. Bayazitov, Sov. Phys. Semicond. **9**, 1309 (1975).
13 M. Yamada, S. Hara, K. Yamamoto, and K. Abe, Jpn. J. Appl. Phys. **19**, 261 (1980).
14 A. Esturo-Breton, T. A. Wagner, J. R. Köhler, and J. H. Werner, in *13th Workshop on Crystalline Silicon Solar Cell Materials and Processes*, edited by B. Sopori (NREL, Golden CO, 2003), p. 186.

THE AUTHORS

Jürgen Köhler

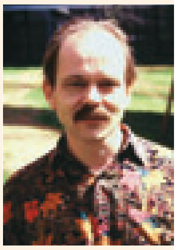

studied Physics in Tübingen and Stuttgart. During his diploma thesis in 1984 he worked at the Institut für Physikalische Elektronik (ipe), faculty of electrical engineering, on optical spectroscopy of molecules in high pressure gases. Between 1985 and 1990 he worked at ipe in the frame of several R&D projects in the field of laser spectroscopy and material processing and towards his Ph. D. thesis. In 1990 he became the head of the research group "applied laser and measurement techniques", where he was responsible for several EC, BMBF and bilateral industrial R&D projects. In 1991 he became member of the permanent scientific staff at ipe. He obtained his Ph. D. from the Universität Stuttgart in 1996. Since 1997, he is heading the laser-processing research group at ipe.

Uwe Rau

received the Ph. D. degree in physics in 1991 from the University of Tübingen, Germany, for his work on temporal and spatial structure formation in the low-temperature electronic transport of bulk semiconductors. From 1991–1994 he worked at the Max-Planck-Institut für Festkörperforschung, Stuttgart, Germany, in the field of Schottky contacts, semiconductor heterojunctions and silicon solar cells. From 1994–1997 he was with the University of Bayreuth, Germany, working on electrical characterization and simulation of silicon and CuInSe2 solar cells. In 1997 he joined the Institut für Physikalische Elektronik at the Universität Stuttgart, where he became leader of the device analysis group. In 2002, he received the habilitation from the Carl-von-Ossietzky Universität Oldenburg. His research interest are electronic, ionic, and photonic transport in solar cells, as well as interface and bulk defects in semiconductors.

Markus B. Schubert

holds a Dipl.-Ing. and a Dr.-Ing. degree, both obtained from the Faculty of Electrical Engineering at the Universität Stuttgart. Since 1985, he worked as a research assistant at Stuttgart University, Institute of Physical Electronics (ipe). Since 1993 he serves as a group leader at ipe, managing various research projects on thin film sensors and solar cells. M. B. Schubert has authored and coauthored more than 100 publications. Since 1999, he assists Prof. J. H. Werner as the associate director of ipe.

Jürgen H. Werner

studied Physics in Tübingen and received the Ph.D. degree in Physics in 1983 from the Universität Stuttgart. The PhD thesis on polycrystalline silicon was carried out at the Max-Planck-Institut für Festkörperforschung, Stuttgart. After working as a scientist at the Max-Planck-Institut, he spent 18 months in the USA as a guest scientist at the IBM T. J. Watson Research Center, Yorktown Heights, N.Y., USA at AT&T Bell Laboratories, Murry Hill, N. J., USA working on Schottky diodes. In 1991, Jürgen Werner received the habilitation from the University of Munich. In these years, his research concentrated on semiconductor interfaces. In 1996 he became the director of the Institute for Physical Electronics (ipe) in 1996, where he has been teaching and researching since then in the field or micro- and optoelectronics. The research emphasis of the ipe is placed on photodectors, solar cells and solar cell materials. Jürgen H. Werner is author and co-author of over 215 publications and the editor of nine books.

Contact

Institut für Physikalische Elektronik, Universität Stuttgart, Pfaffenwaldring 47, 70569 Stuttgart
Tel. +49 (0)711 6857141
Fax +49 (0)711 685 7143
E-mail: sekretariat@ipe.uni-stuttgart.de

zurück zum Inhalt